CANADIAN THESES ON MICROFICHE

THÈSES CANADIENNES SUR MICROFICHE

National Library of Canada
Collections Development Branch

Canadian Theses on
Microfiche Service

Ottawa, Canada
K1A 0N4

Bibliothèque nationale du Canada
Direction du développement des collections

Service des thèses canadiennes
sur microfiche

NOTICE

The quality of this microfiche is heavily dependent upon the quality of the original thesis submitted for microfilming. Every effort has been made to ensure the highest quality of reproduction possible.

If pages are missing, contact the university which granted the degree.

Some pages may have indistinct print especially if the original pages were typed with a poor typewriter ribbon or if the university sent us an inferior photocopy.

Previously copyrighted materials (journal articles, published tests, etc.) are not filmed.

Reproduction in full or in part of this film is governed by the Canadian Copyright Act, R.S.C. 1970, c. C-30. Please read the authorization forms which accompany this thesis.

AVIS

La qualité de cette microfiche dépend grandement de la qualité de la thèse soumise au microfilmage. Nous avons tout fait pour assurer une qualité supérieure de reproduction.

S'il manque des pages, veuillez communiquer avec l'université qui a conféré le grade.

La qualité d'impression de certaines pages peut laisser à désirer, surtout si les pages originales ont été dactylographiées à l'aide d'un ruban usé ou si l'université nous a fait parvenir une photocopie de qualité inférieure.

Les documents qui font déjà l'objet d'un droit d'auteur (articles de revue, examens publiés, etc.) ne sont pas microfilmés.

La reproduction, même partielle, de ce microfilm est soumise à la Loi canadienne sur le droit d'auteur, SRC 1970, c. C-30. Veuillez prendre connaissance des formules d'autorisation qui accompagnent cette thèse.

THIS DISSERTATION
HAS BEEN MICROFILMED
EXACTLY AS RECEIVED

LA THÈSE A ÉTÉ
MICROFILMÉE TELLE QUE
NOUS L'AVONS REÇUE

Canada

NL 339 (r. 88/09)

National Library of Canada / Bibliothèque nationale du Canada

Ottawa, Canada
K1A 0N4

TC –

ISBN 0-315-21255-1

CANADIAN THESES ON MICROFICHE SERVICE – SERVICE DES THÈSES CANADIENNES SUR MICROFICHE

PERMISION TO MICROFILM – AUTORISATION DE MICROFILMER

• Please print or type – Écrire en lettres moulées ou dactylographier

AUTHOR – AUTEUR

Full Name of Author – Nom complet de l'auteur

Robert Wayne King

Date of Birth – Date de naissance
14/06/58

Canadian Citizen – Citoyen canadien
☑ Yes / Oui ☐ No / Non

Country of Birth – Lieu de naissance
Canada

Permanent Address – Résidence fixe
201, 10505-78 Ave
Edmonton, Alberta
T6E 1P3

THESIS – THÈSE

Title of Thesis – Titre de la thèse

Heavy Oil Emulsion Rhedogy

Degree for which thesis was presented
Grade pour lequel cette thèse fut présentée
MSc. Petroleum Engineering

Year this degree conferred
Année d'obtention de ce grade
1985

University – Université
University of Alberta

Name of Supervisor – Nom du directeur de thèse
Donald L. Flock

AUTHORIZATION – AUTORISATION

Permission is hereby granted to the NATIONAL LIBRARY OF CANADA to **microfilm** this thesis and to **lend** or **sell copies of the film.**

The author reserves other publication rights, and neither the thesis nor extensive extracts from it may be printed or otherwise reproduced without the author's written permission.

L'autorisation est, par la présente, accordée à la BIBLIOTHÈQUE NATIONALE DU CANADA de **microfilmer** cette thèse et de **prêter** ou de **vendre des exemplaires du film.**

L'auteur se réserve les autres droits de publication; ni la thèse ni de longs extraits de celle-ci ne doivent être imprimés ou autrement reproduits sans l'autorisation écrite de l'auteur.

ATTACH FORM TO THESIS – VEUILLEZ JOINDRE CE FORMULAIRE À LA THÈSE

Signature
R. W. King

Date
30 January 1985

Canada

THE UNIVERSITY OF ALBERTA

HEAVY OIL EMULSION RHEOLOGY

by

© ROBERT W. KING

A THESIS

SUBMITTED TO THE FACULTY OF GRADUATE STUDIES AND RESEARCH

IN PARTIAL FULFILMENT OF THE REQUIREMENTS FOR THE DEGREE

OF MASTER OF SCIENCE

IN

PETROLEUM ENGINEERING

MINERAL ENGINEERING

EDMONTON, ALBERTA

SPRING 1985

THE UNIVERSITY OF ALBERTA

RELEASE FORM

NAME OF AUTHOR ROBERT W. KING

TITLE OF THESIS HEAVY OIL EMULSION RHEOLOGY

DEGREE FOR WHICH THESIS WAS PRESENTED MASTER OF SCIENCE

YEAR THIS DEGREE GRANTED SPRING 1985

Permission is hereby granted to THE UNIVERSITY OF ALBERTA LIBRARY to reproduce single copies of this thesis and to lend or sell such copies for private, scholarly or scientific research purposes only.

The author reserves other publication rights, and neither the thesis nor extensive extracts from it may be printed or otherwise reproduced without the author's written permission.

(SIGNED) R.W. King

PERMANENT ADDRESS:

201, 10505 - 78 Avenue
Edmonton, Alberta
T6E 1P3

DATED 28 January 1985

THE UNIVERSITY OF ALBERTA

FACULTY OF GRADUATE STUDIES AND RESEARCH

The undersigned certify that they have read, and recommend to the Faculty of Graduate Studies and Research, for acceptance, a thesis entitled HEAVY OIL EMULSION RHEOLOGY submitted by ROBERT W. KING in partial fulfilment of the requirements for the degree of MASTER OF SCIENCE in PETROLEUM ENGINEERING.

.....

Supervisor

.....

.....

.....

Date.....Jan 28/85.....

to Janeen

Abstract

The rheological behavior of stabilized emulsions of dewatered Wainwright B, Epping and Primrose crude oils was examined. With each oil, W/O, O/W, and W/O/W emulsions were created. Each oil exhibited a range of water contents in which no stable emulsions could be produced. As the water content of the emulsions increased, the viscosity of the emulsions increased, reaching a maximum at the boundary between W/O and W/O/W emulsions of Wainwright B. For Epping and Primrose, the maximum viscosity occurred adjacent to the region of unstable emulsions which separates the W/O and W/O/W emulsions. The rheology of each emulsion was examined at four temperatures ranging from 23°C to 75°C and the data was adequately characterized by the power law model. The power law coefficients were observed to be functions of water content, emulsion morphology, oil viscosity, temperature, and the presence of what appear to be natural surfactants. Pseudoplastic behavior was generally observed.

Acknowedgements

Many thanks are extended to Dr. D.L. Flock for his council and support during this study and to Miss C. Crerar for her assistance in gathering some of the data used in this study. I am especially grateful to my wife and to my family, whose generous interest and encouragement were indispensible.

Table of Contents

Chapter		Page
1.	Introduction	1
2.	Emulsion Rheology	6
	2.1 General Developments	6
	2.2 Non-Hydrodynamic Effects	10
	2.2.1 London-van der Waals Forces	10
	2.2.2 Electrostatic Forces	13
	2.2.3 Steric Stabilization	16
	2.2.4 Thermal Influences	18
	2.3 Hydrodynamic Effects	19
	2.3.1 Dispersed Phase Concentration	19
	2.3.2 Particle Shape	20
	2.3.3 Particle Size Distribution	22
	2.3.4 Particle Interactions	24
	2.3.5 Phase Inversion	27
3.	Materials and Methods	30
	3.1 Fluids	30
	3.2 Emulsion Preparation	32
	3.3 Emulsion Examination	34
	3.3.1 Water Content	34
	3.3.2 Classification and Morphology	34
	3.3.3 Particle Size Measurements	34
	3.3.4 Rheometry	38
4.	Results and Discussion	43
	4.1 Water Content and Morphology	43
	4.2 Particle Size Distributions	48
	4.3 Emulsion Rheology	61

5. Conclusions 89
Recommendations 91
Bibliography 92
Appendix A 99
A.1 General Considerations 99
A.2 Theory of Coaxial Cylinder Viscometers 100
A.3 Violation of the Assumptions 105
A.3.1 Fluid Properties 106
A.3.2 Laminar Flow and Circular Streamlines 107
A.3.3 Time-Dependent Effects 109
A.3.4 Wall Adherence Condition 109
A.3.5 Edge and End Effects 109
A.3.6 Viscous Heating 110
A.4 The Haake and Brookfield Viscometers 112
Appendix B 115
Appendix C 194

List of Tables

Table	Description	Page
4.1	Particle size distribution summary for Wainwright B Emulsions	53
4.2	Particle size distribution summary for Epping Emulsions	54
4.3	Particle size distribution summary for Primrose Emulsions	55
B.1	Wainwright B 0.8% (dried) W/O Emulsion Rheology at 22.80 ±0.10°C	116
B.2	Wainwright B 0.8% (dried) W/O Emulsion Rheology at 40.50 ±0.05°C	117
B.3	Wainwright B 0.8% (dried) W/O Emulsion Rheology at 60.00 ±0.05°C	118
B.4	Wainwright B 0.8% (dried) W/O Emulsion Rheology at 79.15 ±0.05°C	118
B.5	Wainwright B 4.8% W/O Emulsion Rheology at 22.65 ±0.05°C	119
B.6	Wainwright B 4.8% W/O Emulsion Rheology at 39.95 ±0.05°C	119
B.7	Wainwright B 4.8% W/O Emulsion Rheology at 59.90 ±0.05°C	120
B.8	Wainwright B 4.8% W/O Emulsion Rheology at 79.45 ±0.05°C	120
B.9	Wainwright B 10.4% W/O Emulsion Rheology at 22.85 ±0.05°C	121
B.10	Wainwright B 10.4% W/O Emulsion Rheology at 40.40 ±0.05°C	121
B.11	Wainwright B 10.4% W/O Emulsion Rheology at 59.05 ±0.05°C	122
B.12	Wainwright B 10.4% W/O Emulsion Rheology at 79.65 ±0.05°C	122
B.13	Wainwright B 18.0% W/O Emulsion Rheology at 23.10 ±0.05°C	123

B.14 Wainwright B 18.0% W/O Emulsion Rheology at 40.10 ±0.05°C 124

B.15 Wainwright B 18.0% W/O Emulsion Rheology at 59.70 ±0.05°C 125

B.16 Wainwright B 18.0% W/O Emulsion Rheology at 79.20 ±0.05°C 125

B.17 Wainwright B 26.5% W/O Emulsion Rheology at 22.80 ±0.15°C 126

B.18 Wainwright B 26.5% W/O Emulsion Rheology at 39.95 ±0.05°C 127

B.19 Wainwright B 26.5% W/O Emulsion Rheology at 59.00 ±0.05°C 128

B.20 Wainwright B 26.5% W/O Emulsion Rheology at 79.15 ±0.05°C 129

B.21 Wainwright B 28.0% W/O/W Emulsion Rheology at 24.70 ±0.05°C 130

B.22 Wainwright B 28.0% W/O/W Emulsion Rheology at 40.90 ±0.30°C 131

B.23 Wainwright B 28.0% W/O/W Emulsion Rheology at 59.25 ±0.10°C 132

B.24 Wainwright B 28.0% W/O/W Emulsion Rheology at 78.20 ±0.05°C 132

B.25 Wainwright B 34.4% W/O/W Emulsion Rheology at 22.75 ±0.05°C 133

B.26 Wainwright B 34.4% W/O/W Emulsion Rheology at 39.50 ±0.05°C 134

B.27 Wainwright B 34.4% W/O/W Emulsion Rheology at 59.70 ±0.05°C 135

B.28 Wainwright B 34.4% W/O/W Emulsion Rheology at 79.20 ±0.05°C 136

B.29 Wainwright B 42.0% W/O/W Emulsion Rheology at 22.95 ±0.05°C 137

B.30 Wainwright B 42.0% W/O/W Emulsion Rheology at 40.55 ±0.05°C 138

B.31 Wainwright B 42.0% W/O/W Emulsion Rheology at 60.00 ±0.05°C 139

B.32 Wainwright B 42.0% W/O/W Emulsion Rheology at 79.50 ±0.05°C 140

B.33 Wainwright B 46.4% W/O/W Emulsion Rheology at 22.60 ±0.10°C 141

B.34 Wainwright B 46.4% W/O/W Emulsion Rheology at 40.15 ±0.10°C 142

B.35 Wainwright B 46.4% W/O/W Emulsion Rheology at 59.25 ±0.15°C 143

B.36 Wainwright B 46.4% W/O/W Emulsion Rheology at 79.60 ±0.10°C 143

B.37 Wainwright B 54.0% W/O/W Emulsion Rheology at 22.90 ±0.10°C 144

B.38 Wainwright B 54.0% W/O/W Emulsion Rheology at 40.00 ±0.10°C 144

B.39 Wainwright B 54.0% W/O/W Emulsion Rheology at 60.00 ±0.10°C 145

B.40 Wainwright B 54.0% W/O/W Emulsion Rheology at 79.00 ±0.10°C 145

B.41 Wainwright B 95.6% O/W Emulsion Rheology at 23.90 ±0.05°C 146

B.42 Wainwright B 95.6% O/W Emulsion Rheology at 39.70 ±0.10°C 146

B.43 Wainwright B 95.6% O/W Emulsion Rheology at 59.30 ±0.10°C 147

B.44 Wainwright B 95.6% O/W Emulsion Rheology at 79.10 ±0.15°C 147

B.45 Wainwright B 97.6% O/W Emulsion Rheology at 22.20 ±0.10°C 148

B.46 Wainwright B 97.6% O/W Emulsion Rheology at 40.30 ±0.10°C 148

B.47 Wainwright B 97.6% O/W Emulsion Rheology at 59.60 ±0.10°C 149

B.48 Wainwright B 97.6% O/W Emulsion Rheology at 74.50 ±0.20°C 149

B.49 Epping 0.9% (dried) W/O Emulsion Rheology at 23.05 ±0.05°C 150

B.50 Epping 0.9% (dried) W/O Emulsion Rheology at 40.55 ±0.10°C 150

B.51 Epping 0.9% (dried) W/O Emulsion Rheology at 59.80 ±0.05°C 151

B.52 Epping 0.9% (dried) W/O Emulsion Rheology at 79.35 ±0.10°C 152

B.53 Epping 14.4% W/O Emulsion Rheology at 23.80 ±0.20°C 153

B.54 Epping 14.4% W/O Emulsion Rheology at 37.00 ±0.20°C 153

B.55 Epping 14.4% W/O Emulsion Rheology at 58.00 ±0.20°C 154

B.56 Epping 14.4% W/O Emulsion Rheology at 74.00 ±0.20°C 154

B.57 Epping 17.0% W/O Emulsion Rheology at 22.30 ±0.10°C 155

B.58 Epping 17.0% W/O Emulsion Rheology at 38.80 ±0.10°C 155

B.59 Epping 17.0% W/O Emulsion Rheology at 57.50 ±0.10°C 156

B.60 Epping 17.0% W/O Emulsion Rheology at 73.00 ±0.50°C 156

B.61 Epping 20.0% W/O Emulsion Rheology at 24.40 ±0.10°C 157

B.62 Epping 20.0% W/O Emulsion Rheology at 40.00 ±0.15°C 157

B.63 Epping 20.0% W/O Emulsion Rheology at 60.60 ±0.15°C 158

B.64 Epping 20.0% W/O Emulsion Rheology at 76.00 ±0.50°C 158

B.65 Epping 20.4% W/O Emulsion Rheology at 23.40 ±0.10°C 159

B.66 Epping 20.4% W/O Emulsion Rheology at 40.00 ±0.15°C 159

B.67 Epping 20.4% W/O Emulsion Rheology at 57.90 ±0.20°C 160

B.68 Epping 20.4% W/O Emulsion Rheology at 75.00 ±0.20°C 160

B.69 Epping 43.2% W/O/W Emulsion Rheology at 22.50 ±0.10°C 161

B.70 Epping 43.2% W/O/W Emulsion Rheology at 39.50 ±0.50°C 161

B.71 Epping 43.2% W/O/W Emulsion Rheology at 59.90 ±0.50°C 162

B.72 Epping 53.2% W/O/W Emulsion Rheology at 22.90 ±0.10°C 163

B.73 Epping 53.2% W/O/W Emulsion Rheology at 39.80 ±0.10°C 163

B.74 Epping 53.2% W/O/W Emulsion Rheology at 59.20 ±0.10°C 164

B.75 Epping 64.0% W/O/W Emulsion Rheology at 22.60 ±0.10°C 165

B.76 Epping 64.0% W/O/W Emulsion Rheology at 40.00 ±0.10°C 165

B.77 Epping 64.0% W/O/W Emulsion Rheology at 59.80 ±0.10°C 165

B.78 Epping 66.8% W/O/W Emulsion Rheology at 21.60 ±0.10°C 166

B.79 Epping 66.8% W/O/W Emulsion Rheology at 38.00 ±0.20°C 166

B.80 Epping 66.8% W/O/W Emulsion Rheology at 59.70 ±0.20°C 166

B.81 Epping 70.4% W/O/W Emulsion Rheology at 22.65 ±0.05°C 167

B.82 Epping 70.4% W/O/W Emulsion Rheology at 39.75 ±0.10°C 167

B.83 Epping 70.4% W/O/W Emulsion Rheology at 59.30 ±0.10°C 168

B.84 Epping 70.4% W/O/W Emulsion Rheology at 75.50 ±0.10°C 168

B.85 Epping 96.8% O/W Emulsion Rheology at 23.80 ±0.10°C 169

B.86 Epping 96.8% O/W Emulsion Rheology at 39.00 ±0.20°C 169

B.87 Epping 96.8% O/W Emulsion Rheology at 59.40 ±0.20°C 170

B.88 Epping 96.8% O/W Emulsion Rheology at 75.40 ±0.20°C 170

B.89 Epping 98.0% O/W Emulsion Rheology at 25.20 ±0.10°C 171

B.90 Epping 98.0% O/W Emulsion Rheology at 39.70 ±0.20°C 171

B.91 Epping 98.0% O/W Emulsion Rheology at 60.00 ±0.20°C 172

B.92 Epping 98.0% O/W Emulsion Rheology at 74.50 ±0.20°C 172

B.93 Epping 98.4% O/W Emulsion Rheology at 22.65 ±0.10°C 173

B.94 Epping 98.4% O/W Emulsion Rheology at 39.75 ±0.10°C 173

B.95 Epping 98.4% O/W Emulsion Rheology at 59.30 ±0.10°C 174

B.96 Epping 98.4% O/W Emulsion Rheology at 75.60 ±0.10°C 174

B.97 Primrose 3.6% (dried) W/O Emulsion Rheology at 22.00 ±0.10°C 175

B.98 Primrose 3.6% (dried) W/O Emulsion Rheology at 40.00 ±0.20°C 175

B.99 Primrose 3.6% (dried) W/O Emulsion Rheology at 59.60 ±0.50°C 175

B.100 Primrose 22.8% W/O Emulsion Rheology at 23.80 ±0.10°C 176

B.101 Primrose 22.8% W/O Emulsion Rheology at 44.80 ±0.20°C 176

B.102 Primrose 22.8% W/O Emulsion Rheology at 54.20 ±0.20°C 177

B.103 Primrose 22.8% W/O Emulsion Rheology at 62.00 ±0.20°C 177

B.104 Primrose 32.0% W/O Emulsion Rheology at 22.80 ±0.10°C 178

B.105 Primrose 32.0% W/O Emulsion Rheology at 43.20 ±0.20°C 178

B.106 Primrose 32.0% W/O Emulsion Rheology at 53.50 ±0.20°C 179

B.107 Primrose 32.0% W/O Emulsion Rheology at 64.00 ±0.30°C 179

B.108 Primrose 44.8% W/O/W Emulsion Rheology at 22.00 ±0.10°C 180

B.109 Primrose 44.8% W/O/W Emulsion Rheology at 44.00 ±0.20°C 180

B.110 Primrose 44.8% W/O/W Emulsion Rheology at 56.00 ±0.20°C 181

B.111 Primrose 44.8% W/O/W Emulsion Rheology at 63.50 ±0.50°C 181

B.112 Primrose 48.0% W/O/W Emulsion Rheology at 22.00 ±0.10°C 182

B.113 Primrose 48.0% W/O/W Emulsion Rheology at 43.50 ±0.10°C 182

B.114 Primrose 48.0% W/O/W Emulsion Rheology at 52.00 ±0.20°C 183

B.115 Primrose 48.0% W/O/W Emulsion Rheology at 64.00 ±0.30°C 183

B.116 Primrose 62.4% W/O/W Emulsion Rheology at 22.50 ±0.10°C 184

B.117 Primrose 62.4% W/O/W Emulsion Rheology at 42.00 ±0.10°C 184

B.118 Primrose 62.4% W/O/W Emulsion Rheology at 56.00 ±0.20°C 184

B.119 Primrose 62.4% W/O/W Emulsion Rheology at 66.00 ±0.30°C 184

B.120 Primrose 64.4% W/O/W Emulsion Rheology at 22.80 ±0.10°C 185

B.121 Primrose 64.4% W/O/W Emulsion Rheology at 44.50 ±0.10°C 185

B.122 Primrose 64.4% W/O/W Emulsion Rheology at 55.00 ±0.20°C 186

B.123 Primrose 64.4% W/O/W Emulsion Rheology at 64.50 ±0.30°C 186

B.124 Primrose 78.5% O/W Emulsion Rheology at 23.50 ±0.10°C 187

B.125 Primrose 78.5% O/W Emulsion Rheology at 41.50 ±0.10°C 187

B.126 Primrose 78.5% O/W Emulsion Rheology at 51.50 ±0.20°C 187

B.127 Primrose 78.5% O/W Emulsion Rheology at 60.50 ±0.30°C 187

B.128 Primrose 82.4% O/W Emulsion Rheology at 23.00 ±0.10°C 188

B.129 Primrose 82.4% O/W Emulsion Rheology at 41.50 ±0.10°C 188

B.130 Primrose 82.4% O/W Emulsion Rheology at 50.10 ±0.20°C 188

B.131 Primrose 82.4% O/W Emulsion Rheology at 60.00 ±0.20°C 188

B.132 Primrose 88.8% O/W Emulsion Rheology at 22.00 ±0.10°C 189

B.133 Primrose 88.8% O/W Emulsion Rheology at 44.00 ±0.10°C 189

B.134 Primrose 88.8% O/W Emulsion Rheology at 51.00 ±0.10°C 190

B.135 Primrose 88.8% O/W Emulsion Rheology at 60.00 ±0.10°C 190

B.136 Primrose 95.2% O/W Emulsion Rheology at 22.80 ±0.10°C 191

B.137 Primrose 95.2% O/W Emulsion Rheology at 45.00 ±0.10°C 191

B.138 Primrose 95.2% O/W Emulsion Rheology at 55.00 ±0.20°C 192

B.139 Primrose 95.2% O/W Emulsion Rheology at 65.00 ±0.20°C 192

B.140 Primrose 98.6% O/W Emulsion Rheology at 23.00 ±0.10°C 193

B.141 Primrose 98.6% O/W Emulsion Rheology at 45.00 ±0.10°C 193

B.142 Primrose 98.6% O/W Emulsion Rheology at 55.00 ±0.20°C 193

B.143 Primrose 98.6% O/W Emulsion Rheology at 64.20 ±0.20°C 193

C.1 Wainwright B 0.8% W/O Emulsion Primary Distribution.....195

C.2 Wainwright B 4.8% W/O Emulsion Primary Distribution.....195

C.3 Wainwright B 10.4% W/O Emulsion Primary Distribution.....196

C.4 Wainwright B 18.0% W/O Emulsion Primary Distribution.....196

C.5 Wainwright B 26.5% W/O Emulsion Primary Distribution.....197

C.6 Wainwright B 28.0% W/O/W Emulsion Primary Distribution.....198

C.7 Wainwright B 28.0% W/O/W Emulsion Secondary Distribution.....198

C.8 Wainwright B 34.4% W/O/W Emulsion Primary Distribution.....199

C.9 Wainwright B 34.4% W/O/W Emulsion Secondary Distribution.....199

C.10 Wainwright B 46.4% W/O/W Emulsion Primary Distribution.....200

C.11 Wainwright B 46.4% W/O/W Emulsion Secondary Distribution.....200

C.12 Wainwright B 54.0% W/O/W Emulsion Primary Distribution.....201

C.13 Wainwright B 54.0% W/O/W Emulsion Secondary Distribution.....201

C.14 Wainwright B 95.6% O/W Emulsion Primary Distribution.....202

C.15 Wainwright B 97.6% O/W Emulsion Primary Distribution.....203

C.16 Epping 0.9% W/O Emulsion Primary Distribution.....204

C.17 Epping 14.4% W/O Emulsion Primary Distribution.....204

C.18 Epping 17.0% W/O Emulsion Primary Distribution.....205

C.19 Epping 20.0% W/O Emulsion Primary Distribution.....206

C.20 Epping 20.4% W/O Emulsion Primary Distribution.....206

C.21 Epping 43.2% W/O/W Emulsion Primary Distribution....207

C.22 Epping 43.2% W/O/W Emulsion Secondary Distribution.....207

C.23 Epping 53.2% W/O/W Emulsion Primary Distribution....208

C.24 Epping 53.2% W/O/W Emulsion Secondary Distribution.....208

C.25 Epping 64.0% W/O/W Emulsion Primary Distribution....209

C.26 Epping 64.0% W/O/W Emulsion Secondray Distribution.....210

C.27 Epping 66.8% W/O/W Emulsion Primary Distribution....211

C.28 Epping 66.8% W/O/W Emulsion Secondary Distribution.....212

C.29 Epping 70.4% W/O/W Emulsion Primary Distribution....213

C.30 Epping 70.4% W/O/W Emulsion Secondary Distribution.....213

C.31 Epping 96.8% O/W Emulsion Primary Distribution.....214

C.32 Epping 98.0% O/W Emulsion Primary Distribution.....214

C.33 Epping 98.4% O/W Emulsion Primary Distribution.....215

C.34 Primrose 3.6% W/O Emulsion Primary Distribution.....216

C.35 Primrose 22.8% W/O Emulsion Primary Distribution....217

C.36 Primrose 32.0% W/O Emulsion Primary Distribution....218

C.37 Primrose 44.8% W/O/W Emulsion Primary Distribution.....219

C.38 Primrose 44.8% W/O/W Emulsion Secondary Distribution.....220

C.39 Primrose 48.2% W/O/W Emulsion Primary Distribution.....221

C.40 Primrose 48.2% W/O/W Emulsion Secondary Distribution.....222

C.41 Primrose 62.4% W/O/W Emulsion Primary Distribution.....223

C.42 Primrose 62.4% W/O/W Emulsion Secondary Distribution.....224

C.43 Primrose 64.4% W/O/W Emulsion Primary Distribution.....225

C.44 Primrose 64.4% W/O/W Emulsion Secondary Distribution.....225

C.45 Primrose 78.5% O/W Emulsion Primary Distribution....226

C.46 Primrose 82.4% O/W Emulsion Primary Distribution....226

C.47 Primrose 88.8% O/W Emulsion Primary Distribution....227

C.48 Primrose 95.2% O/W Emulsion Primary Distribution....228

C.49 Primrose 98.6% O/W Emulsion Primary Distribution....229

List of Figures

Figure	Description	Page
2.1	Newtonian and non-Newtonian relationships between the shearing rate and the shear stress	8
2.2	Schematic of particle collisions and possible outcomes	11
2.3	Particle interaction potential energy curve as described by the DLVO theory	15
4.1	Emulsion Morphology	45
4.2	Typical droplet size distribution	50
4.3	Geometric mean droplet diameters for Wainwright B emulsions	56
4.4	Geometric mean droplet diameters for Epping emulsions	57
4.5	Geometric mean droplet diameters for Primrose emulsions	58
4.6	Viscosity as a function of water content and shear rate for Wainwright B emulsions at 23°C	62
4.7	Viscosity as a function of water content and shear rate for Wainwright B emulsions at 40°C	66
4.8	Viscosity as a function of water content and shear rate for Wainwright B emulsions at 60°C	67
4.9	Viscosity as a function of water content and shear rate for Wainwright B emulsions at 79°C	68
4.10	Viscosity as a function of water content and shear rate for Epping emulsions at 23°C	69
4.11	Viscosity as a function of water content and shear rate for Epping emulsions at 40°C	71
4.12	Viscosity as a function of water content and shear rate for Epping emulsions at 60°C	72
4.13	Viscosity as a function of water content and shear rate for Epping emulsions at 75°C	73
4.14	Viscosity as a function of water content and shear rate for Primrose emulsions at 23°C	75

4.15 Viscosity as a function of water content and shear rate for Primrose emulsions at 43°C.....76

4.16 Viscosity as a function of water content and shear rate for Primrose emulsions at 53°C.....77

4.17 Viscosity as a function of water content and shear rate for Primrose emulsions at 63°C.....78

4.18 Shear thinning index as a function of temperature and water content for Wainwright B emulsions.....80

4.19 Shear thinning index as a function of temperature and water content for Epping emulsions.....81

4.20 Shear thinning index as a function of temperature and water content for Primrose emulsions.....82

4.21 Consistency index as a function of temperature and water content for Wainwright B emulsions.....84

4.22 Consistency index as a function of temperature and water content for Epping emulsions.....85

4.23 Consistency index as a function of temperature and water content for Primrose emulsions.....86

A.1 Schematic of the concentric cylinder viscometer.....101

List of Plates

Plate	Description	Page
4.1	Typical dual emulsion	49

Nomenclature

h - effective viscometer bob length (cm)

N - total number of particles sampled (-)

n - power law flow behavior index (-)

n_s, n_t - viscometer controller set and true angular bob speed (rpm)

R_1, R_2 - radii of inner (bob) and outer (cup) cylinders, respectively (cm)

Re - Reynolds number

S - viscometer dial reading (percentage of full scale torque)

T - temperature (°C)

x_m - geometric mean diameter (microns)

x_i - average particle diameter of a given size interval (microns)

$\dot{\gamma}$ - shearing rate (s^{-1})

ϵ - ratio of the shear stress at the cup wall to the shear stress at the bob surface (-)

η - apparent viscosity, or just viscosity (cP)

η_0 - continuous phase viscosity (cP)

κ - shear thinning index, or inverse flow behavior index (-)

ξ - power law consistency index (dyne·s^n/cm^2)

ρ - density (g/cm^3)

σ - geometric standard deviation

τ - shear stress (dynes/cm^2)

ϕ - volume fraction of the dispersed phase (-)

Ψ - torque (dyne·cm)

Ω - angular velocity of the bob (s^{-1})

$\omega(r)$ - local angular velocity (s^{-1})

1. Introduction

In the petroleum industry, fluid suspensions, and in particular, emulsions, are often encountered. They occur during production operations, are being considered for enhanced recovery techniques, have been proposed as a possible system for pipeline transportation of very viscous crudes, and have been investigated as potential fracturing fluids. Except for flow through porous media, when the suspended particles are of similar size as the flow channels, the scale of these flows is much larger than that of the suspended particles. For these larger scale systems, the heterogeneous suspension behaves like an effectively homogeneous continuum, the bulk suspension.

Such flow behavior can be dealt with on a variety of levels, as indicted by Napper and Hunter (1975): these range from formal mathematical approaches which examine the time evolution of the stress-strain tensor in terms of the properties of the material, to purely empirical correlations between parameters related to the applied stress and to the rate of strain. Within this latter method, two approaches are evident. The microrheological approach, which attempts to establish the detailed behavior of particles of various shapes in response to hydrodynamical forces, has been extensively developed by Mason and various collaborators; see, for example, Goldsmith and Mason (1962), Zia, Cox, and Mason (1966), and Takano, Goldsmith, and Mason (1966, 1969). The macrorheological approach establishes a theoretical

relationship between viscosity and shear rate or between shear stress and shear rate.

Early studies of suspensions sought only to identify an effective viscosity. Such analyses began with Einstein (1906): his theoretical development was restricted to an infinitely dilute suspension of small rigid spherical particles and was free of externally applied forces. Under these conditions the particles behave as individuals and their only response is to rotate passively with the bulk vorticity and to resist the bulk straining. Such resistance leads to an increased dissipation of energy, which may be measured as an increase in viscosity. This is a function of the volume fraction of the suspended particles only. Alternatively, Landau and Lifshitz (1959) found the full bulk stress tensor by applying an ensemble average to the randomly varying stress tensor defined at the microscopic particle level.

Although studies of idealized suspensions should suggest new forms of constitutive equations, and thus provide a means by which different physical phenomena are isolated, such derivations often demand severe idealizations. But, engineering problems concerning complex crude oil-water (brine) systems are beyond the validity of the idealized approaches. In each of the situations indicated earlier, the rheological behavior of the emulsions must be known. For example, the energy requirements for pipelining may be deduced if the viscosity of the emulsion

is known; produced emulsions may be broken if the nature of emulsion formation and stability is understood. Therefore, phenomenological models, based in macrorheology, must be considered.

The rheology of emulsions falls in the general theoretical area of the rheology of disperse systems, and is complicated by the liquid nature of the disperse phase and by the mechanics of the interface. Suspensions of particles derive many of their properties from the same physical and chemical forces responsible for the stability of true colloidal systems.

To reconcile the net macroscopic effect of the physical and chemical phenomena controlling emulsion formation and stability, Flock (1977) examined the dependence of these properties as a fuction of crude oil pH, total acid number, average molecular weight, asphaltene content, viscosity, density, API gravity, conductivity, BS&W, water content, surface tension, and interfacial tension of several crude oils and their produced waters. Results suggest that three parameters are primarily responsible for their behavior: crude oil viscosity, total acid number, and asphaltene content. Flock proposed four hypothetical emulsion classifications, those of:

1. very viscous crudes, containing very high concentrations of asphaltenes and resinous acids.
2. viscous crudes with fairly high concentrations of asphaltenes and resinous acids.

3. moderately viscous crudes with intermediate concentrations of asphaltenes and resinous acids.
4. low viscosity crudes with low concentrations of asphaltenes and/or resinous acids

Crudes from group one (eg. Athabasca bitumen) generally will not form emulsions at room temperature because of their high viscosity, while crudes from group four (eg. Bonnie Glen) also will not form emulsions because of their low natural surfactant content. Crude oils such as Wainwright and Chauvin, from group three, readily form stable emulsions.

However, if an artificial surfactant is employed, stable emulsions of crude oils from each category can be created. The rheology of these stabilized emulsions is of interest since it is governed by the same factors controlling emulsion stability.

This investigation includes the examination of the rheological behavior of stabilized emulsions of Primrose, Epping and Wainwright B crude oils, from categories one, two, and three respectively, as a function of dispersed phase content, morphology, droplet size distribution, shearing rate, and temperature. To better understand the possible interrelationships among the variables, the underlying principles of the forces governing emulsion behavior were surveyed, and are discussed in Chapter 2.

By the nature of this study, the results are not of direct engineering utility. Instead, an attempt has been made to characterize the behavior of different emulsions of

heavy crude oils and only the broad outlines of consistent behavior have been investigated and identified. Similar investigations with other oils, waters, and surfactants will eventually provide a coherent picture of the behavior of the crude oil emulsions encountered in the petroleum industry.

2. Emulsion Rheology

2.1 General Developments

The rheological behavior of fluids may be adequately described by a collective property such as viscosity. As a generic term, it groups together the combined effects of many physical and chemical forces operating at the molecular level, and extending to several microns.

Simplest among flow types is Newtonian flow. Solutions and single phase fluids composed of moderately large molecules or ions, (Einstein 1926; Bird et al. 1960) exhibit Newtonian behavior: the viscosity remains constant up to very high flow rates and the rheology may be described by classical hydrodynamic theory.

For such fluids (regarded as a continuum) the internal frictional resistance to flow, the viscosity, is the ratio of the applied shearing stress to the rate of shear. Van Wazer et al. (1963) distinguishes between a differential viscosity and an apparent viscosity. Consider an infinitesimally thin layer of fluid confined between two planes of infinite extent. The tangential force per unit area (the stress, τ) causes one plane to move with respect to the other, imposing simple laminar flow on the fluid layer. The velocity gradient in the fluid is the rate of shear, $\dot{\gamma}$, and the differential viscosity is therefore $\eta_d = \delta\tau/\delta\dot{\gamma}$. This is just the slope at a given point of a stress versus shear rate curve. The more usual definition

of viscosity (and the one used in this study) is the ratio of the shearing stress per unit area to a unit velocity gradient normal to this area. This is the apparent viscosity and is just the slope of the line joining the origin to a given point of the stress versus shear rate curve. In Figure 2.1, typical shear stress - shear rate curves are illustrated. For the non-Newtonian curves, a representative apparent viscosity is shown by the dashed line.

For Newtonian fluids the apparent and differential viscosity are equivalent; for a non-Newtonian fluid, the apparent viscosity represents the viscosity of an equivalent Newtonian fluid exhibiting the same resistance to flow at the chosen shear rate.

In 1906, Einstein determined the viscosity of an infinitely dilute suspension of neutrally bouyant spheres in an incompressible Newtonian fluid. He considered that the spheres were much larger than the molecules of the fluid (but much smaller than the dimensions of the viscometer) and that only hydrodynamic forces were present. Such suspensions exhibit Newtonian behavior, with the viscosity being expressed in terms of the viscosity of the suspending fluid, η_o, and the fractional volume content of the spheres, ϕ:

$$\eta = \eta_o(1 + 2.5\phi) \qquad (2.1)$$

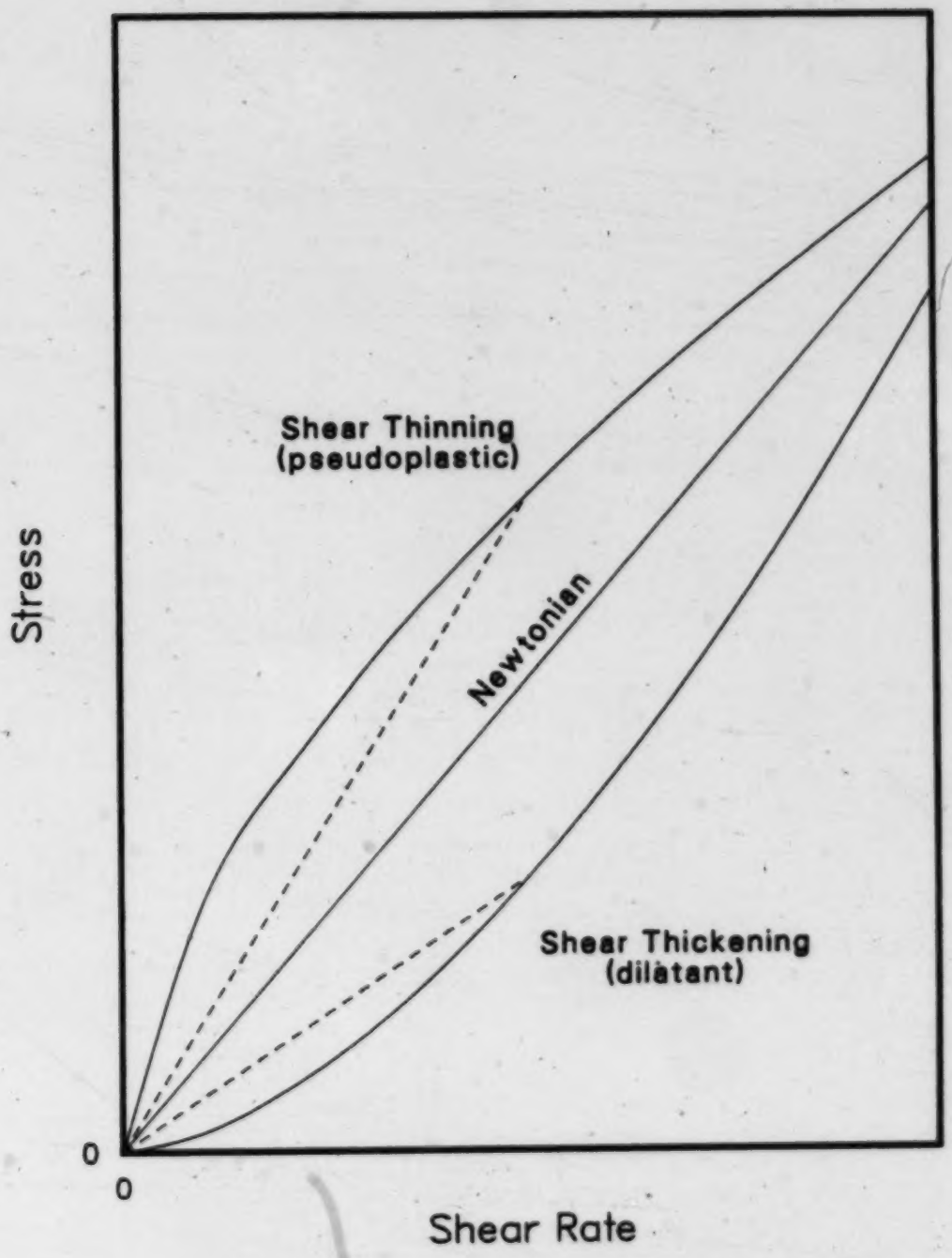

Figure 2.1. Newtonian and non-Newtonian relationships between the shearing rate and the shearing stress. The apparent viscosity is illustrated for the Non-Newtonian curves (------).

Beyond fractional volume contents of about 0.03, equations such as (2.1) are not valid principally because at greater concentrations, the disturbances to the local flow streamlines caused by individual particles cannot be considered separately.

Accordingly, Einstein's equation has been modified to account for higher concentrations but only with moderate success. Guth and Simha (1936) included a quadratic term, ϕ^2, with the subsequent equation being valid for fractional volume contents of less than about 0.06. Oliver and Ward (1953) developed a similar model for suspensions of rigid spheres of varying diameter, valid for concentrations up to 0.20.

The non-Newtonian behavior of concentrated suspensions, and of emulsions generally, arises from the interactions of the particles, interactions of the particles with the continuous phase, and the response of the fluid particles. The factors which influence the rheological behavior of emulsions and suspensions have been identified, but their interrelationships are not well understood. Thus, to date there are no hypotheses comprising more than a few of these factors, and none which can adequately predict rheological behavior.

These factors may be broadly grouped as hydrodynamic and non hydrodynamic influences. Hydrodynamic forces determine if and when particles will interact under shearing stresses, but it is the non-hydrodynamic factors that govern

the destiny of such interactions and hence, the rheological behavior (and stability) of dispersions. Figure 2.2 illustrates how particle collisions, induced hydrodynamically or non-hydrodynamically, are controlled by non-hydrodynamic forces. These forces may cause the particles to separate or remain together. They will also determine if the particles or aggregates are disrupted under the influence of shear. Such interactions will determine the rheological behavior of the emulsion; hence, each of these factors must be considered for its unique influence.

2.2 Non-Hydrodynamic Effects

The forces responsible for non-Newtonian behavior consist of the London-van der Waals forces, electrostatic forces, and steric stabilization. Furthermore, temperature will affect the particle interactions in two ways: Brownian motion and modification of the dispersion forces.

2.2.1 London-van der Waals Forces

Until the advent of quantum mechanics, molecules were regarded as hard objects without long range influence. This simplified approach was successfully applied by van der Waals who recognized the importance of molecular size and intermolecular forces in determining the pressure of a gas (Castellan 1971).

In 1930, London was able to explain the intermolecular attraction of non-polar molecules. Averaged in time, the

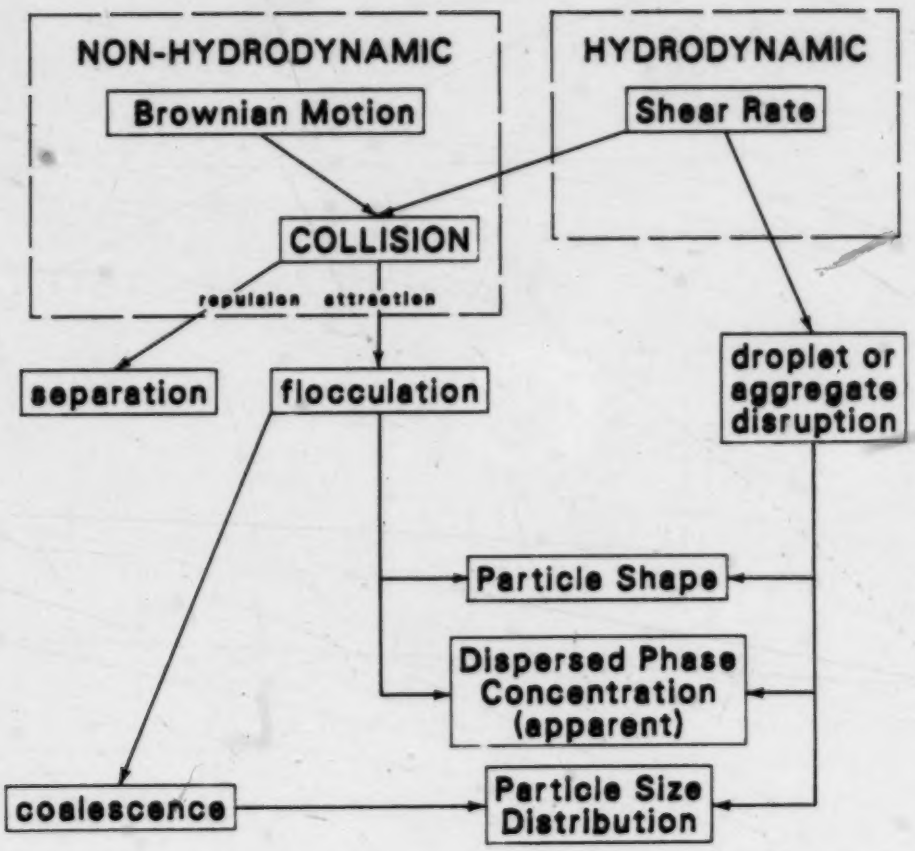

Figure 2.2. Flow diagram of particle interactions and possible results under the influence of hydrodynamic and non-hydrodynamic factors.

molecule or atom has no permanent dipole moment, but it does possess an instantaneous dipole which is randomly oriented. If two such atoms are close together, their electronic motions become synchronized. This results in an attractive force.

De Boer (1936) and Hamaker (1937) used this principle to calculate the attractive force between rigid spherical particles composed of the same material. By assuming pairwise additivity of this dispersion force, they demonstrated that although the range of the force was of atomic dimensions, the summed effect of all the constituent atoms or molecules results in an interaction range of colloidal dimensions. Hamaker also found that the interaction energy is strongly dependent upon the size of the smaller particle: if the size of the particles is scaled by some factor and their separation (shortest surface to surface distance) is also scaled by the same factor, the energy remains unchanged.

The relative importance of this attractive force is strongly affected by distortion of liquid droplets at close separation, by the presence of electrolytes in the intervening phase (Overbeek 1966), and by polymeric molecules adsorbed at the particle surface (or droplet interface). Mahanty and Ninham (1976) and Tabor (1976) summarized the limitations of Hamaker's approach, including the more general considerations of Lifshitz (1956), indicating the theory still needs to consider many-body

effects, the presence of permanent dipoles and free ions, and the borderline area between dispersion forces and chemical bonds.

2.2.2 Electrostatic Forces

The repulsive electrostatic force arises from the double layer of ionic charges surrounding the colloidal particle. In the ideal case, the monolayer of ions next to the surface of the particle have opposite charge to the charge of the particle; it is called the Stern layer. An outer diffuse atmosphere of ions whose charge is predominantly of sign opposite to the charge on the particle also surrounds the particles; it is called the Gouy or Debye-Hückle layer. Together these two layers are called the double layer and exhibit two electroviscous effects.

The first electroviscous effect is due to the resistance of the ionic atmosphere to deformation caused by the shearing flow. Stokes and Mills (1965) explained that the interionic attraction and thermal movements will tend to restore the more stable equilibrium distribution (spherically symmetric). The result is an ellipsoidal distribution with the restoring force acting as a viscous energy sink, contributing to an increase in the viscosity of the system. The second electroviscous effect arises from the overlap of double layers of adjacent particles. Although the double layers of like particles are always repulsive, the coulombic repulsion must compete with the

dispersion forces.

Derjaguin and Landau (1941), and Vervey and Overbeek (1948) independently considered the combined influence of the dispersion and coulombic interaction forces; the result was the DLVO theory (after Derjaguin, Landau, Verwey, and Overbeek). Whereas the London-van der Waals force decays as an inverse function of the particle separation, the electrostatic force falls off exponentially with separation. The resultant potential energy of interaction curve generally exhibits both minima and maxima (see Figure 2.3; recall that a positive potential energy is an unfavorable configuration, resulting in repulsion, and that negative potential energy results in attraction). With reference to Figure 2.3, note that at large particle separations, the interaction potential energy is essentially zero. As the distance between the particles decreases, the strength of the dispersion force increases until at some moderate distance, the effect of coulombic repulsion becomes influential. At this distance, the balance of the attractive and repulsive forces yields a shallow minimum, the secondary minimum. As the separation decreases further, the repulsive force increases in strength, resulting in the primary maximum. At very small separations, the dispersion force again dominates (primary minimum), until Born repulsion' becomes dominant. The depth and position of the secondary minimum depends on the balance of repulsive and

---

'Born repulsion arises from the apparent rigidity of atoms. This is due to the mutual repulsion of the electron clouds.

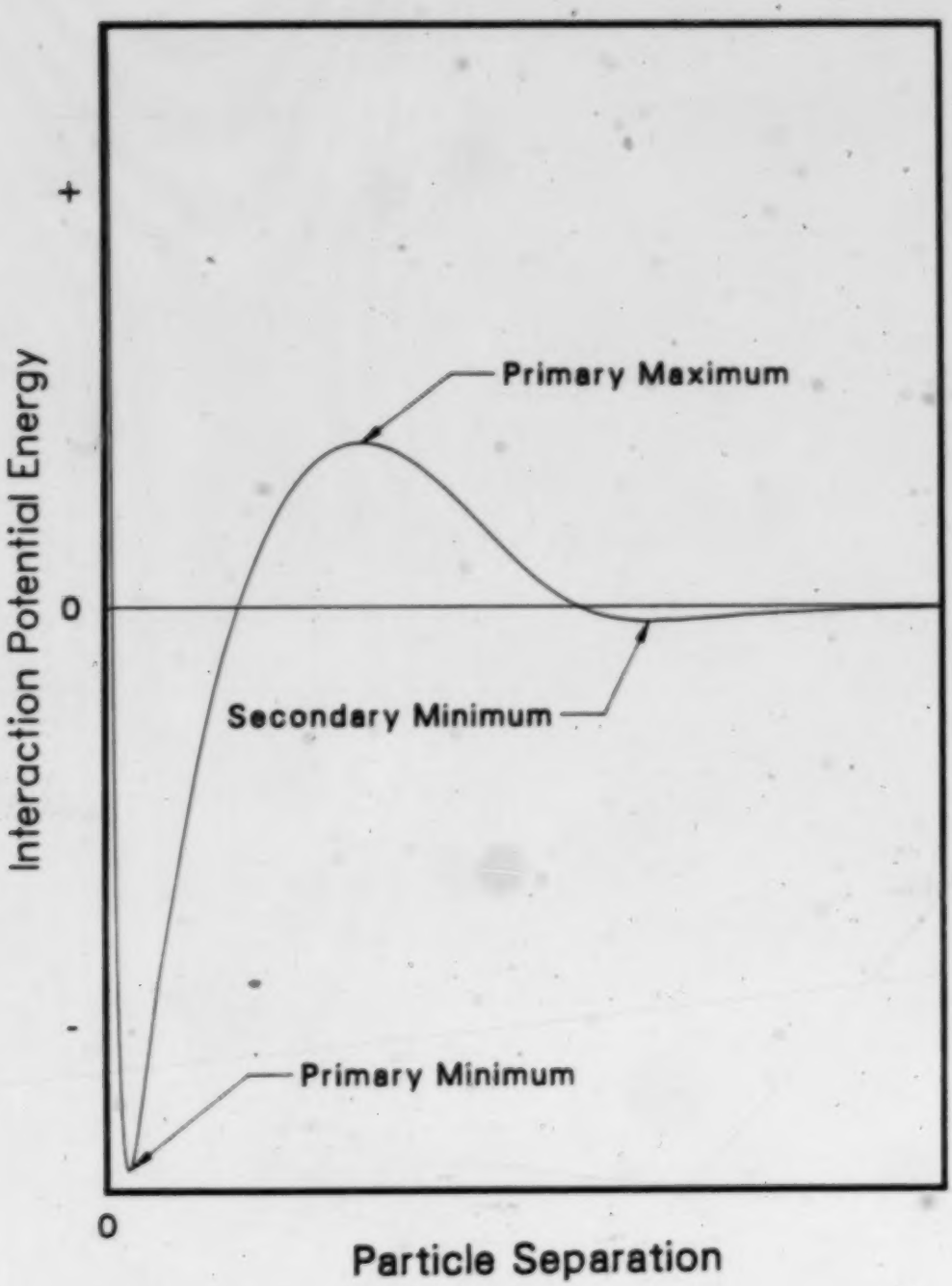

Figure 2.3. Particle interaction potential energy curve as described by the DLVO theory.

attractive forces in the system and is, in part, responsible for the stability and structure of some colloidal systems.

The secondary minimum may result in reversible aggregation of the particles. Since the particles prefer to remain in the shallow potential well, the viscosity of the dispersion is increased. Trapped between the particles is a small amount of the suspended medium, and since this fluid is immobilized, the effective dispersed phase content of the dispersion is increased, resulting in non-Newtonian behavior of W/O (water-in-oil) emulsions (van den Temple 1963). However, de Vries (1963) states that if the shearing rate imposed on the dispersion is sufficiently high, the flocculated particles will be redispersed, resulting in decreasing viscosity with increasing shear.

Israelichvili and Ninham (1977) discussed an alternative source of colloidal stability: the particles may be situated at a separation where repulsive forces dominate, but the system is still ordered and stable because the particles are confined by the finite size of the dispersion. This ordered state may be either a one phase system, such as in an O/W (oil-in-water) emulsion, or a two phase system, such as occurs when a mixture of two immiscible fluids completely separates.

2.2.3 Steric Stabilization

Steric stabilization is a term that encompasses all aspects of stabilizing mechanisms involving adsorbed

non-ionic macromolecules. The stabilization of emulsions requires a surface active agent which is often a poly(ethylene oxide) surfactant (Shaw 1980). These nonionic molecules are oriented at the interface since they have a lyophobic part which strongly imbeds itself in the aqueous phase, and have a long lyophilic part that trails freely in the oleic phase. The size and orientation of the polymer acts as a physical barrier to close approaches of dispersed particles and acts independently of the double layer interaction.

Steric interactions may be attractive or repulsive when two particles collide (Shaw 1980). If the dispersion medium is a good solvent for the lyophilic ends of the polymer, interpenetration of the trailing ends is not favoured and repulsion results. If the dispersing medium is a poor solvent, interpenetration is favoured and attraction results. The polymer tails may further interpenetrate until elastic repulsion, due to the tension between adjacent molecules, stops the process.

The presence of steric stabilizers causes the Stern layer of ions to be displaced away from the particle surface thus increasing the range of the double layer repulsion. They may also mask the effect of van der Waals attractive forces. The net effect is enhanced stability (Overbeek 1977). (An excellent and thorough discussion of steric stabilization is presented by Napper 1977.)

2.2.4 Thermal Influences

Thermal energy can have many profound influences on the stability and rheology of emulsions. These include Brownian motion, the temperature dependence of the viscosity of the constituent fluids, and chemical responses.

Thermal agitation of the molecules of the continuous phase of a dispersion will cause the dispersed particles to undertake small quick random motions (Brownian Motion). These motions are both rotational and translational and are more pronounced for smaller particles. Krieger and Dougherty (1959) and Brenner (1972) considered that translational effects are more important in dilute dispersions since the particles will be displaced from the secondary minimum if there is sufficient thermal energy. In concentrated systems, the rotation of a particle will affect the motion of adjacent particles.

Becher (1965) states that the viscosity of an emulsion is strongly correlated with the viscosity of the continuous phase, which is not unexpected. Therefore one would expect the suspension viscosity to react in a manner very similar to the continuous phase and to be modified by any physical and chemical changes which may occur in the emulsion. Bennett et al. (1968) indicated that freezing likely destroys the interfacial membrane enclosing the dispersed phase, and heating will break an emulsion (unstable to separation) by causing coalescence of the dispersed droplets. This happens because the lyophilic/lyophobic

nature of the surfactant (nonionic) is a function of temperature: a nonionic surfactant containing ethylene oxide chains as hydrophilic groups suffers dehydration of the ethylene oxide moieties as the temperature increases (Mitsui et al. 1972). These same investigators found that surfactant behavior is dependent on the number of ethylene oxide units. Surfactants containing less than ten ethylene oxide units caused an increase in the interfacial tension as the temperature rose, while a surfactant with more than ten units caused a decrease; the result is a decrease and increase of stability, respectively.

2.3 Hydrodynamic Effects

2.3.1 Dispersed Phase Concentration

In the introduction to this chapter, it was indicated that the concentration of the dispersed phase serves to increase the viscosity of the suspension or emulsion, as indicated by Einstein and others. Since the 1920s similar investigations have considered the shape and finite sizes of the particles, and how they interact under varied conditions; these will be discussed below.

One more recent contribution to understanding the role of dispersed phase concentration was the attempt by Frankel and Acrivos (1966) to calculate the viscosity of a very concentrated suspension from first principles. They considered a suspension of rigid spheres near its maximum

concentration (about 74% by close packing of rigid spheres). Under this assumption, the particles are nearly touching and lubrication theory is applied. The suspension viscosity was found to be:

$$\eta = \frac{9\eta_o(\phi/\phi_m)^{1/3}}{8(1 - \phi/\phi_m)^{1/3}} \qquad (2.2)$$

in the limit as ϕ approaches ϕ_m, the maximum concentration. This approach is of limited use because the rigid particles were assumed to be of uniform size, and the number of nearest neighbors was arbitrarily chosen as six.

2.3.2 Particle Shape

Elaborations of Einstein's now classic equation proceeded to consider non-spherical particles, since Einstein's infinitely dilute limit is not influenced by the size or shape of the spheres (each sphere is considered independently). Investigations by, for example, Jeffery (1923) and Simha (1923, 1940) demonstrated that ellipsoidal particles increase the viscosity of the suspension, moderated by the randomizing influence of Brownian motion. Since the effects of Brownian motion, double layer and van der Waals interactions are relatively more important for sub-micron particles, viscosities of suspensions of such particles are often higher than similar suspensions of larger particles. Inertial forces influence the larger

particles more strongly.

When the dispersed phase is liquid, the velocity gradient in the neighborhood of the particle will cause the particle to deform, and if the gradient is steep enough, the particles may even be broken apart into several smaller droplets. Taylor (1934) balanced the surface tension forces and the normal surface stress caused by the flow, and the resultant droplet shape is ellipsoidal, to a first approximation. As the shear rate is increased, the droplet is further distorted until the viscous stretching forces dominate the restoring surface tension forces. At this point, the particle is rapidly distended, becomes unstable, and ruptures. However, if the viscosity of the liquid comprising the droplet is sufficiently higher than that of the continuous phase, the droplet may not be ruptured.

The interfacial viscoelasticity alluded to arises from the surface elasticity, the exchange of surfactant between the oleic and aqueous phases and the interface, and reorientation of the polymeric molecules in the interface (Oosterbroek and Mellema, 1981).

In conjunction with deformation, the particle will rotate with the local vorticity and the tangential stresses on the interface may induce circulation of the fluid within the droplet (Sherman 1968). If the interfacial layer is strong, it will resist the external tangential stresses, inhibiting the development of internal circulation. It is for this reason that small droplets in a stabilized emulsion

behave as solid spheres. As indicated by Bartok and Mason (1959), internal circulation is usually observed in deformed droplets and as the rate of shear increases, the interface becomes progressively less resistant to the viscous forces exerted by the continuous medium. Such deformations are an additional energy sink, resulting in an increased viscosity. Under steady state conditions, the viscosity of the emulsion is not affected by the deformation unless the droplets are very large or the shear rate very high and disruption ensues.

2.3.3 Particle Size Distribution

When an emulsion is created, the particles are present in a variety of sizes. The distribution may be modified as a result of shear induced droplet rupturing, as described above. Sweeny and Geckler (1954) found that bimodal suspensions of widely different particle sizes had consistently lower viscosities than a monomodal suspension of the same volume fraction. Eveson and Mill (1959) concluded that in multimodal suspensions, the relative viscosity of the suspension (the quotient of the suspension viscosity to the continuous phase viscosity) is proportional to the product of the relative viscosities of the separate monomodal suspensions.

Continuing the same reasoning, Farris (1968) presented a method of predicting the viscosity of multimodal suspensions from monomodal viscosity data. By assuming a

large particle size ratio, the larger particles are considered as being suspended in a homogeneous fluid comprising the continuous phase and the smaller particles. Extended to multimodal suspensions, the system's viscosity is:

$$\eta_r = \eta_0 \prod_i h(\phi_i) \qquad (2.3)$$

where $h(\phi_i)$ is the relative viscosity of the unimodal suspension of the ith size of particles, with volume fraction ϕ_i. Farris also showed that for suspensions with several particle sizes, and with any dispersed phase content, the minimum viscosity occurs when the volume fraction of all the particle sizes are equal. It may also occur when the number of particle sizes becomes infinite, for a fixed dispersed phase content. However, application of this technique to emulsions is probably not practical because the relative viscosity function for each droplet size is not calculable.

The viscosity of suspensions with uniform particle size will increase with increasing fractional concentration, becoming very large near the maximum packing configuration. Polydisperse suspensions can achieve higher maximum particle concentrations because the smaller particles can be packed into the interstices of the larger particles.

In addition to the concentration induced crowding, the particles will be brought together if their trajectories

nearly or completely intersect. This will occur in shear flow of non-dilute systems.

2.3.4 Particle Interactions

Under static conditions particles will come into contact under the action of Brownian motion, sedimentation and chance convection currents (Kitchener and Musselwhite 1968); these are classed as perikinetic phenomena. When the suspension undergoes flow such as simple shear the particles may come into close proximity; this is an orthokinetic phenomenon.

Attempts to determine the contribution of particle interactions during the first half of this century were generally unsuccessful because they only summed all possible two-particle interactions and considered only hydrodynamic forces. Batchelor and Green (1972) resolved this problem by realizing that there is a multiparticle effect. This means that two-particle interactions occur not in an unbound continuous solvent, but rather in an unbound suspension of the other particles, which has an increased viscosity. This is the essence of the ensemble averaging technique.

Neglecting all but purely hydrodynamic influences, two particles brought together by their trajectories will interact. In the neighborhood of each (spherical, rigid) particle, streamlines are curvilinear and are either open or closed (van de Ven 1981). The limiting open streamline determines the mimimum separation of the particle centers

for a glancing encounter. However, it is the ratio of the particle radii which determines the smallest separation of the particle surface. Consequently, particles of similar radii can approach much more closely than particles of significantly dissimilar radii (Adler 1981).

Mason (1977) differentiates between two types of doublets (the association of two particles) which depend on the trajectory of approach. The transient doublet occurs in a glancing collision: the particles approach along open streamlines, execute a partial orbit and then receed from one another. Permanent doublets arise if the particle centers approach within the surface of limiting (closed) trajectories. This occurs in several ways: three-body collisions, interparticle attraction (van der Waals forces), Brownian diffusion, and polymer bridging. The addition of coulombic forces will restrict the distance of nearest approach to approximately the secondary minimum described by the DLVO theory. (Two particle interactions under a variety of conditions have been extensively investigated by Mason and various collaborators. Refer to Mason and Manley 1952; Bartok 1957, 1959; Allan 1962.)

The fate of the permanent doublets depends on the nearness of the particles and the shearing rate. For collisions of particles energetic enough to overcome the primary maximum of the interaction potential energy, the particles may contact one another. Then, the possibility of coalescence exists for fluid particles. This process is

hindered by two factors: surfactant at the interface is capable of withstanding a certain amount of pressure and may therefore keep the droplet interiors from touching; viscous flow of fluid from between the approaching droplets is also a retardant.

Kitchener and Musselwhite (1968) discussed the viscous flow of the surrounding fluid from between the approaching droplets. Because of the viscous flow, a region of high pressure exists between the approaching droplets. This has occasionally been termed the disjoining pressure and causes radial flow of fluid from between the droplets, and dimpling of the local surface of the droplets. The radial flow of fluid applies a tangential stress to the interface which might sweep away the layer of protective surfactant, possibly conducing coalescence.

Many particles may become grouped together to form aggregates. These structures may be constructed at moderate shear rates by the combination of the hydrodynamic and non-hydrodynamic processes discussed above. Within the interstices of the flocculated particles, some of the continuous phase is immobilized and the apparent fractional volume concentration of the dispersed phase is thus increased. Additionally, these aggregates will behave as large, irregularly shaped droplets.

The build-up of aggregates and the immobilization of some of the continuous phase contributes to an increase of viscosity, perhaps explaining, in part, dilatant behavior.

Shear thinning behavior occurs if this loose structure is broken down. At higher rates of shear, outer members of the aggregate spall, and the aggregate decreases in size. At sufficiently high shear rates, the aggregates can be completely dismembered. Cohesive van der Waals forces, entangled steric polymers, and particle deformation complicate these processes.

2.3.5 Phase Inversion

Unique to liquid-liquid suspensions, phase inversion can cause abrupt changes in rheological behavior. According to Dickinson (1981, p. 284), "The phenomena of phase inversion, whereby an oil-in-water (O/W) emulsion changes abruptly to a water-in-oil (W/O) emulsion, or vice versa, is not well understood." It is thought that the phase volume at which this behavior can occur depends on the temperature, the type and amount of emulsifier, and the mechanical agitation imposed on the emulsion. Herrmann, Klar, and Kahlweit (1981) reported a water-oil-nonionic surfactant system that exhibited a temperature dependent inversion. The system contained 5 wt% surfactant and equal amounts (47.5 wt%) of water and cyclohexane. At room temperature, two phases are present: one is rich in oil, and contains some water and surfactant; the other is rich in water and contains most of the surfactant and some oil. As the temperature was elevated, the volume fraction of the water rich phase increased at the expense of the oil rich phase,

until the phase inversion temperature (PIT) was almost attained. At this point, a third phase, rich in water and containing little oil or surfactant, appeared. Over a narrow temperature range around the PIT, these three phases coexist. As the temperature increases in this narrow range, the original oil rich phase is diminished and finally disappears, while the new water rich phase grows. Two phases once again exist, one is rich in oil and contains most of the surfactant and some water, while the other is rich in water and contains little surfactant or oil. Evidence of Mitsui et al. (1972) explains the transfer of surfactant. The hydrophilic nature of the polar group of the nonionic surfactant is very sensitive to temperature, such that the surfactant has a high water solubility at low temperatures, but becomes progressively more oil soluble as the temperature increases.

In addition to the change of surfactant solubility, Becher (1965) mentioned that chemical reactions between the surfactant and one of the principle phases may permit phase inversion, as well as permitting an increase of the dispersed phase concentration if the surfactant is fairly soluble in both phases.

Dickinson (1982) determined that phase inversion usually requires mechanical agitation. An emulsion with dispersed volume fraction of about 50%, behaves as if the O/W and W/O configurations are separated by a large free energy barrier. The emulsion can be inverted from one

morphological state to the other by either changing the composition to reduce the height of the energy barrier or by adding sufficient energy to the system by heating and agitating so it is able to overcome the barrier and invert. There is also the likelihood of a partial inversion, that is, when a portion of the continuous phase is present within the droplets of dispersed phase (a dual emulsion).

Ross and Kornbrekke (1981) have also examined the statistical nature of emulsion formation. They found that for any given volume ratio of two liquids there is a certain probability of obtaining one type of dispersion rather than the other (for unstabilized liquid-liquid mixtures). The phase inversion point is the volume ratio for which there is a 50% probability of obtaining one morphology or its conjugate. As the temperature increases, the inversion point tends toward a volume ratio of 50:50.

3. Materials and Methods

3.1 Fluids

The stabilized emulsions of Wainwright B, Epping and Primrose crude oils were examined. The Wainwright B and Epping crudes were dried by vacuum distillation at 40°C until 0.8% and 0.9%, by volume, water remained in the crudes, respectively. During the drying process some of the light hydrocarbons were incidentally evaporated; these light ends were collected during the drying process and returned to the remainder of the dried oil when acceptable water contents were achieved. The Primrose crude was dried in 1979 and had been in refrigerated storage since then; it contained 3.6% water.

The dried oils each exhibit slightly non-Newtonian behavior, having approximate viscosities at room temperature as follows: Wainwright B, 880 cP (10.9 s^{-1}); Epping, 10700 cP (10.9 s^{-1}); Primrose, 72000 cP (1.3 s^{-1}). Since stabilized emulsions were required in this study, an incidental background examination of the interfacial tension between the surfactant solution and the oils was conducted. These investigations only served to determine the amount of surfactant necessary to produce stable emulsions, and so, only the conclusions are discussed below.

The oils were emulsified with distilled water, and the non-ionic surfactant Triton X-100. Steinborn (1981) reported that Triton X-100 is a water soluble polymer with 8

to 10 ethylene oxide units (iso-ocyl pheoxypoly ethoxy ethanol) and has a density of 1.065 g/cm³. The appropriate concentration of surfactant was determined by finding the concentration of Triton X-100 in distilled water which minimized the interfacial tension between the surfactant solution and the crude oil. For the Wainwright B crude, this was measured with the Du Nouy Tensiometer at room temperature. The procedure was that given in ASTM D971-82 (Standard Method of Testing Interfacial Tension) and the readings were corrected using the formula of Zuidema and Waters (1941). Rubin and Radke (1979) demonstrated that when two immiscible liquid phases are in contact (either phase may contain the surfactant), the interfacial tension falls to an equilibrium value, perhaps passing through a minimum. In light of their results, the oil and surfactant solutions used in this study were left in contact for approximately 30 minutes before the interfacial tension was measured. This was to ensure that equilibrium interfacial tension conditions were attained. For the Wainwright B oil, a shallow minimum in interfacial tension was found: 0.8 dynes/cm at a surfactant concentration of 0.7% by volume.

The Epping oil is of similar density to the surfactant solutions, and thus, a more sensitive method, the pendant drop technique, was used to measure interfacial tension, at room temperature. To increase the density difference between the two phases, deuterium water was used for the aqueous phase. For a discussion of the pendant drop

technique, see Stauffer (1965) and Ambwani and Fort (1979). No true minimum interfacial tension was observed, it declined only slightly from a value of 0.61 dynes/cm for surfactant concentrations above 0.6%.

The Primrose crude is also heavier than the surfactant solutions, and due to its high viscosity, the pendant drop apparatus could not be used. Consequently, the optimum surfactant concentration was not obtained for the Primrose crude. However, since the surfactant concentration is not a variable in these rheological examinations, a constant surfactant concentration of 0.7% by volume was adopted for all three oils.

3.2 Emulsion Preparation

All of the emulsions were prepared by mixing appropriate quantities of water (surfactant solution) and dried oil with a Gifford Wood Homogenizer Mixer[2] (actually a high impact turbine). Generally, W/O emulsions were produced by adding the aqueous phase to the oleic phase while mixing, and O/W emulsions are produced by the converse procedure. Such was the case with the Wainwright B and Epping crudes. For intermediate water contents (30% to 70%, depending upon the oil used), water continuous dual emulsions were produced, regardless of which phase was added to the other.

---

[2]for mixing suggestions see the "Operating Manual", Gifford-Wood Homogenizer Mixer Model 1-LV, Greerco Corporation, USA.

Because of the very high viscosity of the Primrose crude, the homogenizer would not function in just the oil; therefore, the Primrose emulsions were produced only when the oil was added to the water while mixing. Both water continuous and oil continuous Primrose emulsions were prepared by the same process. At low water contents (less than 35%), W/O emulsions were still produced because the emulsion created while adding more oil eventually inverts from an O/W emulsion to a W/O emulsion. This behavior was evident for all three oils. W/O emulsions produced in this way appeared to be less stable to creaming after quiescent storage at room temperature for several weeks.

To create the emulsions, the constituent fluids were mixed for about ten minutes, poured into a separatory funnel and left undisturbed for twenty-four hours. Those emulsions containing intermediate volumes of water invariably separated into two distinct emulsions. One of these was rich in water (at least 90% water by volume), and the other was a water continuous dual emulsion. In this way, two relatively stable emulsions were obtained simultaneously. Emulsions prepared with low dispersed phase content retained their integrety.

Once a stable emulsion was obtained, it was tested for its water content, classified, and was then ready for particle size and rheological examinations.

3.3 Emulsion Examination

3.3.1 Water Content

A 25 mL sample of emulsion and sufficient toluene was boiled under reflux for ninety minutes. The water vapour was condensed and collected in a graduated receiving tube and the fractional water content was thus determined. Each emulsion was named according to its percentage water content, regardless of the emulsion type.

3.3.2 Classification and Morphology

Classification as either a water or oil continuous dispersion may be quickly determined by placing a small sample of the emulsion into a bath of toluene or acetone. If the emulsion is oil continuous, the oil, which is miscible with toluene, is leached from the sample; if the sample is water continuous, the water is leached out by the acetone: this process is readily observable. However, this technique cannot distinguish between a dual and a simple emulsion with the same continuous phase. This distinction was accomplished with an optical microscope, and was done in conjunction with the photomicrography and particle size analysis of the emulsions.

3.3.3 Particle Size Measurements

The particle size data was aquired in two stages, photomicrography and image measurements. A sample of the

emulsion was placed on a microscope slide, beneath a cover slip, and illuminated by white light if the emulsion was oil continuous, and by near ultraviolet light if the emulsion was water continuous. The choice of light source was governed by the opacity of the continuous phase, water being opaque to ultraviolet light, and oil to white light. This enhanced the contrast between the suspended droplets and the dark continuous phase.

Hecht and Zajac (1976) showed that the limit of resolution of a microscope is proportional to the wavelength of the light used for illumination, and inversely proportional to the numerical aperture of the objective lens. For the system used, the limiting resolution is about 0.3 μm for ultraviolet illumination and about 0.4 μm for white light illumination.

Once an appropriate field of stationary particles was in focus, a photograph was taken (KODAK Tech Pan 100 high contrast film). Since illumination with ultraviolet light requires exposures of four to seven seconds (depending on the optical transmission of the sample), obtaining a stationary field is important. Particles severely influenced by Brownian motion generally moved too erratically to be photographed by this method.

For each emulsion, a 21.6 cm by 25.4 cm print was made from the negative. At this stage the droplet images had been magnified by a factor of 1400 ±20. Now, microscopes have a relatively narrow depth of field, thus not all of the

droplet images on a photograph will be in focus. Those images properly in focus were blackened with ink and the photograph was then bleached in an iodine solution to remove all other images. Only black images of the in-focus droplets remained and were in strong contrast to the white background (the converse representation could also be established if necessary). In this form, the photographs were examined with an optical comparator.

The Bausch and Lomb Omnicon Alpha™ Image Analysis System[3] was used to measure the total number of identified droplet images on the photograph which were greater in size than a chosen diameter, yielding cumulative frequency data. This diameter is the maximum horizontal chord and is therefore orientation dependent for non-circular objects. In most of the emulsions, the dispersed phase existed as spherical droplets; in those few cases for which droplet crowding was evident, this distortion was not strong, and so it was ignored.

The instrument was calibrated with test circles of known dimensions, and the reproduciblity of the calibration factor was ±0.55%. The smallest discrete (photographic) image discernible was approximately 0.5 mm in diameter. At a magnification of 1400 ±20, this corresponds to droplets with a minimum diameter of 0.36 ±0.07 μm which agrees well with the minimum resolvable diameter of the microscope.

---

[3]see the operator's manual: The Bausch and Lomb Omnicon Alpha™ Image Analysis System Operator's Manual, Rochester, N.Y. (1976).

Coupled with the instrument reproduciblity, a measurement uncertainty of 0.1 μm was adopted.

Allen (1968) reported that particle sizes measured by optical microscopy can be in serious error for diameters less than a few times the limit of resolution. For a particle with a true diameter of 1.0 μm, a typical visual estimate would be 1.13 μm; for a true diameter of less than 0.2 μm a typical estimate would be 0.5 μm. Hence, a useful lower limit of resolution is on the order of one micron (below this value even the measurement error is greater than 10%). In this study droplet diameters below one micron were included with the proviso that these measurements may be subject to considerable error.

The droplet distributions occurred as two types, primary and secondary. Primary distributions are those occurring as simple dispersions, such as O/W or W/O types. For dual emulsions, such as W/O/W, water droplets exist within oil droplets which, in turn, are dispersed in a continuous water phase. The water dispersed within the oil droplets constitute the secondary distribution; the distribution of oil droplets, regardless of their interior structure, would be the primary distribution. To obtain enough secondary droplets for a statistical analysis, the distributions within several primary droplets were examined and combined. However, the number of secondary droplets in one such sample was still too low for a strictly proper statistical analysis.

The cumulative frequency data for the primary and secondary distributions of emulsions of all three oils is tabulated in Appendix C.

3.3.4 Rheometry

Measurements of the shear stress-shear rate relationship employed two coaxial cylinder viscometers: the Haake Rotovisco RV3, with a MK500 type measuring head, and the Brookfield Synchrolectric Digital LVTD. Each instrument imposes Couette flow (specifically Searle flow geometry) by rotating the inner cylinder (bob) at a constant angular velocity, Ω, sustained by a torque, Ψ; the outer cylinder (cup) is stationary.

For the Haake viscometer, an approximately 450 mL sample was placed into a thermally jacketed vessel, and the cup and bob assembly was then lowered into the sample. Narrow slots in the cup permit the sample to completely fill the annulus between the cup and the bob, and to cover the bob. During this entire procedure, numerous air bubbles were entrapped by the fluid; several hours were necessary for these bubbles to escape (more time was needed for fluids with a viscosity greater than about 5000 cP).

The temperature of the sample, cup, and bob was controlled by circulating an appropriately heated thermal oil through the thermal jacket, and a Haake HT22 constant temperature circulator was used to control the thermal oil temperature. The temperature of the emulsion was monitored

with two iron-constantan thermocouples, one adjacent to the outside of the cup and the other located beneath the cup. When the temperature controller was adjusted, it was assumed that the desired fluid temperature was attained when the two thermocouples indicated the same temperature to within one degree (absolute) of each other; this occurred about two hours after the change of temperature was initiated, and of course, depended upon the amount of change desired.

The bob was rotated at the desired angular frequency by selecting the appropriate value, n_s, on the viscometer control unit. The torque necessary to overcome the viscous drag of the fluid is indicated on a scale of 0 to 100. This value, S, is proportional to the actual torque required, and a full scale (S=100) deflection is equivalent to a torque of 427775 dyne·cm. The rotational speed may be chosen discretely or varied continuously.

Attempts to calibrate the Haake viscometer for Newtonian fluids were frustrated by the discovery that the angular frequency of the bob was not equal to the frequency indicated by n_s on the control unit. A functional relationship between the actual frequency, Ω, and the indicated frequency, n_s, was obtained, and is presented in section A.4 of Appendix A. Precautions for the use of the Haake and Brookfield viscometers is also discussed in section A.4. The warnings about possible damage to the Haake viscometer cannot be overemphasized: to protect the precision torsion spring, the bob should be rotated at

speeds such that the S dial never exceeds 100 units. Furthermore, the cup and bob assembly should never be subjected to a jolting motion as this may severely damage the saphire bearings which guide the bob axle.

The Brookfield Synchrolectric Digital Viscometer was used for emulsions with very high or with very low viscosities. Although the Haake viscometer is capable of measuring fluid viscosities over an extremely broad range, using the Brookfield viscometer was more expedient. The UL Adapter of the Brookfield viscometer is particularly well suited for low viscosity measurements. It is a narrow annulus viscometer requiring only a 25 mL sample. To measure higher viscosity fluids, the LVTD series of spindles was used, and 600 mL of the test emulsion were held in a 600 mL beaker, the cup. In either setup, the frequency of the bob was set at any of eight discrete values. Here too, the torque necessary to overcome the viscous resistance of the fluid is indicated on a scale of 0 to 100, a full scale deflection being equivalent to a torque of 673.7 dyne·cm.

The temperature of the sample, cup and bob, were maintained by immersing the beaker of test fluid in a constant temperature water bath. The temperature of the sample was measured with an iron-constantan thermocouple before and after a particular rheological test; the bath temperature was monitored continuously.

For the more viscous fluids, the advantage of the Brookfield viscometer over the Haake viscometer is that when

an emulsion is removed from the separatory funnel, it may be directly drained into a 600 mL beaker. Any entrapped air then has plenty of time to escape before the rheological tests are performed. The necessity of repouring the air-free emulsion into another container, as with the Haake viscometer, was thus eliminated.

Once the test fluid reached an appropriate steady temperature its rheological behavior was examined. Both viscometers were operated in the same way: when the rotational speed of the bob was changed, the instrument was allowed to reach equilibrium (indicating steady motion in the liquid) before the dial reading was taken. The instructions provided by the Haake[4] and Brookfield[5] viscometer manufacturers state that the apparent viscosity, shear rate and shear stress are determined from the dial reading, the angular velocity of the bob, and manufacturer supplied constants. The formulae and procedures indicated are correct when the fluid is Newtonian, but for non-Newtonian behavior, the relationship between the shear rate and the shear stress is non-linear. Following a somewhat generalized procedure, a relationship between the shear stress, τ, and the shear rate, $\dot{\gamma}$, is developed in Appendix A. Also discussed in Appendix A are the potential

---

[4] see the Haake information booklet by G. Schramm, "An Introduction to Rheology and Viscometry," Haake Mess-Technik, Karlsruhe, West Germany. n.d.

[5] see Brookfield information sheet 66-0112, "Brookfield Synchro-Lectric Viscometer, Shear Rate and Shear Stress Formulas", Brookfield Engineering Laboratories, Inc., Stoughton, Mass. n.d.

problems that may arise from violations of the assumptions underlying the adopted relationship between the shear stress and the shear rate.

For both viscometers, dial readings below about 5.0 were rejected, except for the UL Adapter for which values below 1.0 were rejected. Below these limits dial readings are unreliable. Additionally, both viscometers produced comparable measurements when calibrated with a Newtonian calibration oil.

The rheological data presented in Appendix B includes estimates of the measurement uncertainty. In most cases, the uncertainty is on the order of a few percent (for viscosity). The measurement uncertainty was generally assumed to be about one third of the smallest scale division. The uncertainty in the dial reading of the viscometers was estimated from the fluctuation of the S scale indicator. For the Brookfield viscometer no uncertainty was assumed for the angular frequency of the bob, whereas for the Haake viscometer, the rotational speed and its uncertainty was calculated, as indicted in Appendix A. These uncertainties were propagated by the usual rules of error propagation (see, for example, Taylor 1982).

4. Results and Discussion

The discussions presented below consider the interrelationships of the water content and morphology, the particle size distribution, and the shear viscosity of the emulsions at ambient and elevated temperatures. Three different oils were used; thus, a class comparison is also presented.

Since the determinations of water content, emulsion morphology, and particle size distribution were performed on the emulsions at room temperature, the relationship of these variables to the rheology of the emulsion is restricted to room temperature. These variables may be regarded as initial conditions when the rheology at elevated temperatures is considered.

4.1 Water Content and Morphology

With the inclusion of the nonionic surfactant Triton X-100 (at a concentration of 0.7%, by volume), stable emulsions of each oil were produced. However, each oil exhibited particular water content ranges for which stable emulsions could not be produced (usually within a few hours of mixing, these mixtures separated into two stable water continuous emulsions). Wainwright B emulsions, with water contents in the range of 55% to 95%, could not be produced. Epping exhibited a narrower upper range, 72% to 95%, and a second low range, 22% to 43%, in which emulsions were unstable and could not be produced; Primrose displayed only

a low range, 32% to 44%, in which stable emulsions could not be produced. Figure 4.1 shows the regions in which no stable emulsions could be produced, as a function of the oil employed. It also shows the regions in which particular types of stable emulsions were created.

The zones of instability appear to be related to the oil classification of Flock (1977), as does the emulsion morphology. Flock hypothesized that crude oils could be broadly classified according to the crude oil viscosity and natural surfactant content, with class one having the highest values, and class four the lowest. Although only three oils (Primrose, Epping, and Wainwright B, from classes one, two, and three, respectively) were examined, results suggest that the ability to produce a stabilized emulsion of a particular morphology depends upon either the oil viscosity or the natural surfactant content, or both.

In conjunction with the nonionic surfactant Triton X-100, oils in lower classes exhibit a zone of instability for low water content which separates regions of emulsions with W/O and W/O/W morphologies. As the classification number decreases, this zone disappears, and another appears at higher water contents. This new region separates emulsions with W/O/W and O/W morphologies.

The location of the unstable zones and of the boundaries between emulsion morphology types may be explained by examining the unstable state in which an emulsion is created. Dickinson (1982) has proposed that

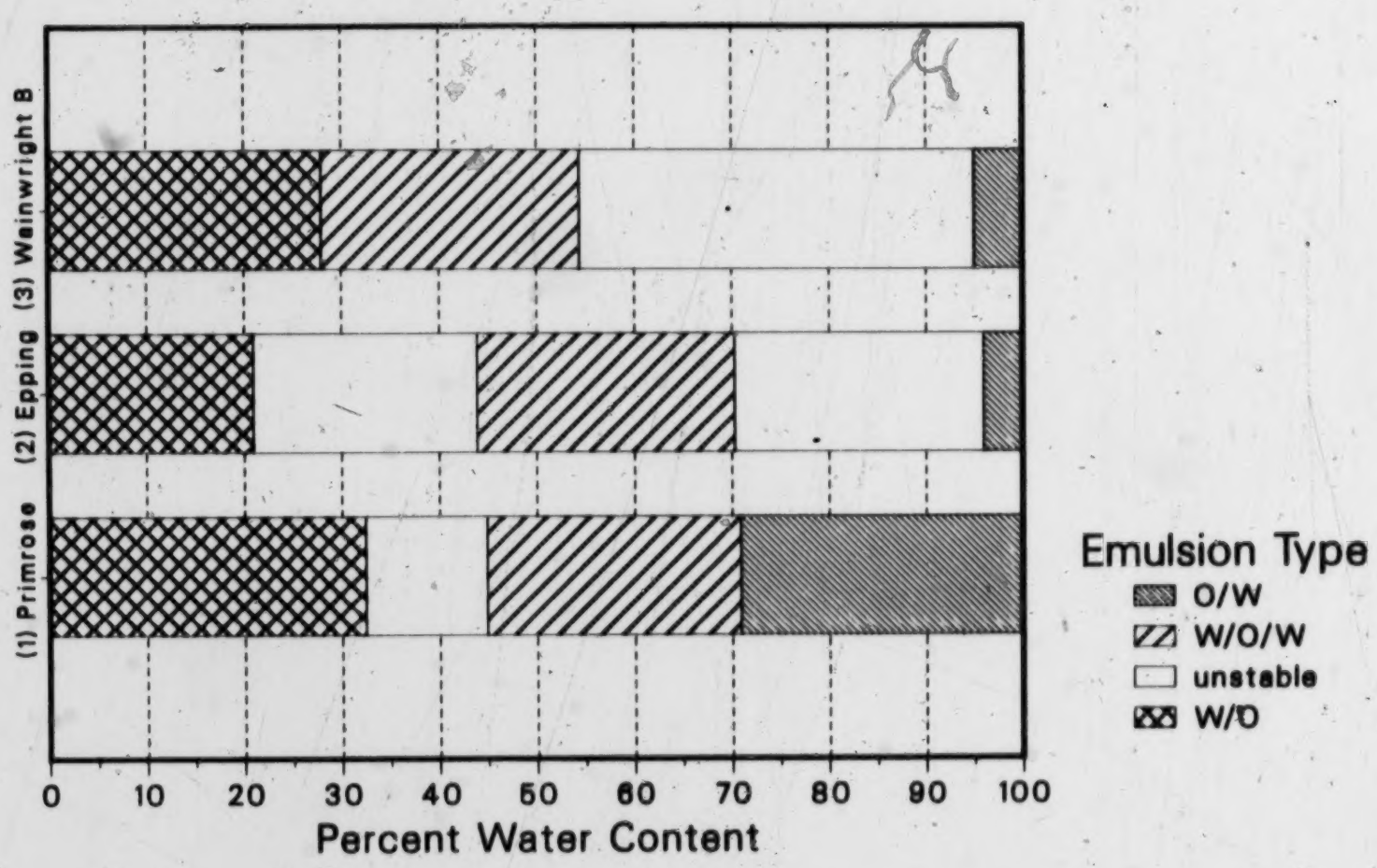

Figure 4.1 Emulsion morphology as a function of water content and oil classification.

after an infinite amount of mixing, the system of fluids is completely homogeneous in the sense that all of its molecules are arranged randomly. When agitation ceases, two sets of evolving states, the W/O and the O/W, coexist, and depending upon the dispersion free energy and volume ratios of the system, the eventual stable emulsion created is determined. By this theory, either a W/O or an O/W emulsion should form. These emulsion types are separated by a narrow zone (the phase inversion concentration), within which it is possible to produce either type of emulsion.

Realistically, the mixing of fluids to create an emulsion takes a finite amount of time meaning that inadequate mixing and uneven viscous heating will occur. Such random inhomogeneities in the initial configuration determine the initial evolution towards a stable emulsion. Consequently, any existing morphology will tend to dominate the evolutionary process.

The existence of dual emulsions (W/O/W emulsions for all three oils) must also be a result of incomplete mixing. Nascent O/W and W/O emulsions coexisting immediately after mixing would compete until one type dominated; in these experiments water continuous emulsions dominated. It is conceivable that the combination of natural and artifical surfactants present in each of these systems stabilized the nascent W/O emulsions sufficiently that at least some of them became isolated entities within a dominant O/W emulsion, resulting in a W/O/W emulsion.

The phase inversion volume concentration for Wainwright B appears to be 28.0%. At lower water contents, oil is the continuous phase. The Wainwright B 28.0% emulsion is unique among all of the emulsions created. Microscopic examination could not determine which phase was continuous. Large regions of W/O and W/O/W seem to coexist (several samples of this emulsion were observed). The viscosity of this emulsion is similar to other water continuous dual emulsions, thereby suggesting that it is water continuous. However, its primary droplets would be extremely large oil droplets, and these, in turn, contain a significant amount of water.

The phase inversion concentration for Epping and Primrose emulsions is not clearly evident. But, since this is the division between oil continuous and water continuous emulsions, the region of instability that occurs at relatively low water contents for both of these oils might be representative of the inversion point.

At water contents above about 70%, the Primrose emulsions are O/W. Below this mark the emulsions are W/O/W. This marks the division of compositional states where nascent W/O regions may or may not exist. Above this point, the volume content of oil is sufficiently low that very few if any W/O regions could exist and grow. Throughout the duration of the mixing process the compositional imbalance is so strong that the water continuous morphology remains.

For the Wainwright B and Epping oils, the upper regions of instability exist because of their low natural surfactant content. Even though the oil content is sufficiently low, the combination of natural and artificial surfactants is likely insufficient to stabilize the required interfacial area: increasing the amount of artificial surfactant might alleviate this situation, but this was not investigated.

4.2 Particle Size Distributions

The particle size distribution is intimately connected to the morphology of the emulsions and is significant in their rheological behavior. For each emulsion, cumulative frequency data for the primary and secondary distributions (when present) are displayed in Appendix C. Plate 4.1 shows an example of a dual emulsion (specifically Wainwright B 34.4% W/O/W). Within most droplets which comprise the primary distribution, are droplets of the continuous phase. These enclosed droplets comprise the secondary distribution. Such photographs were used to determine the emulsion type and the the primary and secondary droplet size distributions. The droplet crowding that is evident was the most severe of any of the emulsions examined. Figure 4.2 shows a typical log-normal distribution, in this case, the primary distribution of Epping 20.4% W/O. As described below, the mean droplet diameter and the distribution standard deviation are the desired distribution characteristics. In Figure 4.2, the geometric mean droplet

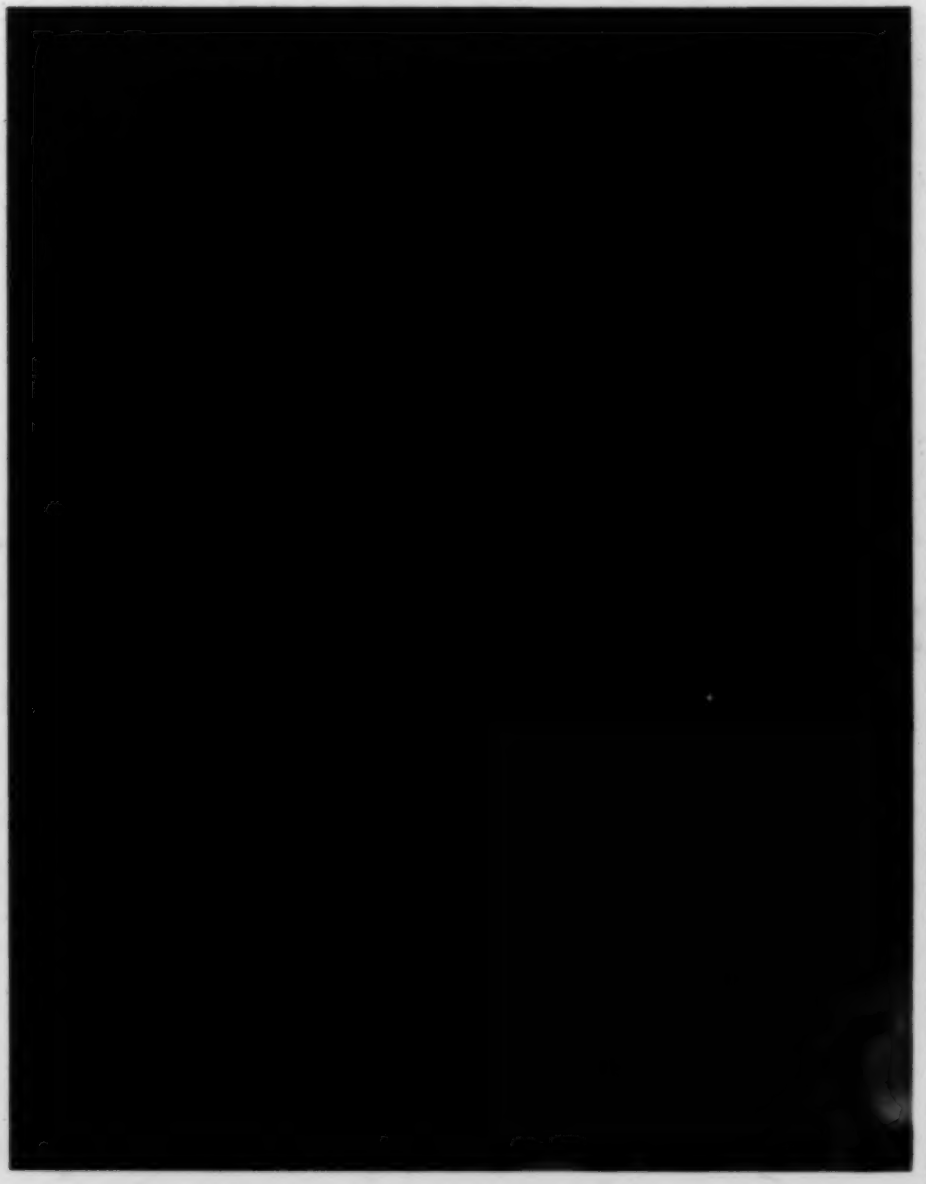

Plate 4.1. A typical dual emulsion showing secondary droplets of the continuous phase within the primary droplets (Wainwright B 34.4% W/O/W).

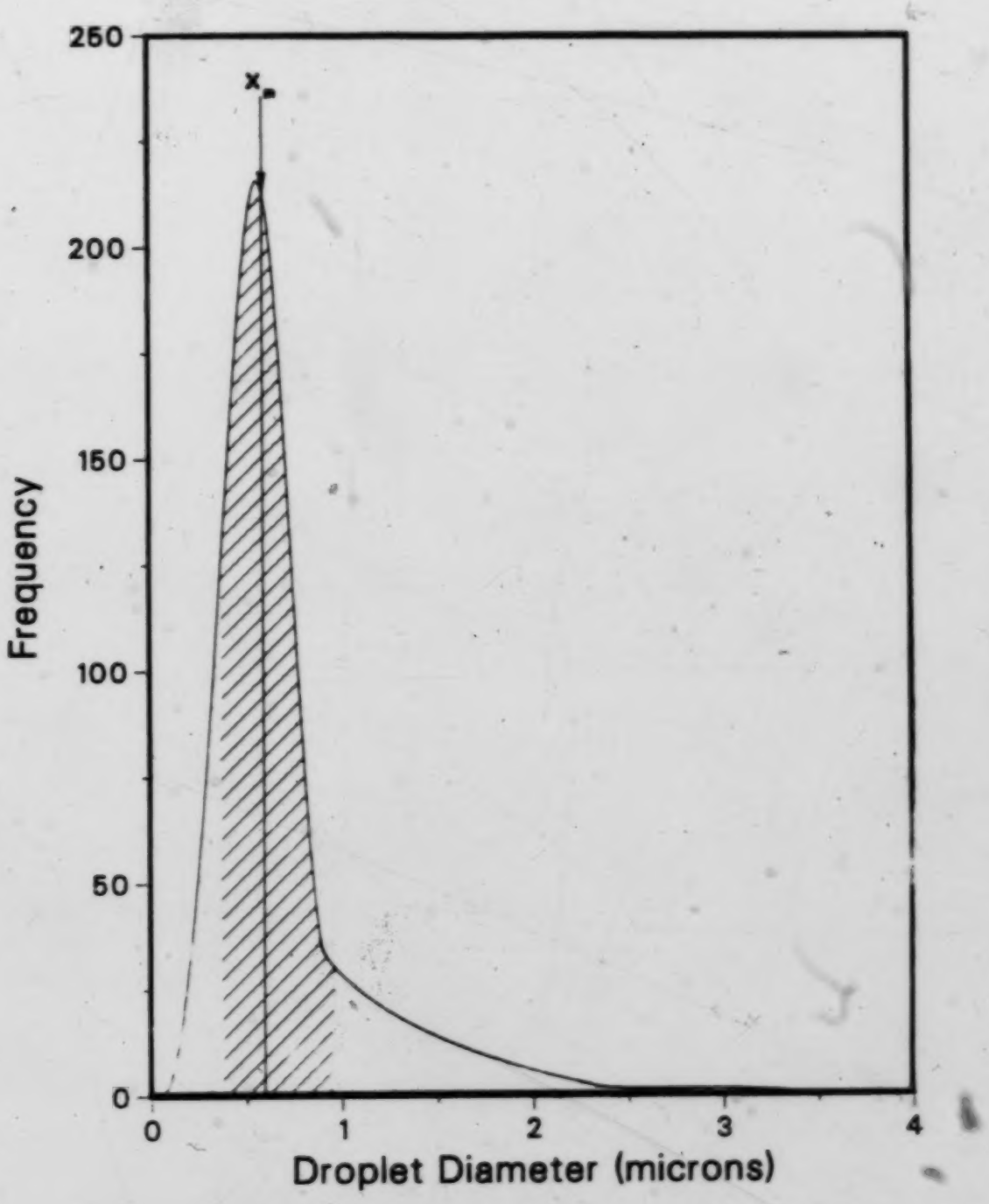

Figure 4.2. Typical distribution of droplet diameters described by a log-normal distribution. The shaded region is the 68% inclusion zone. (Epping 20.4% W/O, primary distribution.)

diameter is shown as x_m. The width of the distribution is characterized by the geometric standard deviation and about 68% of the droplet diameters are within one standard deviation of the mean; this is shown by the shaded region (the 68% inclusion zone).

Since the droplet distributions are polydisperse, they may often be adequately described by two parameters: a mean size, and the degree of spread around this mean. Groves (1980) suggests that the log-normal distribution tends to fit mixtures prepared by homogenization; hence, the geometric mean particle diameter and the geometric standard deviation are the desired parameters. (Particle size analysis is described by many authors: see for example, Allen 1974, Cadle 1965, or Mercer 1973.) Calculating these values is a natural extension of the common mean and standard deviation. If the count of N particles is subdivided into i intervals such that x_i is the average particle diameter for the ith interval, and δN_i is the number of particles in that interval, then the geometric mean diameter and standard deviation are determined as follows:

Geometric mean diameter

$$\ln x_m = \frac{\Sigma \ln x_i \, \delta N_i}{N} \qquad (4.1)$$

Geometric standard deviation

$$\ln\sigma = \left[\frac{\Sigma[\delta N_i(\ln x_i - \ln x_m)]^2}{N - 1}\right]^{0.5} \qquad (4.2)$$

For simplicity, the geometric standard deviation is called the dispersity. The advantage of using the above conventions is that the dispersity has a value of at least unity, a value of 1.0 representing a truly monodisperse system. The mean diameter and dispersity of the distributions present in each emulsion is summarized in Tables 4.1, 4.2, and 4.3. In Figures 4.3, 4.4, and 4.5, the geometric mean droplet diameter is plotted as a function of percent water content and emulsion morphology, and the 68% inclusion zones for the primary distributions are also shown. These boundaries delineate the diameters between which 68% of the particle diameters lie.

Inspection of Figures 4.3, 4.4, and 4.5 reveals several features consistent among all of the emulsions of similar type. The simple emulsions of all oils (W/O and O/W) have mean particle sizes in the range of one to two microns and fairly low dispersity. For the dual emulsions of each oil, the mean particle diameter is considerably larger and the dispersity is significantly broader. It is also noteworthy that the secondary distributions of each oil's dual emulsions have mean particle size and dispersities that are virtually the same as these for the simple emulsions

Table 4.1

Wainwright B Emulsions Particle Distribution Summary

Type	Percent water content	Primary		Secondary	
		Geometric mean diameter (microns)	Dispersity	Geometric mean diameter (microns)	Dispersity
W/O	0.8	1.9	1.6	-	-
W/O	4.8	1.7	1.8	-	-
W/O	10.4	1.0	1.7	-	-
W/O	18.0	2.0	2.1	-	-
W/O	26.5	1.5	2.5	-	-
W/O/W	28.0	4.9	2.0	5.8	2.2
W/O/W	34.4	6.6	3.1	0.9	1.6
W/O/W	46.4	6.0	2.6	2.1	1.7
W/O/W	54.0	4.4	4.5	2.0	1.6
O/W	95.6	1.4	2.0	-	-
O/W	97.6	1.1	2.1	-	-

Table 4.2

Epping Emulsions Particle Distribution Summary

Type	Percent water content	Primary		Secondary	
		Geometric mean diameter (microns)	Dispersity	Geometric mean diameter (microns)	Dispersity
W/O	0.9	1.1	1.7	-	-
W/O	14.4	0.5	2.0	-	-
W/O	17.0	0.7	1.8	-	-
W/O	20.0	0.8	1.7	-	-
W/O	20.4	0.6	1.6	-	-
W/O/W	43.2	8.6	2.0	1.0	1.8
W/O/W	53.2	1.4	2.7	0.7	2.4
W/O/W	64.0	2.4	2.4	2.1	1.8
W/O/W	66.8	2.1	2.3	0.9	2.1
W/O/W	70.4	3.2	2.3	2.0	2.1
O/W	96.8	1.2	2.0	-	-
O/W	98.0	1.4	1.6	-	-
O/W	98.4	1.0	1.5	-	-

Table 4.3

Primrose Emulsions Particle Distribution Summary

Type	Percent water content	Primary		Secondary	
		Geometric mean diameter (microns)	Dispersity	Geometric mean diameter (microns)	Dispersity
W/O	3.6	0.4	2.0	-	-
W/O	22.8	1.1	2.6	-	-
W/O	32.0	0.6	2.5	-	-
W/O/W	44.8	3.5	2.3	1.2	2.1
W/O/W	48.2	1.1	2.6	1.1	2.7
W/O/W	62.4	9.3	4.1	1.3	2.3
W/O/W	64.4	9.9	2.1	0.8	1.7
O/W	78.5	1.2	2.5	-	-
O/W	82.4	1.5	2.2	-	-
O/W	88.8	1.9	1.8	-	-
O/W	95.2	1.2	2.4	-	-
O/W	98.6	1.1	2.4	-	-

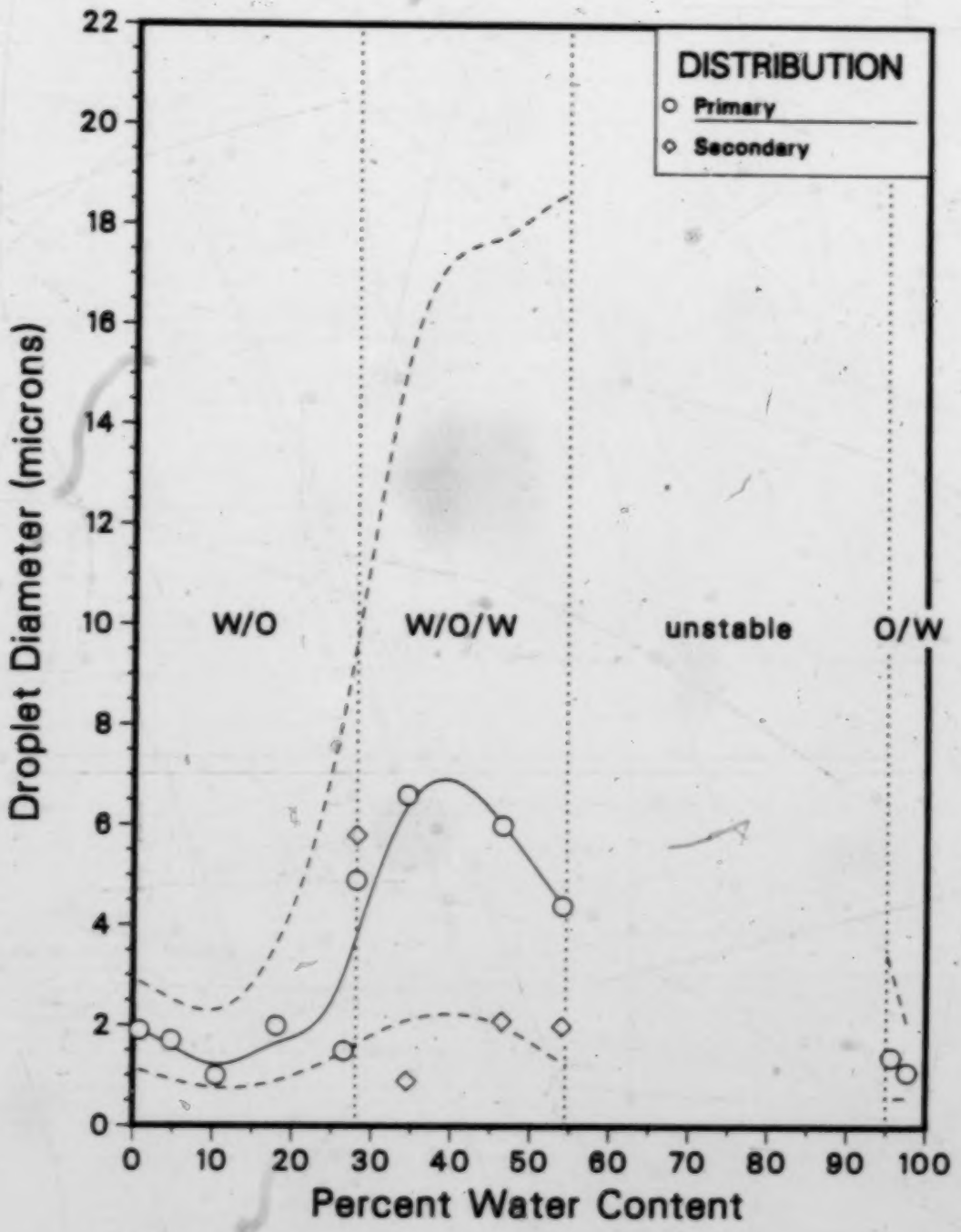

Figure 4.3. Geometric mean droplet diameters for Wainwright B emulsions. For the primary distribution the 68% inclusion boundaries are shown (-----).

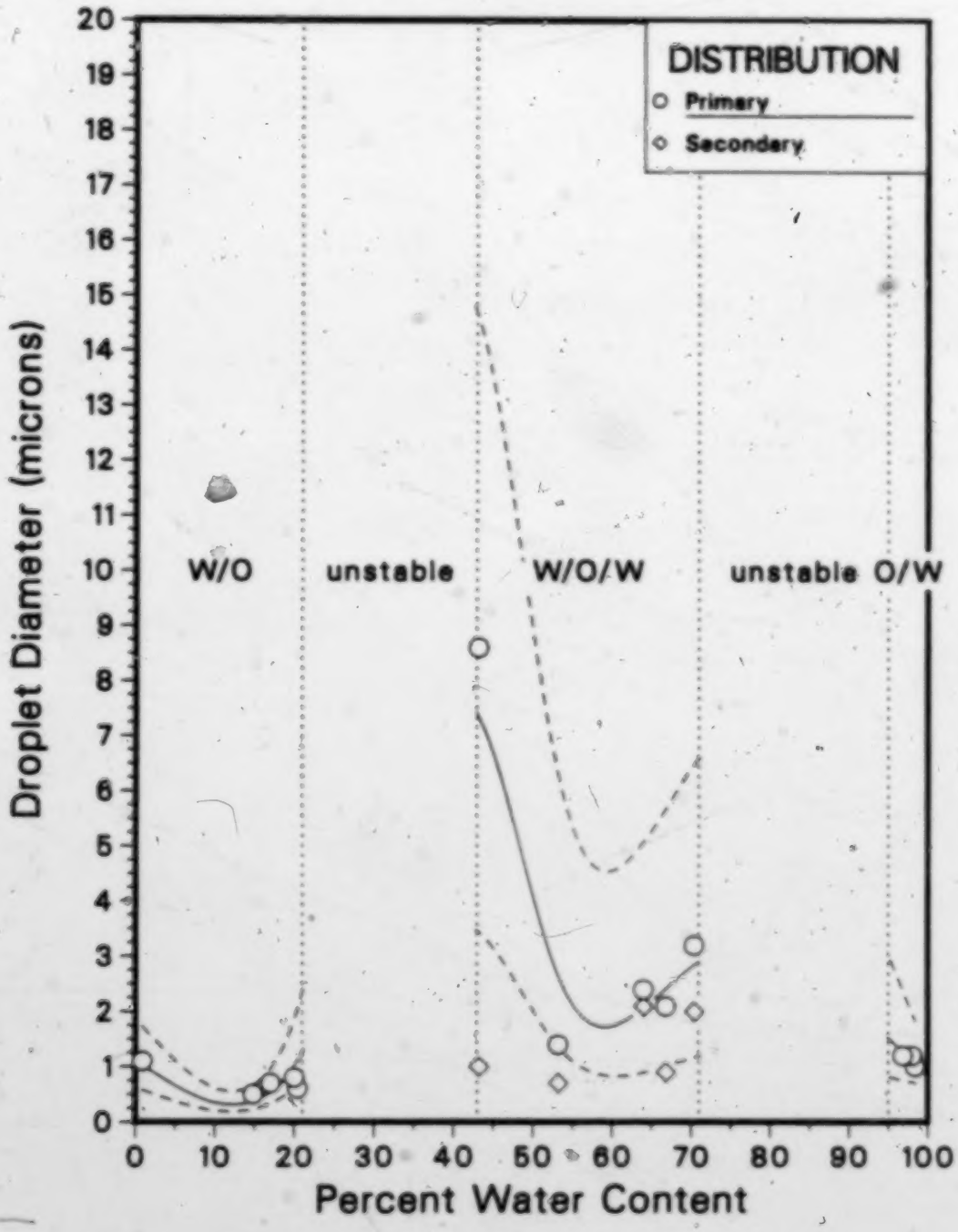

Figure 4.4. Geometric mean droplet diameter for Epping emulsions. For the primary distribution, the 68% inclusion boundaries are shown (-----).

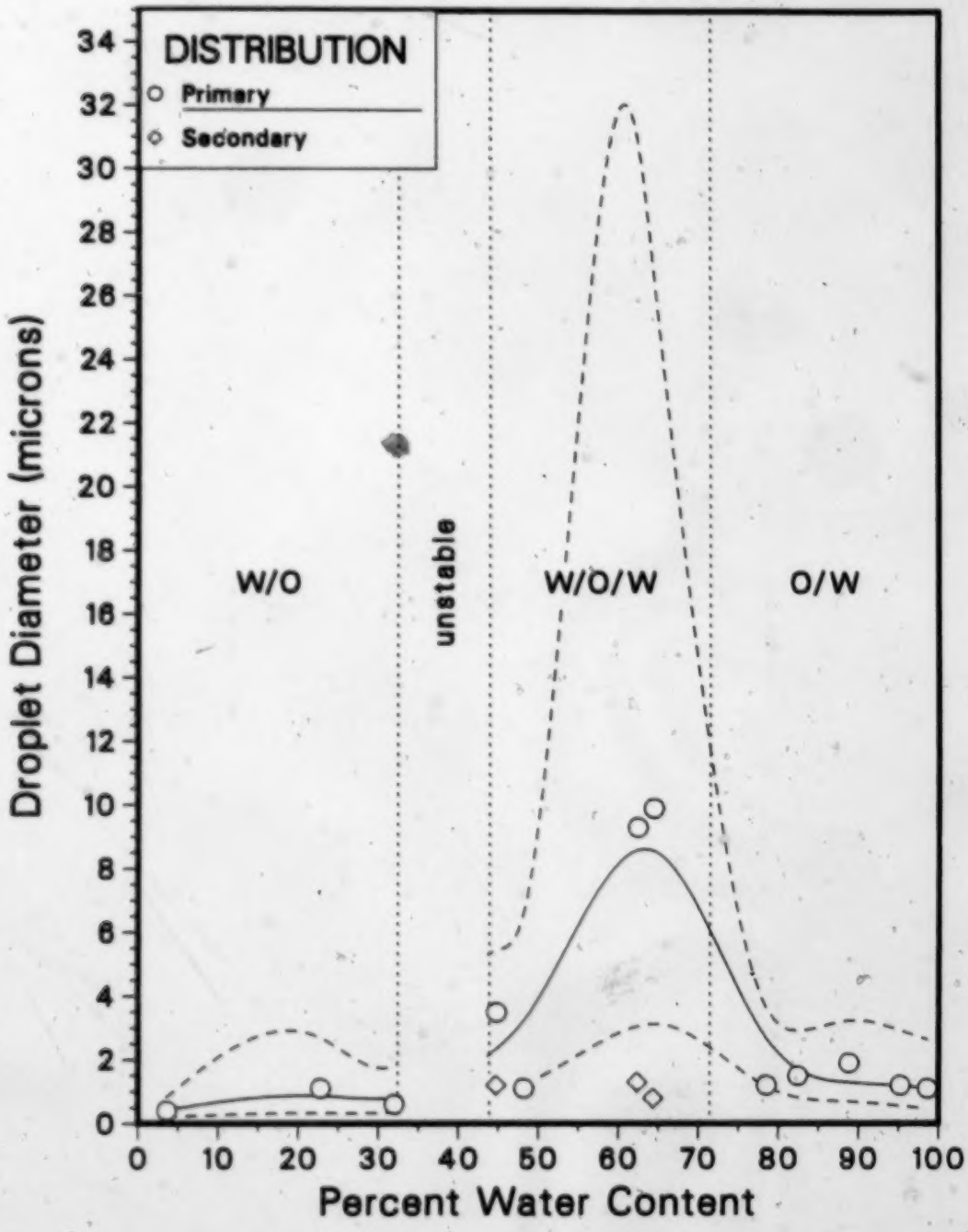

Figure 4.5. Geomtric mean droplet diameter for Primrose emulsions. For the primary distribution, the 68% inclusion boundaries areshown (-----).

(considered on an individual oil basis; also see Tables 4.1, 4.2, and 4.3).

These distributions are expected if the statistical nature of emulsion formation is accepted. During the homogenization process, mechanical energy is added to the system, but the total amount of heat generated is considerably higher for those mixtures containing similar volumes of oil and water. Consequently, the degree of inhomogeneity of incipient dual emulsions is lower than for incipient W/O or O/W emulsions. When mixing ceases, W/O and O/W emulsions coexist and grow until one phase dominates. But until this occurs, each continuous region develops within itself a primary distribution. Ultimately, one region becomes discontinuous, forming the primary distribution. The mean size of the primary particles, in this case, is expected to be large since this phase was competing for dominance. The secondary distribution should not exhibit any unusual characteristics.

The dual emulsions produced from each oil are water continuous although the water to oil ratios are varied enough that some oil continuous dual emulsions would be expected. The fact that all of the dual emulsions are water continuous may be explained by the presence of the nonionic surfactant. Because the surfactant Triton X-100 is water soluble, water continuous emulsions are expected. W/O emulsions exist at low concentrations (that is, below the phase inversion point) since there is insufficient water to

encapsulate the oil during the evolutionary period.

As indicated above, considerable heating occurs during the homogenizing process. For high water content emulsions, the temperature after mixing was approximately 30°C, and for low water contents the final temperature was closer to 40°C. The temperature rise that occurred when mixing similar volumes of oil and water depended upon the oil used: about 40°C for Wainwright B, 45°C for Epping, 50° C for Primrose. Since heating removes ethylene oxide moieties from the surfactant polymer, the surfactant becomes less water soluble. Consequently, the lower limit of water content for which water continuous emulsions (both W/O/W and O/W) are produced increases as the oil becomes more viscous.

The temperature dependence of emulsion formation has adverse consequences for the rheological examinations at elevated temperatures. If the change in surfactant solubility is irreversible, the emulsion may undergo significant, irreversible change of morphology when the temperature of formation is exceeded. Such changes appear to have occurred in several of the emulsions and are discussed below.

The size of the droplets also governs the importance of the influence of non-hydrodynamic forces. With the exception of Epping 53.2% W/O/W and Primrose 48.2% W/O/W dual emulsions, the size of the primary particles in each of the dual emulsions is large enough that Brownian motion, double layer, and steric effects are small or even

negligible. Secondary particles will act to inhibit internal circulations of the primary particles.

4.3 Emulsion Rheology

The shear stress, shear rate and apparent viscosity data for each emulsion at various temperatures is presented in tabular form in Appendix B.

The shear rate at the surfacce of the inner cylinder was determined with equation A.9 of Appendix A: the first two terms of the series were considered. Since the second term is usually small ($f_1(t)$ never exceeds 0.11), it can often be neglected, especially if κ' is small.

A graphical illustration of the rheological data is presented in figures such as Figure 4.6, where the contours of the logarithm of the apparent viscosity are plotted as a function of the emulsion water content and of the shear rate. Each of the plots shows both the shear dependence of emulsion viscosity at constant water content and the water content dependence of emulsion viscosity at constant shear rate.

Consider Figure 4.6 as a example of how to interpret such diagrams. The region between about 55% and 95% water content is that within which no stable emulsions could be created. Prom Figure 4.3, the regions of W/O, W/O/W, and O/W emulsions may be recalled; these regions are not identified in figures such as Figure 4.6 for reasons of clarity. To compare the viscosity of different emulsions at

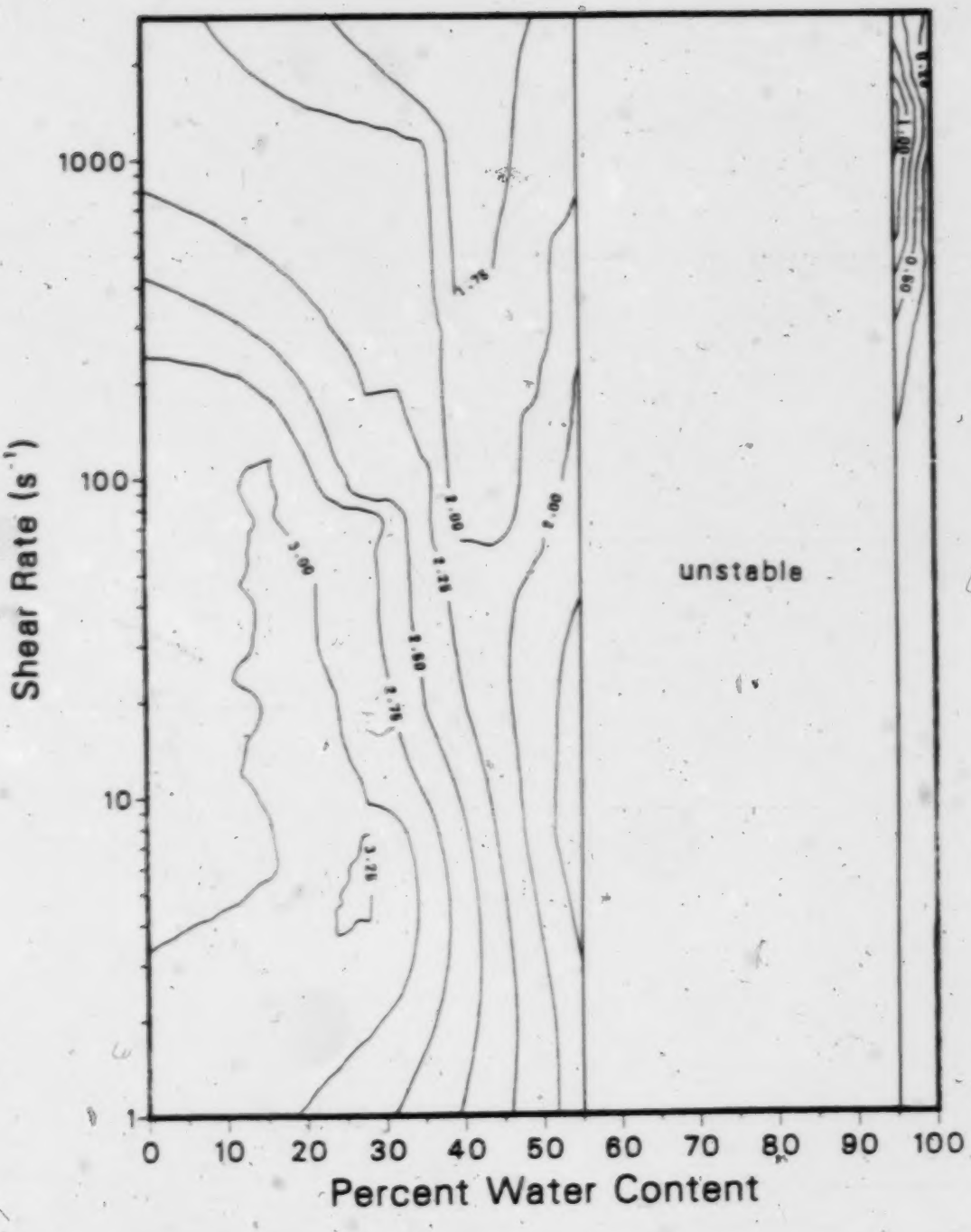

Figure 4.6. Log_{10} viscosity as a function of water content and shear rate for Wainwright B emulsions at 23°C.

a constant shear rate, traverse the contour plot on a line parallel to the abscissa axis. For example, at a shear rate of 10 s^{-1}, the viscosity of W/O emulsions increases with increasing water content, attaining a maximum at a water content of about 25%. As the water content is further increased in the W/O/W region, the viscosity declines by more than an order of magnitude. Above water contents of 95%, the emulsions are O/W and the viscosity is very low and unchanging, at the resolution of the plot.

The rheological behavior of a particular emulsion is obtained by following a line parallel to the ordinate axis. For example, an emulsion containing 10% water shows very slight shear thinning behavior for shear rates up to about 200 s^{-1} and stronger shear thinning behavior above this rate.

The FORTRAN program[1] used to determine and plot the contours automatically extrapolates the contours to an internally defined limit. If there is insufficient data in some region, contours will not be drawn. Caution, therefore, should be exercised when interpreting the contours within about one half of an order of magnitude of the extremes of shear rate on the ordinate axis. Also, the temperature reported for each contour plot is a mean value; all the data contoured on a particular plot was obtained at a temperature within 2.5°C of the indicated temperature.

---

[1] as adapted by the University of Alberta Computing Services from R.J. Sampsom, Surface II Graphics System, Computer Services Section, Kansas Geological Survey, n.p., Lawrence, Kansas. 1978.

For Wainwright B (see Figure 4.6), a region of maximum viscosity occurs for water contents approaching 26.5%, at 23°C. For this and lower concentrations, water is the dispersed phase, so while particle sizes are essentially the same (see Figure 4.3), the droplets are becoming increasingly more crowded. Under these concentrated conditions, strong hydrodynamic and non-hydrodynamic interactions would increase the viscosity. Increasing the shear rate under these conditions should eventually overcome any loose structure built-up among the particles resulting in shear thinning behavior.

At higher water concentrations the phase inversion concentration (PIC) is surpassed, and the emulsions are dual, water continuous. Just above the PIC, the viscosity is still high because the dispersed phase droplets (now oil) are quite concentrated. As the water content increases, the dispersed phase becomes less crowded, hydrodynamic interactions are weaker, and the viscosity falls. Emulsions in this region exhibit significant shear thinning. Because of the low continuous phase viscosity, the oil droplets are very mobile and are thus able to flocculate easily. But such structure will be broken down with increasing shear, conducing shear thinning behavior.

At high water contents, the dispersed phase particles are sufficiently separated that there are few interactions, These emulsions exhibit essentially Newtonian behavior; an Einstein-type dependence on dispersed phase content is

likely applicable to these emulsions. Emulsion Wainwright B 95.6% O/W appears to have exhibited shear thickening behavior (see Tables B.41 to B.44 of Appendix B). As the shear rate was increased towards 1500 s^{-1}, the viscosity increased (also see Table B.41 in Appendix B). This anomalous behavior (by comparison to similar emulsions of Wainwright, Epping, and Primrose) remains unexplained and no systematic experimental errors were encountered.

As the temperature of the Wainwright B emulsions is increased (see Figures 4.7, 4.8 and 4.9), the general features exhibited at 23°C remain. However, the region of high viscosity around the PIC shifts towards higher water contents above 40°C. The shift towards higher water contents is consistent with the temperature dependence of the PIC. Ross and Kornbrekke (1981) found that the PIC tends toward 50% as the temperature increases. As the water solubility of the surfactant declines with increasing temperature, a change of morphology will occur. The Wainwright B emulsions containing 28.0%, 34.4%, 42.0% and to a small extent 46.4% water, suffered phase separation. Unfortunately, the design of the Haake viscometer prevents visual confirmation of just when this occurs (phase separation is discovered after the viscometer vessel is partially dismantled for cleaning).

The contour plot of the Epping emulsions at 23°C is quite featureless (see Figure 4.10). The dried oil (0.9% water) appears to have the highest viscosity; similar Epping

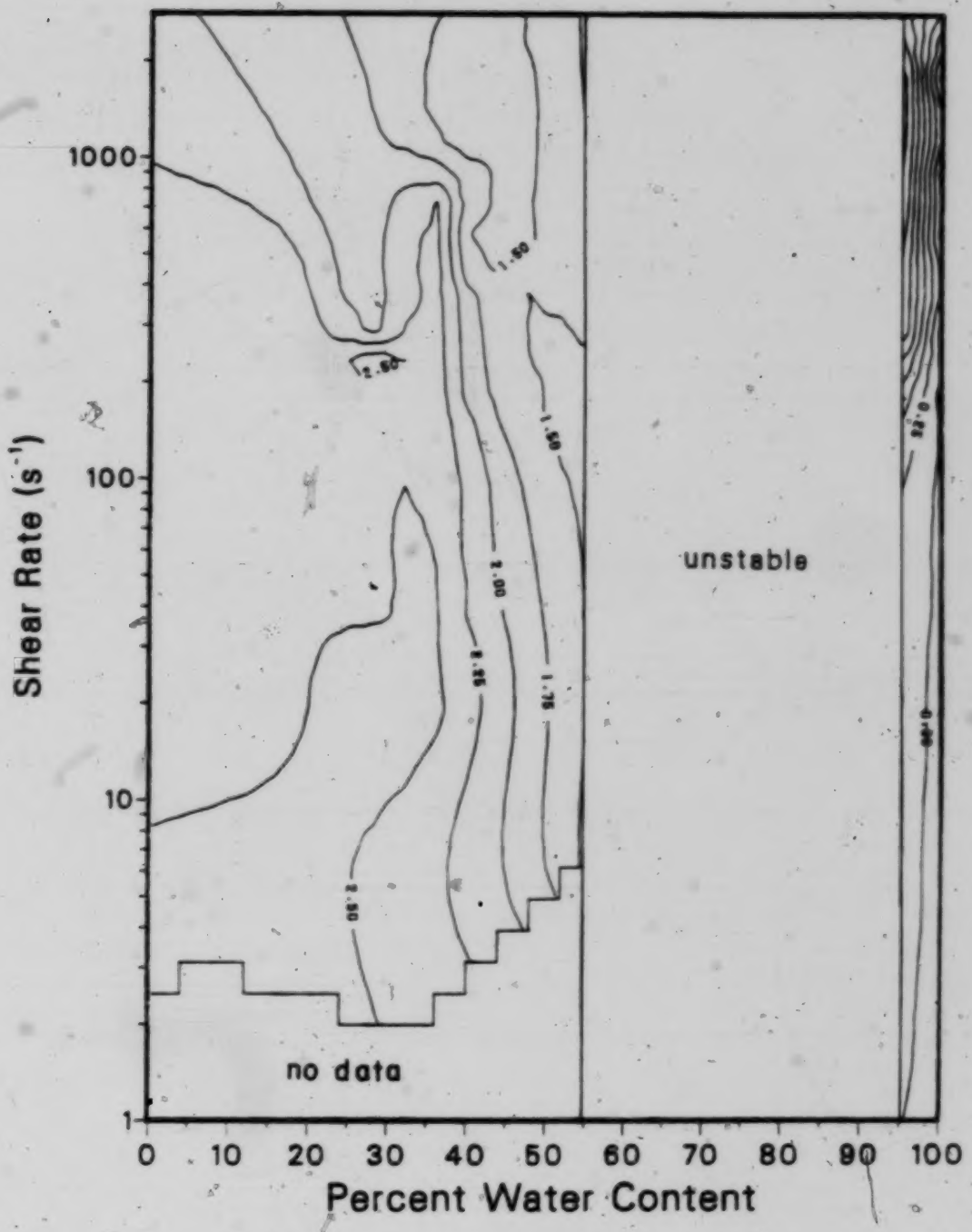

Figure 4.7. Log_{10} viscosity as a function of water content and shear rate for Wainwright B emulsions at 40°C.

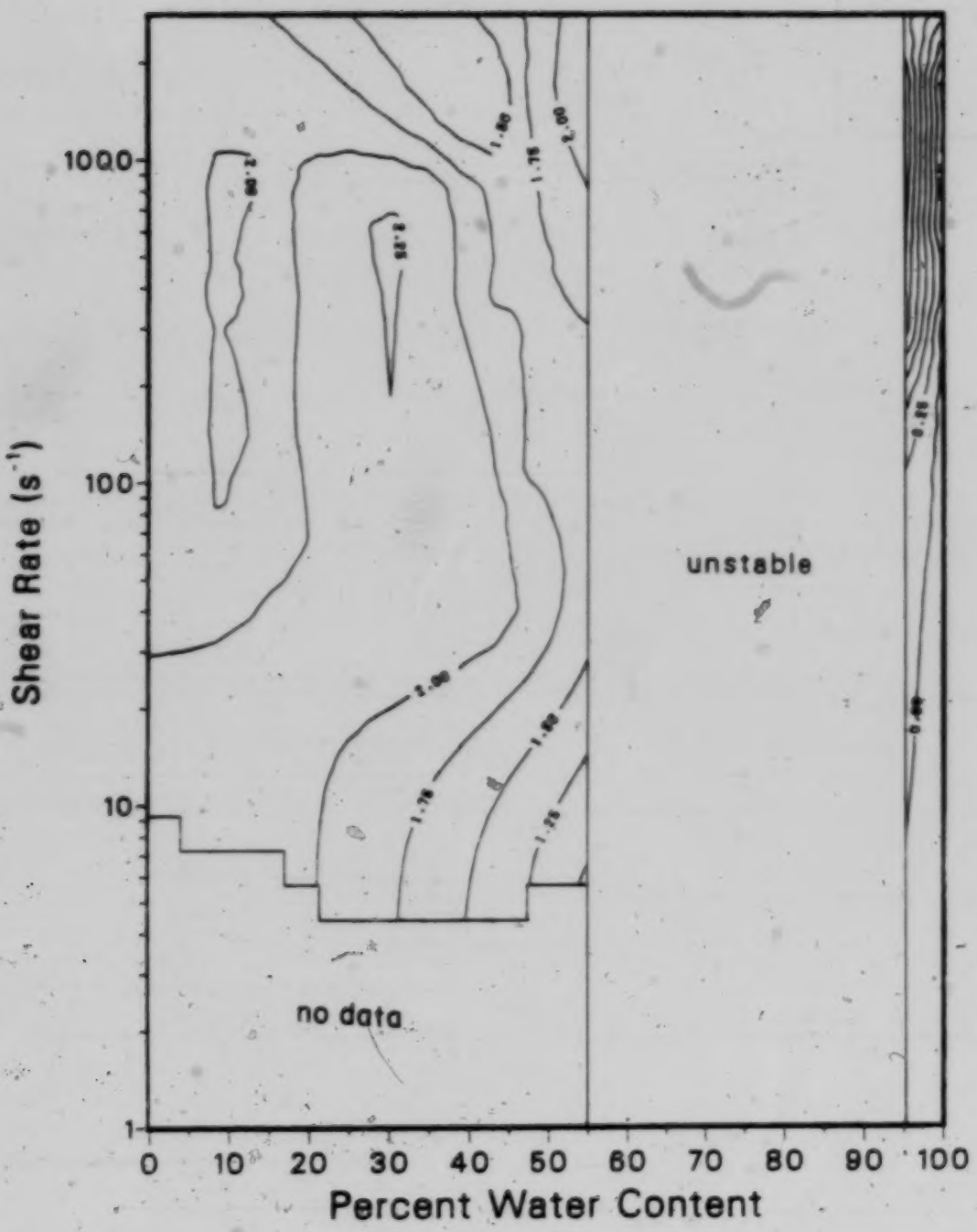

Figure 4.8. Log_{10} viscosity as a function of water content and shear rate for Wainwright B emulsions at 60°C.

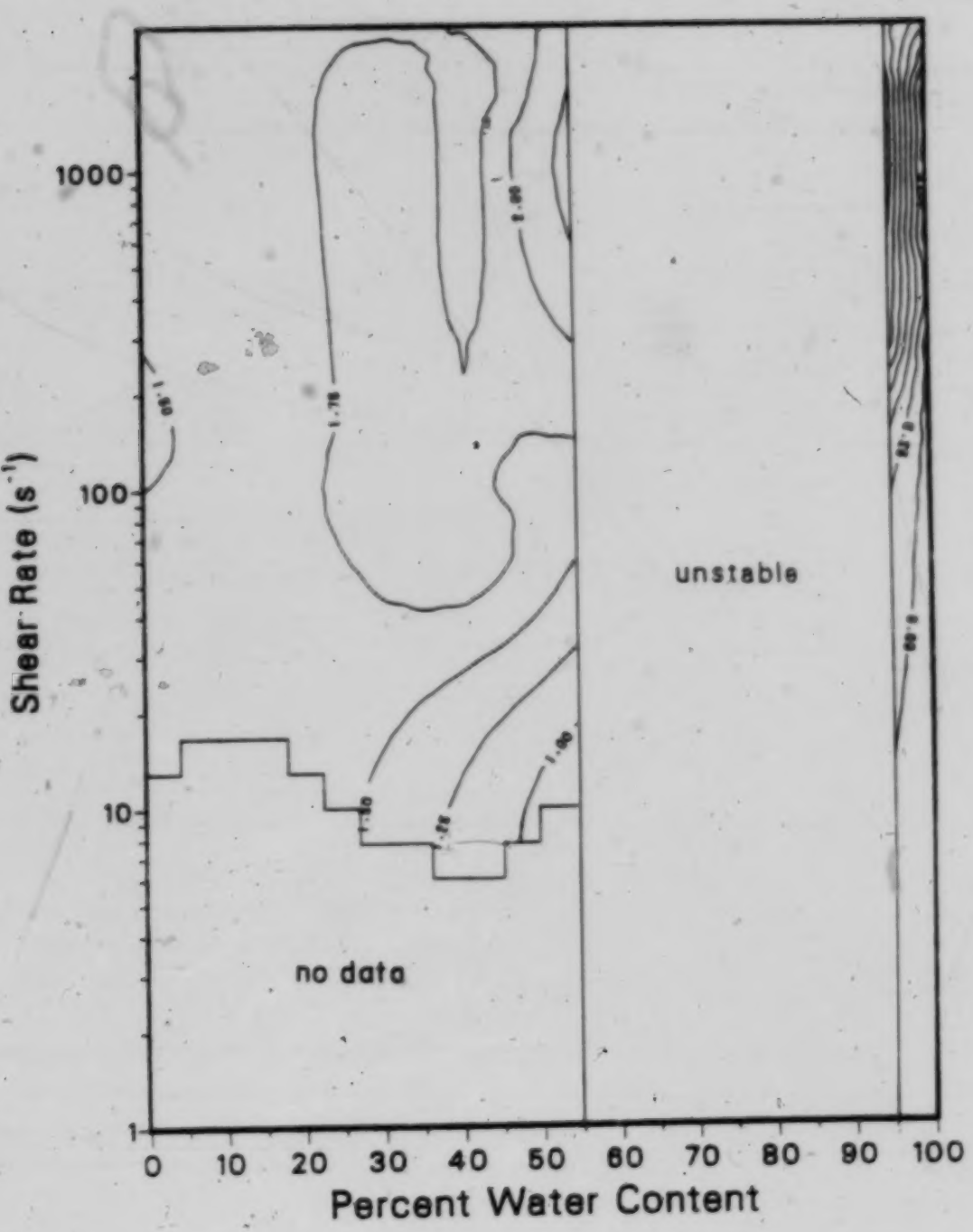

Figure 4.9. Log_{10} viscosity as a function of water content and shear rate for Wainwright B emulsions at 79°C.

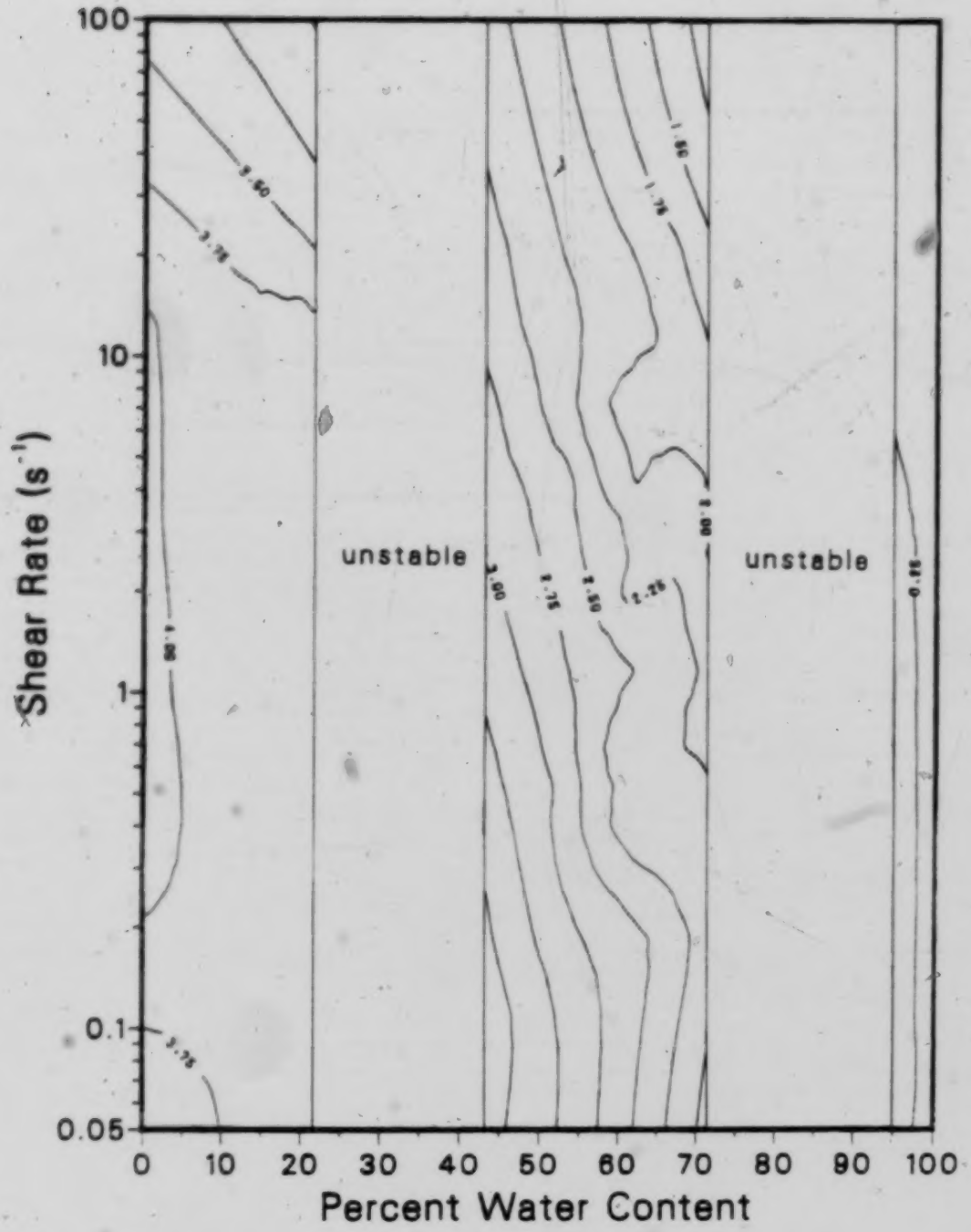

Figure 4.10. Log_{10} viscosity as a function of water content and shear rate for Epping emulsions at 23°C.

emulsions with higher water contents have lower viscosities, an unexpected result (see Tables B.49, B.53, B.57, B.61, and B.65 in Appendix B for details). From the literature, and from data for similar Wainwright B and Primrose emulsions, the viscosity is expected to increase with increasing water content. As only the Haake viscometer was used for this emulsion, and the Brookfield for the others, this apparent result may be due to systematic error.

As the water content of the Epping W/O emulsions increases, the viscosity increases slightly, reaching a maximum for the 20.4% W/O emulsion. In the W/O/W region the viscosity maximum occurs for 43.2% water content and declines as the amount of water in the emulsion increases. This too is an expected result for the same reasons as those discussed for the Wainwright B emulsions. These emulsions also exhibit shear thinning behavior. The fact that the region of unstable emulsions (20.4% to 43.2%) is bounded by emulsions with maximum viscosity implies that this region represents a broad, unstable phase inversion concentration zone rather than a unique PIC, as observed for Wainwright B. Epping emulsions of high water content possess essentially Newtonian behavior like similar Wainwright B emulsions.

Increasing the temperature of the Epping emulsions does not appreciably change the features of the contour plots (see Figures 4.11 to 4.13). All of the dual emulsions, except Epping 70.4% W/O/W, suffered minor phase separation at temperatures approaching 60°C. Consequently, there is no

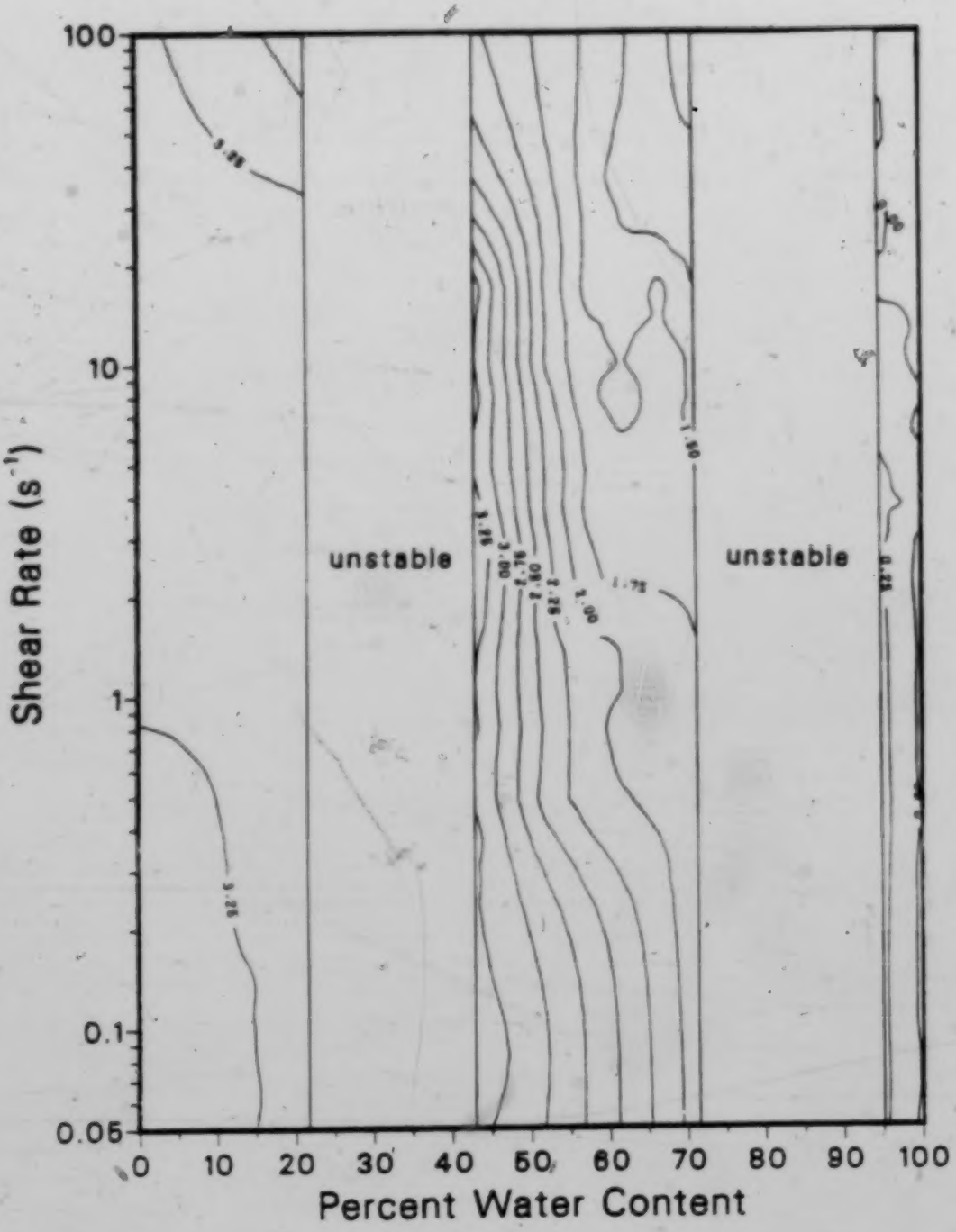

Figure 4.11. Log_{10} viscosity as a function of water content and shear rate for Epping emulsions at 40°C.

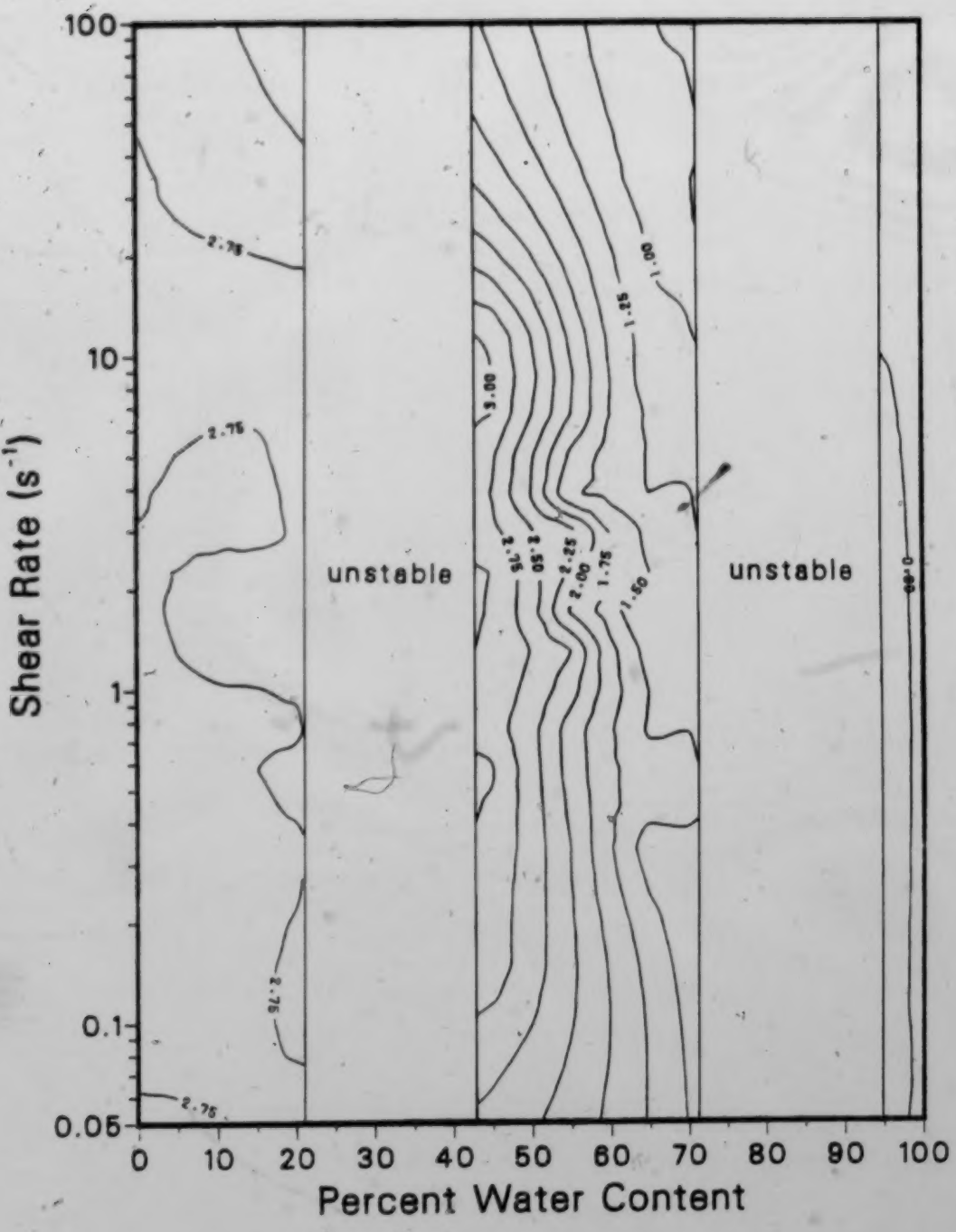

Figure 4.12. Log_{10} viscosity as a function of water content and shear rate for Epping emulsions at 60°C.

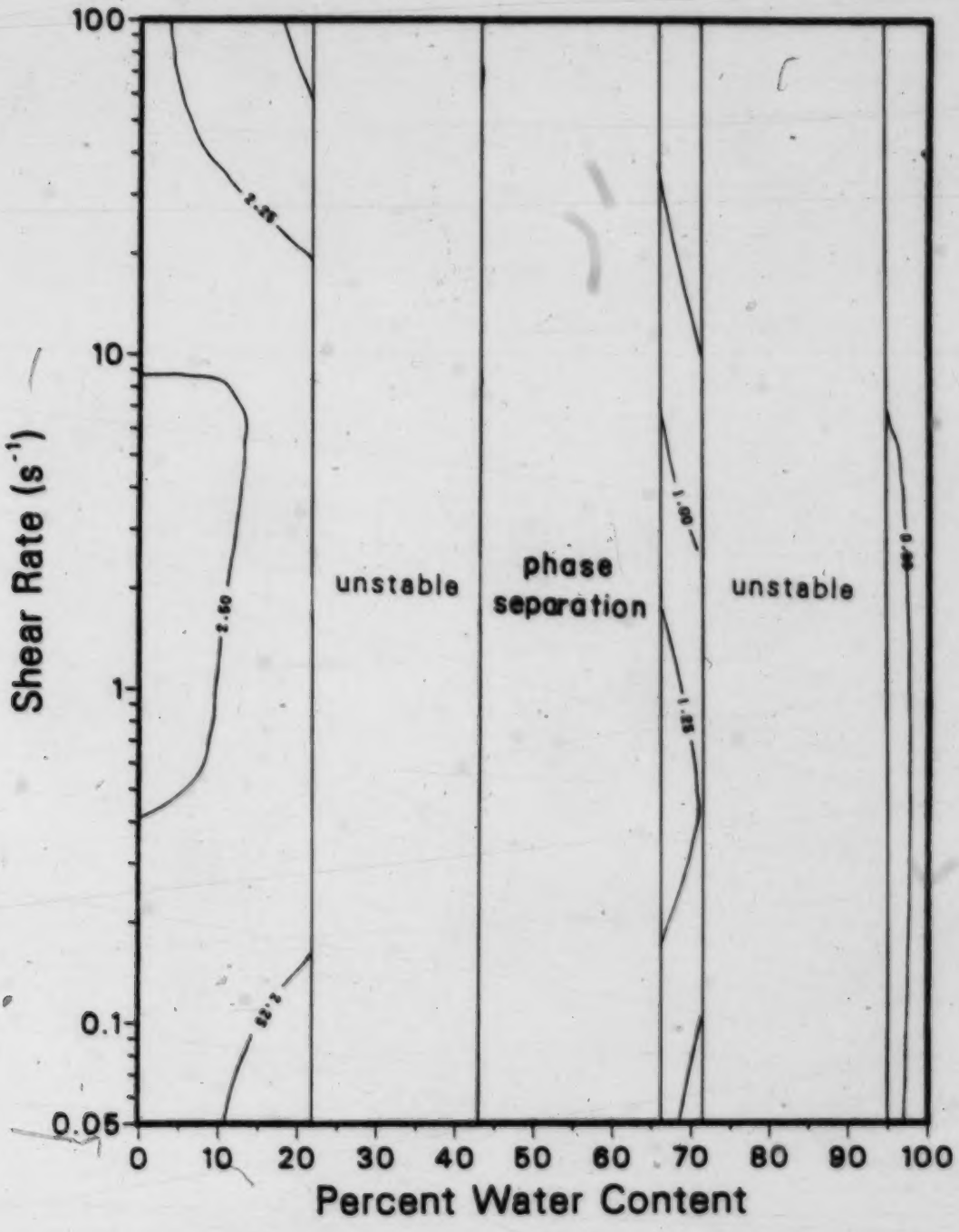

Figure 4.13. Log_{10} viscosity as a function of water content and shear rate for Epping emulsions at 75°C.

data for the Epping emulsions with water contents between 43% and 67%, at 75°C. Epping 43.2% begins to separate at 40°C, suggesting that the phase inversion region is shifting towards the 50:50 water to oil ratio.

Much of the above descriptions apply to the Primrose emulsions (see Figures 4.14 to 4.17). As the water content of the emulsions increases the viscosity increases, until the instability region is reached (32% to 40%). Above the instability region, dual emulsions exhibiting shear thinning behavior exist. The viscosity of the emulsions also decreases as the water content increases, and for this oil, there is a smooth transition from water continuous dual emulsions to water continuous simple emulsions at about 72%. This occurs because the size of the water droplets in the dispersions of 72% or more are too small to accommodate the similarly sized secondary droplets.

Primrose dual emulsions also suffered phase separation, but not to the same degree as the Epping and Wainwright B dual emulsions. Primrose 44.8% and 48% both suffered some separation while being heated from 43°C to 60°C. The separation was more significant for Primrose 44.8% emulsion above 60°C. This again suggests shifting of the instability zone, and degradation above the temperature of formation. Generally though, the Primrose emulsions were less sensitive to thermal degradation, perhaps due to the presence of natural surfactants.

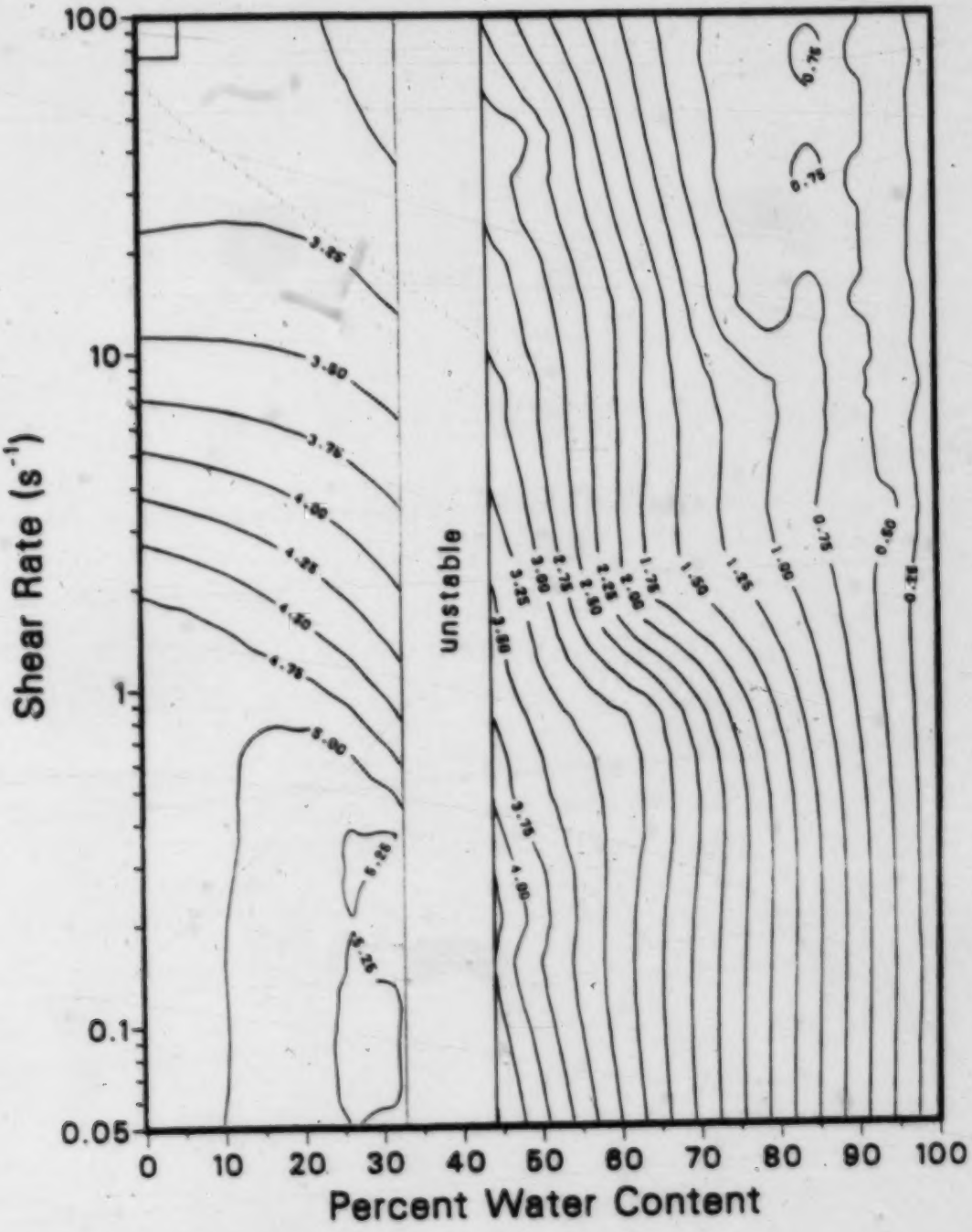

Figure 4.14. Log_{10} viscosity as a function of water content and shear rate for Primrose emulsions at 23°C.

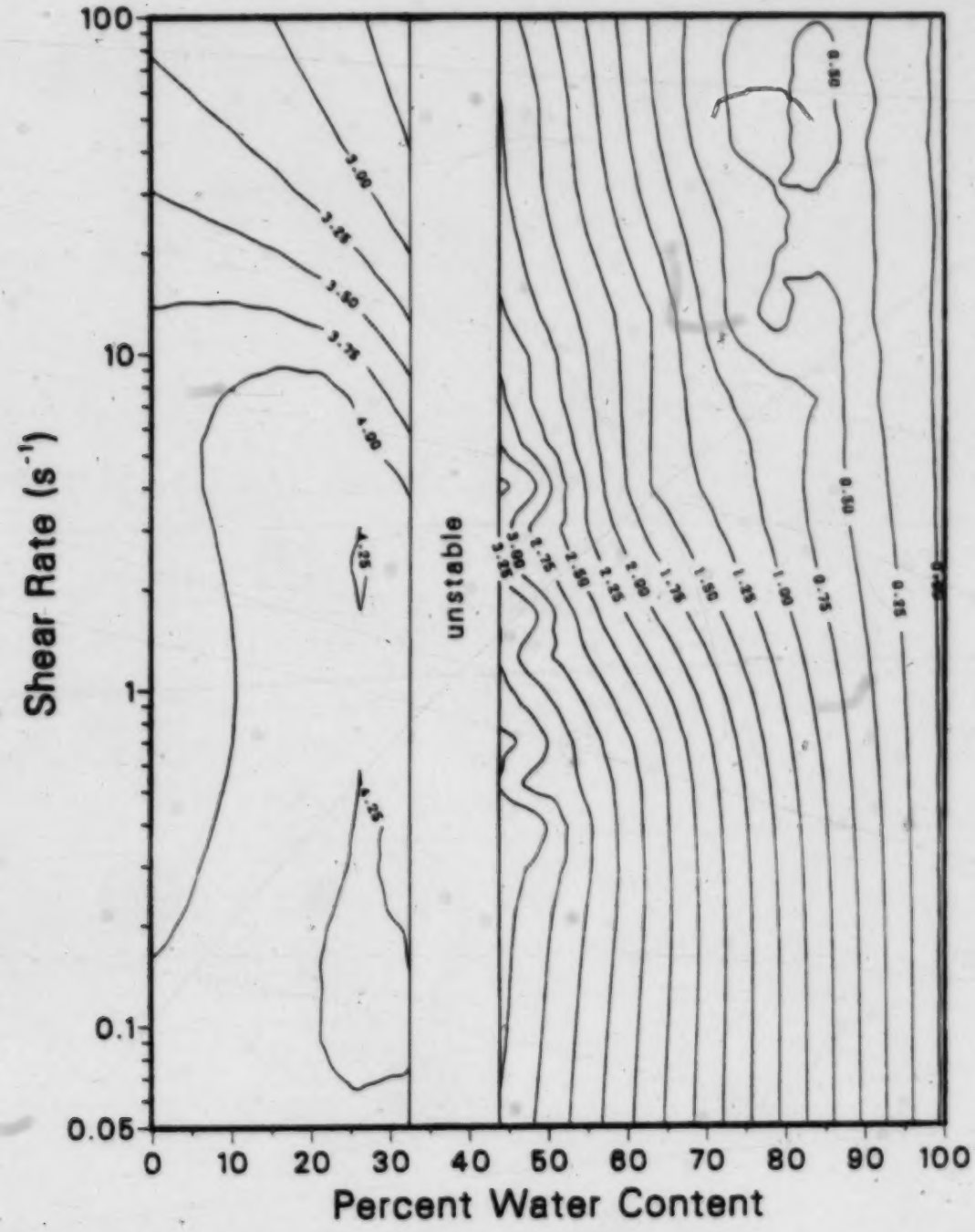

Figure 4.15. Log_{10} viscosity as a function of water content and shear rate for Primrose emulsions at 43°C.

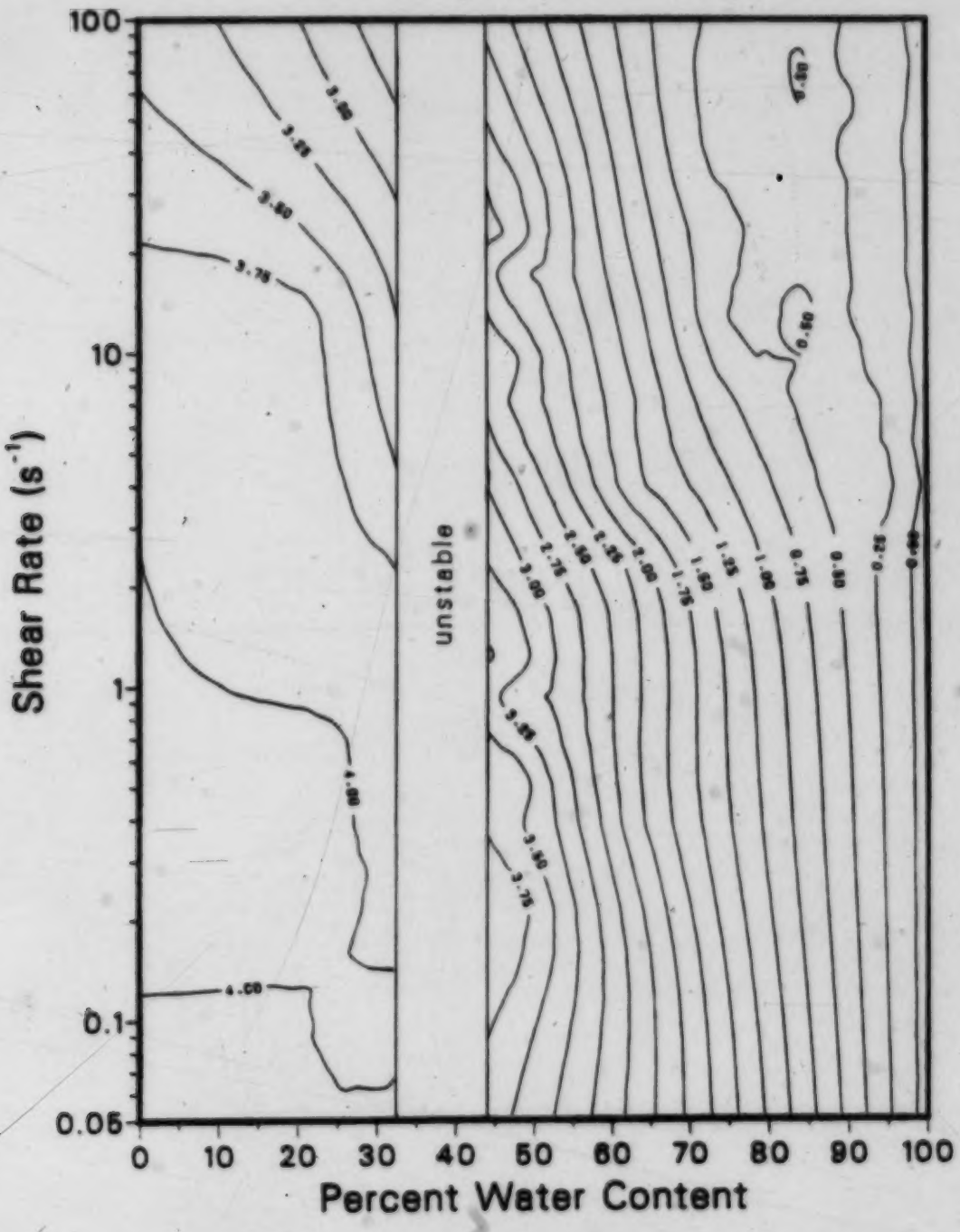

Figure 4.16. Log_{10} viscosity as a function of water content and shear rate for Primrose emulsions at 53°C.

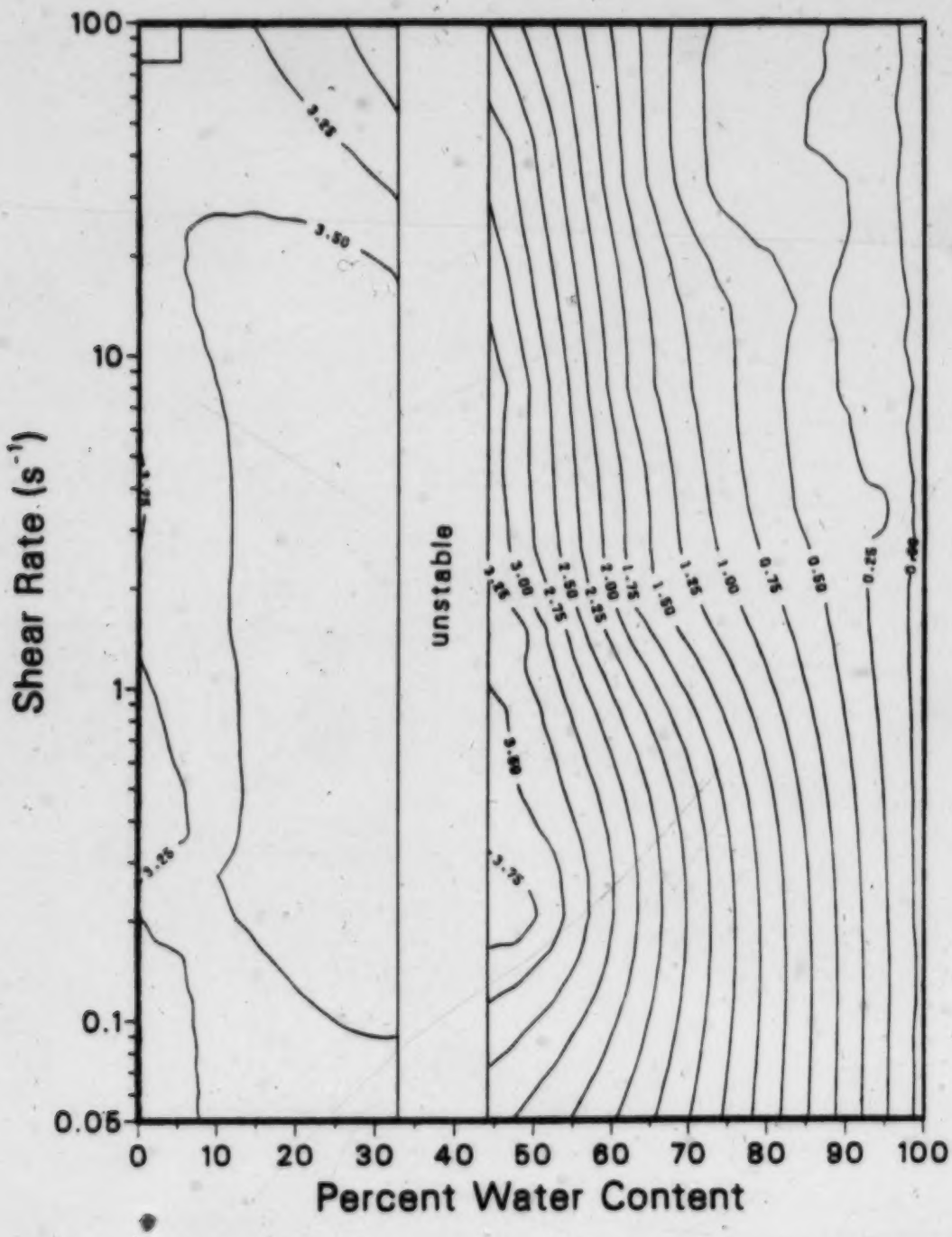

Figure 4.17. Log_{10} viscosity as a function of water content and shear rate for Primrose emulsions at 63°C.

Characterization of the rheological behavior of the emulsions was achieved by fitting the power law model to the data. This was appropriate since the second term of equation A.9 (of Appendix A) was negligibly small (κ' was very small). Employing a logarithmic transformation, the power law model was fitted to the data by linear regression (correlation coefficients squared of a least 0.95, and often 1.00 were obtained). The dependence of the power law coefficients on temperature, emulsion water content, morphology and oil type was then examined.

For each emulsion, the consistency index and the shear thinning index were determined from the shear stress and shear rate data of Appendix B. Figures 4.18, 4.19, and 4.20 show the dependence of the shear thinning index as a function of temperature and water content. Each line in Figure 4.18, for example, indicates the temperature dependence of a particular emulsion. Since there are at most four datum points for each curve, the points are connected rather than curve-fit with a best-fit line or curve, indicating, therefore, trends only.

Each of the dried oils shows slightly shear thinning behavior, as do all of the low dispersed phase content Primrose emulsions; this behavior is independent of temperature. The Epping and Wainwright B W/O emulsions have very slightly shear thinning, almost Newtonian, behavior, which is independent of temperature (see Figures 4.18 and 4.19). With the exception of the anomalous Wainwright B

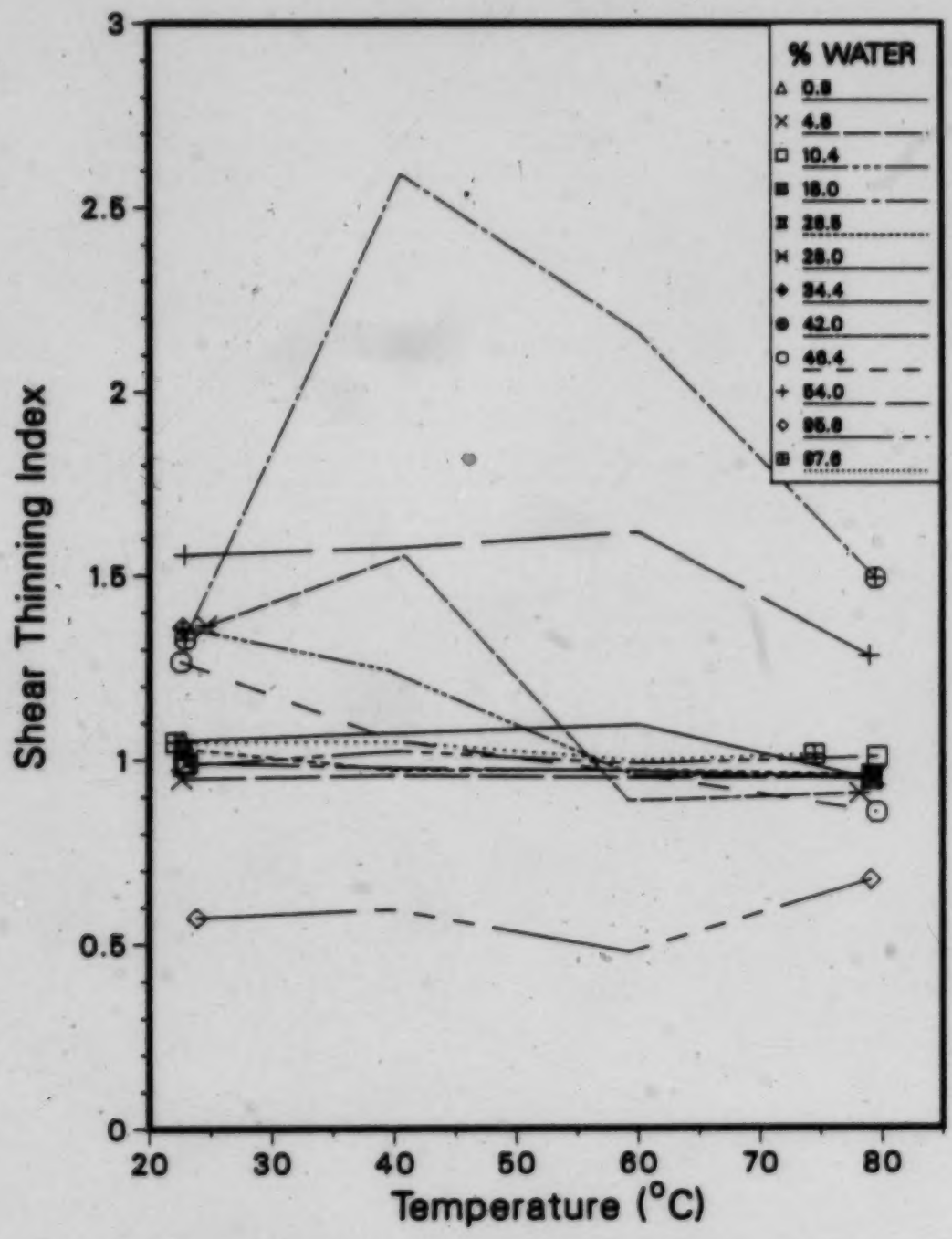

Figure 4.18. Shear thinning index as a function of temperature and water content for Wainwright B emulsions.

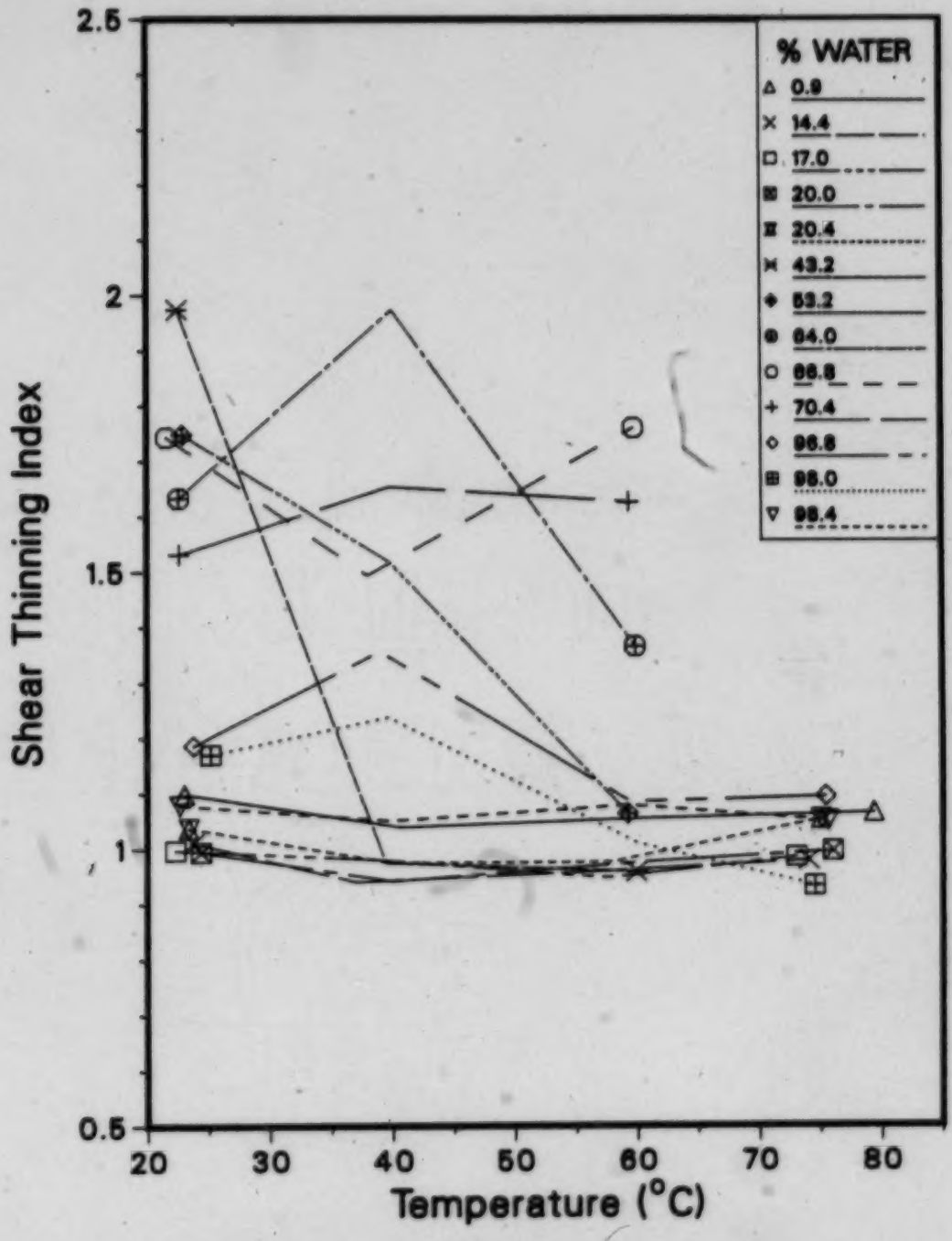

Figure 4.19. Shear thinning index as a function of temperature and water content for Epping emulsions.

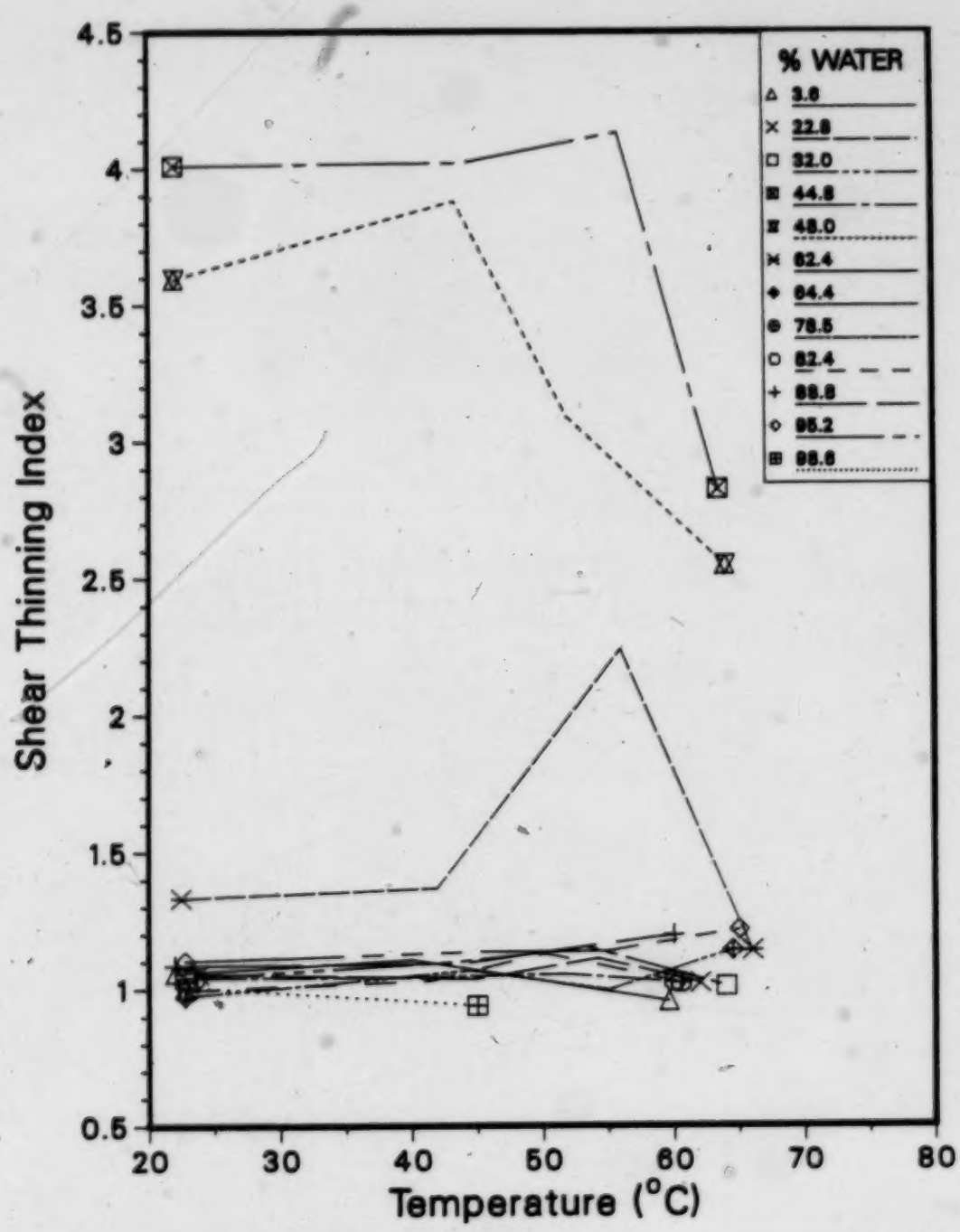

Figure 4.20. Shear thinning index as a function of temperature and water content for Primrose emulsions.

95.6% emulsion, all of the Epping and Wainwright B O/W emulsions have essentially temperature independent shear thinning behavior.

The dual emulsions of each oil show varying degrees of shear thinning behavior at low temperature. As the temperature rises the shear thinning index varies, but generally seems to decline towards unity, as indicated in Figures 4.18, 4.19, and 4.20. For the Wainwright B and Epping emulsions, the variability of the shear thinning index begins at about 40°C and for the Primrose emulsions, begins between 40°C and 60°C. This suggests that a morphological change begins at this temperature, implying that the emulsion's formation temperature is important to the stability of dual emulsions.

Figures 4.21, 4.22, and 4.23 show the dependence of the consistency index on temperature and water content for the Wainwright B, Epping, and Primrose emulsions respectively. The consistency indices of the emulsions of each oil appear to be proportional to the inverse of the temperature: the data suggest a non-linear relationship, but more data would be needed to confirm this. There are a few exceptions to this trend (for example, Epping 70.4% and Wainwright B 42.0%), but generally, the consistency index decreases with increasing temperature.

Most equations proposed in the literature to describe the viscosity of a suspension are in the form of some function of concentration multiplied by the viscosity of the

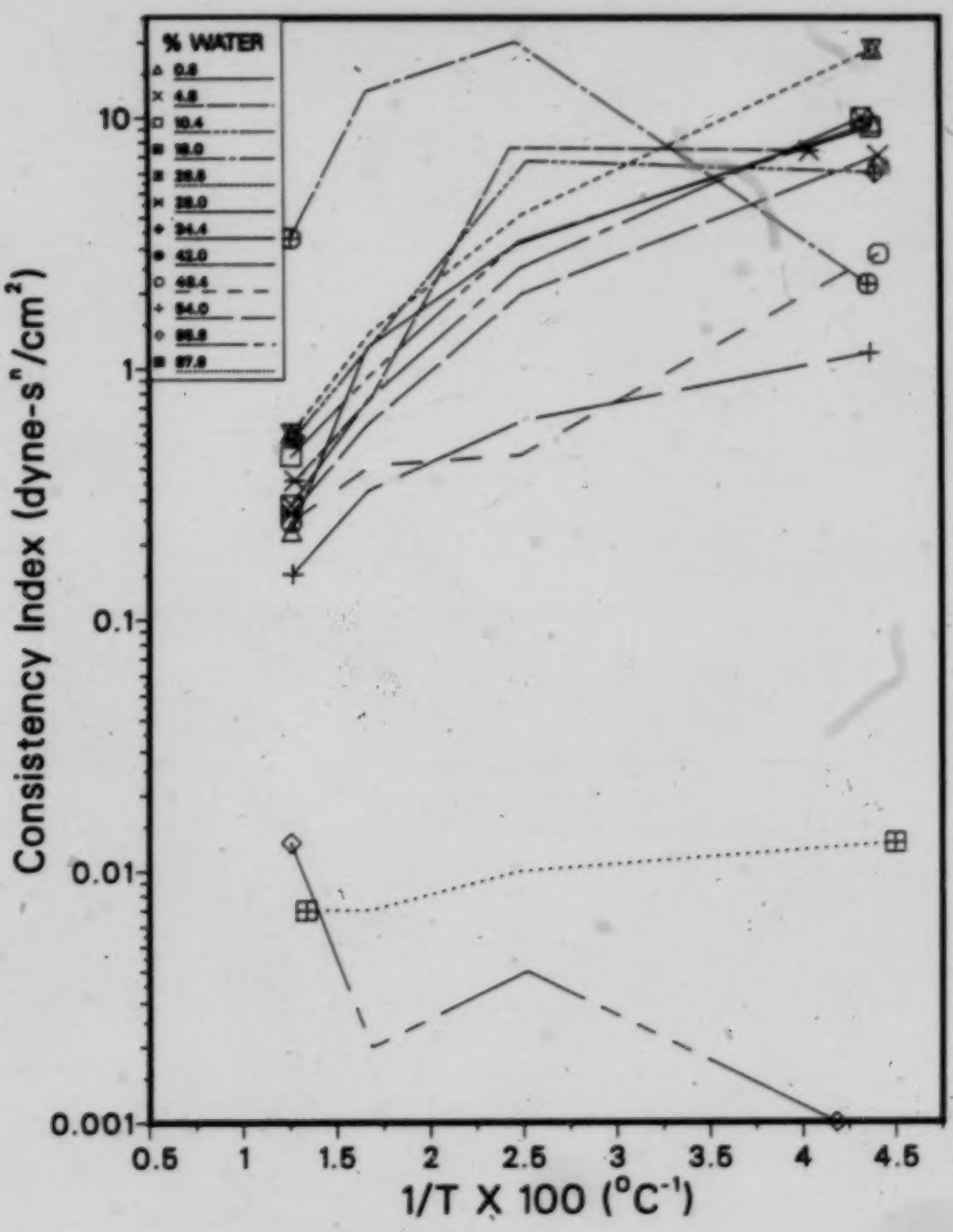

Figure 4.21. Consistency index as a function of inverse temperature and water content for Wainwright B emulsions.

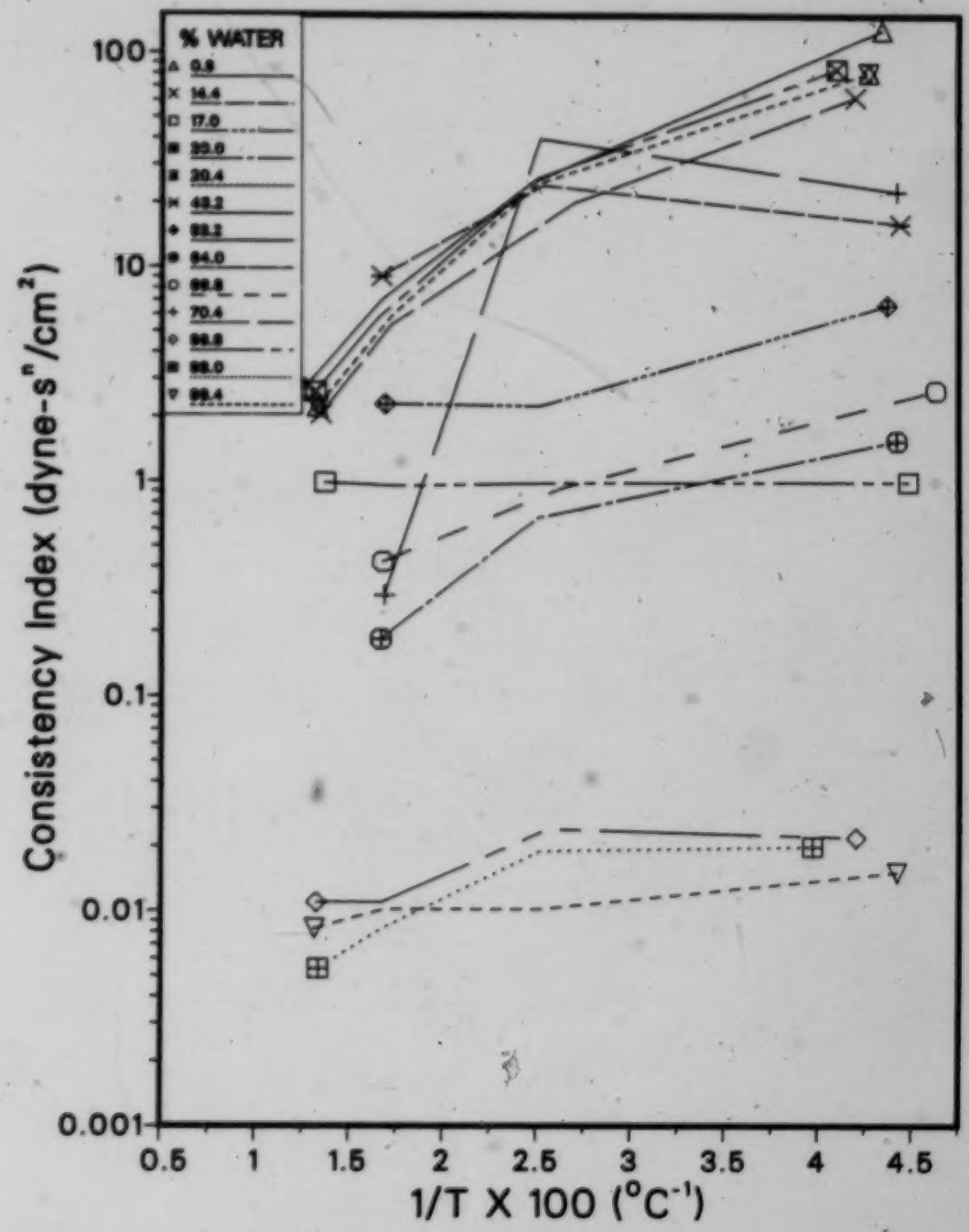

Figure 4.22. Consistency index as a function of inverse temperature and water content for Epping emulsions.

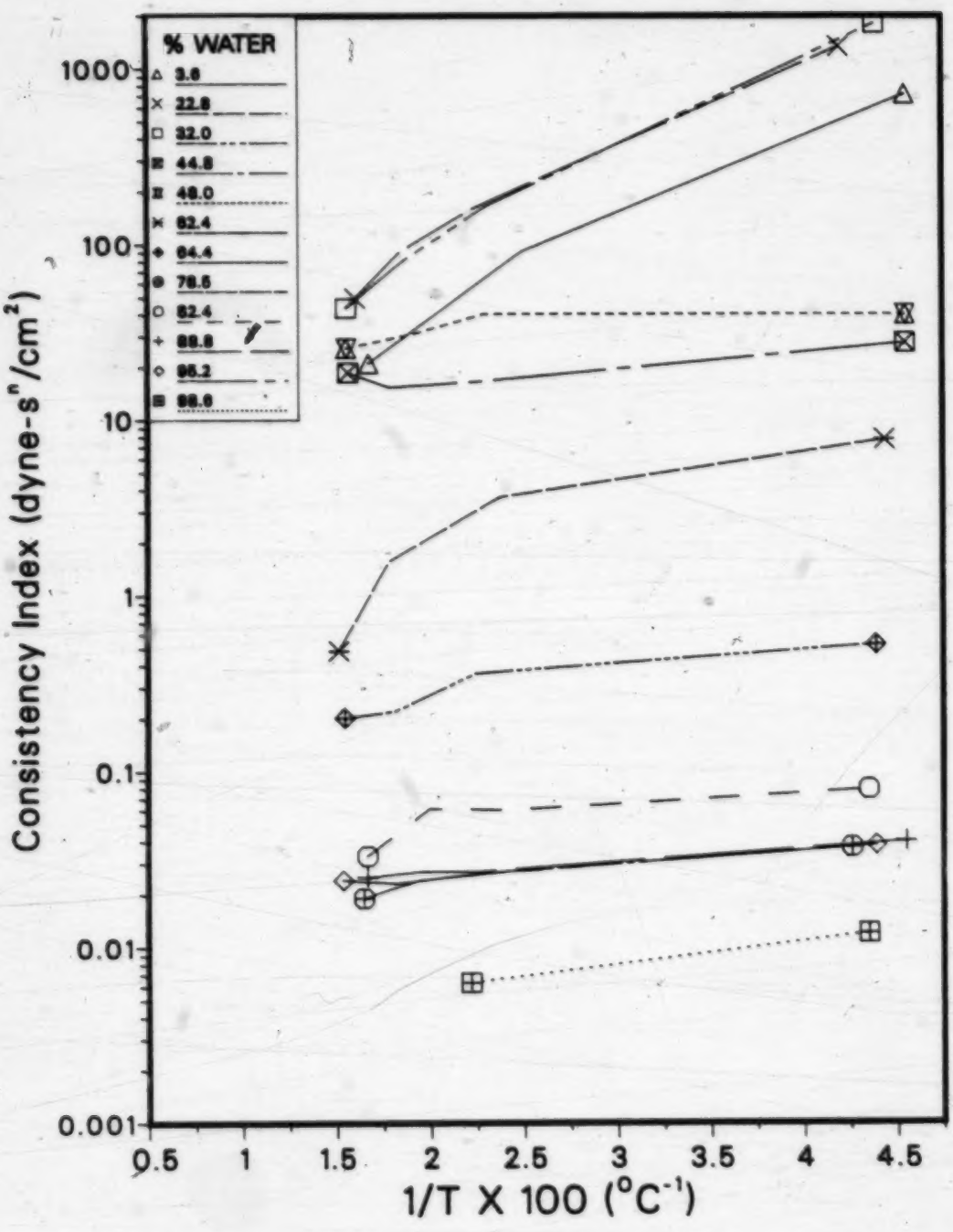

Figure 4.23. Consistency index as a function of inverse temperature and water content for Primrose emulsions.

continuous phase. The behavior of the observed consistency indices conforms to the general fact that fluid viscosity decreases with increasing temperature; but the data also imply that the consistency index is a function of the water content and hence, a function of the emulsion morphology. The simple emulsions (W/O and O/W) have viscosities similar to their respective continuous phase but modified by the hydrodynamic and non-hydrodynamic influences of the dispersed phase interactions. These observations are consistent with the findings of Griskey and Green (1968). By dimensional analysis, they found that fluids for which the shear thinning index is essentially independent of temperature, the consistency index is dependent on the viscosity of the continuous phase. These observations also apply to the water continuous dual emulsions for which the dispersed phase content is low enough: this includes the Epping and Primrose dual emulsions with at least 64.0% and 64.4% water respectively.

Griskey and Green also suggest that the consistency index will increase as the concentration of the dispersed phase increases. This is also observed, as illustrated most clearly on the contour plots. The dependence of the consistency index on the inverse of the temperature as predicted by Grisky and Green can be ascribed to the temperature sensitivity of the artificial surfactant and the consequential temperature dependence of the system morphology. However, the morphological change in the dual

emulsions has a greater effect on the shear thinning index than on the consistency index.

5. Conclusions

Based upon the examination of the morphology, particle size distribution, and rheological behavior of emulsions of Wainwright B, Epping, and Primrose dewatered crude oils, over temperatures ranging from 23°C to 79°C, the following conclusions can be drawn:

1. Each of the oils was emulsified with the nonionic surfactant Triton X-100 (0.7% by volume) and exhibited a water content dependent morphology. For low dispersed phase content, simple emulsions were produced: either W/O or O/W. For emulsions with similar water and oil contents, water continuous dual emulsions were formed.
2. The dispersed phase droplet size distribution of the simple emulsions and of the secondary particles of the dual emulsions were similar. The primary droplet size distribution of the dual emulsions was considerably broader than that for the simple emulsions.
3. Wainwright B exhibited a phase inversion concentration, whereas Epping and Primrose exhibited a region of unstable emulsions which plays the role of the phase inversion concentration.
4. As the dispersed phase content increases, the viscosity of the emulsion increases, reaching a maximum at the division between oil continuous and water continuous emulsions. Shear thinning behavior was generally observed but was more pronounced for the dual emulsions.
5. The descriptions in points 3 and 4 remain essentially

unchanged at elevated temperatures. But, the stability of the a dual emulsion appears to depend on the temperature at which it was created; if the emulsion is heated beyond this temperature, phase separation occurs.

6. The rheological behavior of the emulsions is well described by the power law model. Of the power law coefficients, the shear thinning index was observed to be dependent on temperature for dual emulsions and independent of temperature for simple emulsions. The consistency index was observed to be a function of the continuous phase viscosity and hence, temperature, and the dispersed phase concentration for all of the emulsions.
7. Dual emulsions exhibited a strong dependence on the primary particle size and evolution of morphology.

Recommendations

1. These tests should be expanded to include oils from other classifications and to consider the surfactant concentration and type as variables.
2. Data over a broader range of temperatures and at smaller temperature intervals should be obtained to permit a quantitaive correlation of the power law coefficients with temperature to be deduced.

Bibliography

Adler, P.M. 1981. Interaction of Unequal Spheres: I. Hydrodynamic Interaction: Colloidal Forces. J. Coll. Int. Sci. 84:461-474.

Allan, R.S. and Mason, S.G. 1962. Particle Motions in Sheared Suspensions: XIV. Coalecence of Liquid Drops in Electric and Shear Fields. J. Coll. Sci. 17:383-408.

Allen, T. 1974. Particle Size Measurement, 2nd ed. Chapman and Hall, London.

Allen, T. 1968. Particle Size Measurement. Chapman and Hall, London.

Ambwani, D.S. and Fort Jr., T. 1979. "Pendant Drop Technique for Measuring Liquid Boundary Tensions," in Surface and Collid Science, vol. 11: Experimental Methods, ed. R.J. Good and R.R. Stromberg. Plenum Press, New York.

American Society for Testing and Materials. ASTM D971-82 Standard Test Method for Interfacial Tension of Oil Against Water by the Ring Method. 1982 Annual Book of ASTM Standards, pt.23: Petroleum Products and Lubricants. p. 451-453.

Bartok, W. and Mason, S.G. 1957. Particle Motions in Sheared Suspensions: V. Rigid Rods and Colliosion Doublets of Spheres. J. Coll. Sci. 12:243-262.

Bartok,W. and Mason, S.G. 1959. Particle Motions in Sheared Suspensions: VIII Singlets and Doublets of Fluid Spheres. J. Coll. Sci. 14:13-26.

Batchelor, G.K. and Green, J.T. 1972. The Determination of the Bulk Stress in a Suspension of Spherical Particles to Order C^2. J. Fluid Mech. 56:401-427.

Bauch and Lomb Omnicon Alpha™ Image Analysis System Operator's Manual. Catalogue No. 37-20-09. Rochester, New York. 1976.

Becher, P. 1965. Emulsions: Theory and Practice. 2nd ed., Reinhold Publishing Corp., New York.

Bennett, H., Bishop Jr., J.L., Wulfinghoff, M.E. 1968. Practical Emulsions. vol.1, Chemical Publishing Co. Inc., New York.

Bird, R.B., Stewart, W.E. and Lightfoot, E.N. 1962.

Transport Phenomena. John Wiley and Sons, New York.

Brenner, H. 1972. Suspension Rheology. Prog. in Heat and Mass Transfer. 5:89-129.

Brookfield Engineering Laboratories, Inc. n.d. Brookfield Synchro-Lectric Viscometer, Shear Rate and Shear Stress Formulas. Stoughton, Mass.

Cadle, R.D. 1965. Particle Size. Reinhold Publishing Corp., New York.

Castellan, G.W. 1971. Physical Chemistry, 2nd ed. Addison-Wesley Publising Corp. n.p.

Coleman, B.D., Markovitz, H., and Noll W. 1968. Viscometric Flows of Non-Newtonian Fluids. Springer-Verlag, Berlin.

de Boer, J.H. 1936. The Influence of van der Waals' Forces and Primary Bonds on Binding Energy, Strenth and Orientation, with Special Considerations to Some Artificial Resins: Part I. The Calculation of Sublimation Energies. Trans. Faraday Soc. 32:10-38.

de Vries, A.J., 1963. "Effect of Particle Aggregation on the Rheological Behavior of Disperse Systems," in Rheology of Emulsions, ed. P. Sherman. Proc. Symp. Brit. Soc. Rheology, Oct. 1962, The Macmillan Co., New York. pp.43-58.

Derjaguin, B.V. and Landau,L., Acta Phys. Chem. USSR, 14:663 (1941), and Verwey, E.J.W. and Overbeek, J.Th.G., Theory of the Stability of Lyophobic Colliods, Elsevier (1948), cited by D.J. Shaw, Introduction to Colloid and Surface Chemistry, 3rd ed., Butterworths, Toronto (1980). p. 184.

Dickinson, E. 1981. Interpretation of Emulsion Phase Inversion as a Cusp Catastrophe. J. Coll. Int. Sci. 84:284-287.

Dickinson, E. 1982. Thermodynamic Aspects of Emulsion Phase Inversion J. Coll. Int. Sci. 87:416-423.

Einstein, A. 1906. Ene neue Bestimmung der Molekuldimensionen Annln. Phys. 19:289-306, cited by A. Einstein, Investigations on the Theory of Brownian Movement. Metheun and Company, Ltd., London. 1926.

Einstein, A. 1926. The Brownian Movement, Methuen and Company, Ltd., London.

Eveson, G.F. and Mill, C. ed. 1959. "Rheology of Disperse Systems," cited by P. Becher in Emulsions: Theory and

Practice, 2nd ed. Reinhold Publishing Corp., New York. 1965. p. 82.

Farris, R.J. 1968. Predictions of the Viscosity of Multimodal Suspensions from Unimodal Viscosity Data. Trans. Soc. Rheol. 12:281-301.

Feynman, R.P., Leighton, R.B., and Sands, M. 1966. The Feynman Lectures on Physics, vol. 2: Mainly Electromagnetism and Matter. Addison-Wesley Publishing Co., Reading, Mass.

Flock, D.L. 1977. unpublished communication.

Frankel, N.A. and Acrivos, A. 1967. On the Viscosity of Concentrated Suspensions of Solid Spheres. Chem. Eng. Sci. 18:713-732.

Goldsmith, H.L. and Mason, S.G. 1962. The Flow of Suspensions Through Tubes: I. Singlet Spheres, Rods, and Discs. J. Coll. Sci. 17:448-476.

Greerco Corporation. n.d. Gifford-Wood Homogenizer Mixer, Model 1-LV Operating Manual. n.p.

Griskey, R.G. and Green, R. G. 1968. Rheological Behavior of Dilatant (Shear Thickening) Fluids. Part 1: Experimental and Data. Trans. Soc. Rheol. 12:13-25.

Griskey, R.G. and Green, R. G. 1968. Rheological Behavior of Dilatant (Shear Thickening) Fluids. Part 2: Mechanism and Theory. Trans. Soc. Rheol. 12:27-37.

Groves, M.J. 1980. Particle Size Characterization in Dispersions. J. Disp. Sci. Tech. 1:97-124.

Guth, E. and Simha, R. 1936. Kolloid-Z. 74:266, cited by P. Becher, Emulsions: Theory and Practice, 2nd ed. Reinhold Publishing Corp., New York, 1965. p. 62.

Hamaker, H.C. 1937. The London-van der Waals Attraction Between Spherical Particles. Physica. 4:1058-1072.

Harris, J. 1977. Rheology and Non-Newtonian Flow. Longman Group Ltd., London.

Hecht, E. and Zajac, A. 1976. Optics. Addison-Wesley Publishing Co., Reading, Mass.

Herrmann, C.U., Klar, G., and Kahlweit, M. 1980. On the Phase Inversion of H_2O-Oil-Nonionic Surfactant Systems and Related Phenomena. J. Coll. Int. Sci. 82:6-13.

Israelachvili, J.N. and Ninham, B.W. 1977, "Intermolecular

Forces – the Long and Short of It," in Colloid and Interface Science, vol. 1, pp. 15-26, ed. M. Kerker, R.L. Rowell, and A.C. Zettlemoyer. Academic Press, New York.

Jeffrey, G.B. 1923. The Motion of Ellipsoidal Particles Immersed in a Viscous Fluid. Proc. Roy. Soc. A102:161-179.

Kell, G.S. 1967. Precise Representation of Volume Properties of Water at One Atmosphere. J. Chem. Eng. Data. 12:66-69.

Kitchener, J.A. and Musselwhite, P.R. 1968 "The Theory of Stability of Emulsions," in Emulsion Science, ed. P. Sherman. Academic Press, London.

Krieger, I.M. 1968. Shear Rate in the Couette Viscometer. Trans. Soc Rheol. 12:5-11.

Krieger, I.M. and Dougherty, T.J. 1959. A Mechanism for Non-Newtonian Flow in Suspensions of Rigid Spheres. Trans. Soc. Rheol. 3:137-152.

Krieger, I.M. and Elrod, H. 1953. "Direct Determination of the Flow Curve of Non-Newtonian Fluids: II. Shearing Rate in the Concentric Cylinder Viscometer. J. App. Phys. 24:134-136.

Krieger, I.M. and Maron, S.H. 1952. Direct Determination of the Flow Curves of Non-Newtonian Fluids. J. App. Phys. 23:147-149.

Landau, L.D. and Lifshitz, E.M. 1959. Fluid Mechanics. Pergamon Press, Oxford.

Lifshitz, E.M. 1956. The Theory of Molecular Attractive Forces Between Solids. Soviet J.E.P.T. 2:73-83.

London, F. 1930. Cited by D.J. Shaw, Introduction to Colloid and Surface Chemistry, 3rd ed. Butterworths, Toronto. 1980. p. 188.

Mahanty, J. and Ninham, B.W. 1976. Dispersion Forces. Academic Press, London.

Manley, R. St. J. and Mason, S.G. 1952. Particle Motions in Sheared Suspensions: II. Collisions of Uniform Spheres. J. Coll. Sci. 7:354-369.

Mason, S.G. 1977. "Orthokinetic Phenomena in Disperse Systems," in Colloid and Interface Science, vol. 1, pp. 293-303, ed. M. Kerker, R.L. Rowell, and A.C. Zettlemoyer. Academic Press, New York.

Mercer, T.T. 1973. Aerosol Technology in Hazard Evaluation. Academic Press, New York.

Mitsui, T., Nakamura, S., Harusawa, F., and Machida, Y. 1972. Changes in the Interfacial Tension with Temperature and Their Effects on Particle Sizes and Stability of Emulsions. Kolloid-Z. U. Z. Polymere. 250:227-230.

Napper, D.H. 1977. "Steric Stabilization," in Colloid and Interface science, vol. 1, pp. 413-430, ed. M. Kerker, R. L. Rowell, and A. C. Zettlemoyer. Academic Press, New York.

Napper, D.H. and Hunter, R.S. 1975 "Hydrosols", in Physical Chemistry, Ser. 2, vol. 7, ed. M. Kerker. Butterworths, London. pp. 201-213.

Neter, J., and Wasserman, W. 1974. Applied Linear Statistical Models. Richard D. Irwin, Inc., Homewood, Illinois.

Oliver, D.R. and Ward, S.G. 1953. A Relationship Between Relative Viscosity and Volume Concentration of Stable Suspensions of Spherical Particles. Nature. 171:396-397.

Oosterbroek, M. and Mellema, J. 1981. Linear Viscoelasticity of Emulsions: I. The Effect of an Interfacial Film on the Dynamic Viscosity of Nondilute Emulsions. J. Coll. Int. Sci. 84:14-26.

Overbeek, J. Th. G. 1966. Colloid Stability in Aqueous and Non-Aqueous Media. Disc. Faraday Soc. No. 42. p. 7-22.

Overbeek, J. Th. G. 1977. "Recent Developments in the Understanding of Colloid Stability," in Colloid and Interface Science, vol. 1, pp. 431-445, ed. M. Kerker, R.L. Rowell, and A.C. Zettlemoyer. Academic Press, new York.

Porter, R.S. and Johnson, J.F. 1959. Laminar Flow Degredation of Polyisobutene. J. Phys. Chem. 63:202-205.

Rosen, M.R. 1971. A Rheogram Template for Power Law Fluids: a Technique for Characterizing the Rheological Properties of Emulsions and Polymer Solutions. J. Coll. Int. Sci. 36:350-358.

Rosen, M.R. 1972. A Rheogram Template for Power Law Fluids: II. Rapid Rheological Characterization in a Coaxial Cylinder. J. Coll. Int. Sci. 39:413-417.

Ross, S. and Kornbrekke, R.E. 1981. Change of Morphology of

a Liquid-Liquid Dispersion as a Stochastic Process. J. Coll. Int. Sci. 81:58-68.

Rubin, E. and Radke, C.J. 1979. Dynamic Interfacial Tension Minima in Finite Systems Chem. Eng. Sci. 35:1129-1138.

Sampson, R.J. 1978. Surface II Graphics System, Computer Services Section, Kansas Geological Survey. n.p. Lawrence, Kansas.

Schramm, G. n.d. An Introduction to Rheology and Viscometry Haake Mess-Technik, Karlsrhue, West Germany.

Segré, G. and Silverberg, A. 1961. Radial Particle Displacements in Poiseuille Flow of Suspensions. Nature 189:209-210.

Segré, G. and Silverberg, A. 1962. Behavior of Marcroscopic Rigid Spheres in Poiseuille Flow. J. Fluid Mech. 14:115-135.

Shaw, D.J. 1980. Introduction to Colloid and Surface Chemistry, 3rd ed. Butterworths, Toronto.

Sherman, P., ed. 1968. Emulsion Science. Academic Press, London.

Simha, R. 1940. The Influence of Brownian Movement on the Viscosity of Solutions J. Phys. Chem. 44:25-34.

Stark, P.A. 1970 Introduction to Numerical Methods. Macmillan Publishing Co., Inc., New York.

Stauffer, C.E. 1965. The Measuremwnt of Surface Tension by the Pendant Drop Technique. J. Phys. Chem. 69:1933-1938.

Steinborn, R. 1982. Emulsion Rheology, M.Sc. Thesis. University of Alberta.

Stokes, R.H. and Mills, R. 1965. Viscosity of Electrolytes and Related Properties. Pergamon Press, Oxford.

Sweeny, K.H. and Geckler, R.D. 1954. The Rheology of Suspensions. J. App. Phys. 25:1135-1144.

Tabor, D. 1977. "Surface Forces and Surface Interactions," in Colloid and Interface Science, vol. 1, pp.3-15, ed. M. Kerker, R.L. Rowell, and A.C. Zettlemoyer. Academic Press, New York.

Takano, M., Goldsmith, H.L., and Mason, S.G. 1966. Flow of Suspensions Through Tubes: VII. Rotation and Deformation of Particles in Pulsatile Flow. J. Coll. Int. Sci. 23:248-265.

Takano, M., Goldsmith, H.L., and Mason, S.G. 1969. Flow of Suspensions Through Tubes: IX. Particle Interactions in Pulsatile Flow. J. Coll. Int. Sci. 27:268-281.

Taylor, G.I. 1923. Stability of a Viscous Liquid Contained Between Two Rotating Cylinders. Phil. Trans. A223:289-343.

Taylor, G.I. 1934. The Formation of Emulsions in Definable Fields of Flow. Proc. Roy. Soc. (London). A146:501-523.

Taylor, J.R. 1982. An Introduction to Error Analysis. Oxford University Press, U.S.A.

van Wazer, J.R., Lyons, J.W., Kim, K.Y., and Colwell, R.E. 1963. Viscosity and Flow Measurement. Interscience Publishers, New York.

van de Ven, T.G.M. 1981. Effects of Polymer Bridging on Selective Shear Flocculation. J. Coll. Int. Sci. 81:290-291.

van den Temple, M. 1963 "Effect of Droplet Flocculation on Emlusion Viscosity," in Rheology of Emulsions, ed. P. Sherman, Proc. Symp. Brit. Soc. of Rheology, Oct. 1962, The MacMillan Co., New York.

Walters, K. 1975. Rheometry. Chapman and Hill, London.

Weast, R.C., et al. ed. 1975. CRC Handbook of Chemistry and Physics, 56th ed. CRC Press Inc., U.S.A.

Whorlow, R.W. 1980. Rheological Techniques. Elis Horwood Ltd., Chichester.

Zia, I.Y.Z., Cox, R.G., and Mason, S.G. 1966. Chains of Particles in Shear Flow. Science 153:1405-06.

Zuidema, H.H. and Waters, G.W. 1941. Ring Method for the Determination of Interfacial Tensions. Ind. Eng. Chem. 13:312-313.

Appendix A

A.1 General Considerations

The measurement of the shear stress - shear rate relationship employed two coaxial cylinder viscometers: the Haake Rotovisco RV3 and the Brookfield Synchrolectric Digital viscometers. Each instrument imposes Searle flow by rotating the inner cylinder (bob) at a constant angular velocity, Ω, sustained by a torque, Ψ. The apparent viscosity, shear rate, and shear stress are determined from the dial reading, S (proportional to Ψ), the angular velocity, and manufacturer supplied equations and constants.

This proceedure is correct when the fluid is Newtonian. For non-Newtonian behavior the relationship between the shear rate, $\dot{\gamma}$, and the shear stress, τ, is non-linear. The general relation is presented as:

$$\dot{\gamma} = \dot{\gamma}(\tau) \qquad (A.1)$$

Equation A.1 must be integrated to obtain relationships among the experimental variables, and this is readily done if the form of $\dot{\gamma}(\tau)$ is known. If it is desired to obtain $\dot{\gamma}(\tau)$ from the experimental variables it is necessary to solve an integral equation (Krieger and Maron 1953). Consider then, the general problem of flow between rotating concentric cylinders.

A.2 Theory of Coaxial Cylinder Viscometers

The test fluid is contained between two coaxial cylinders which are in relative rotational motion. The inner cylinder (bob), of radius R_1 and length h, rotates at a fixed angular velocity, Ω, while the outer cylinder (cup), of radius R_2, is stationary: refer to Figure A.1. After van Wazer et al. (1963), the following assumptions are adopted:

1. stable fluid properties
2. laminar flow
3. circular flow streamlines
4. steady motion (time derivatives vanish)
5. no slip at the fluid-cylinder wall interface
6. edge and end effects are neglected
7. system is isothermal

A fluid element at a distance r from the axis of rotation flows tangentially with angular velocity $\omega(r)$. The shear rate at r is then defined as

$$\dot{\gamma} = r\frac{d\omega}{dr} \qquad (A.2)$$

in cylindrical coordinates.

The torque, Ψ, acting across the cylindrical surface of radius r is the product of the shear stress, $\tau(r)$, the moment arm, r, and the surface area, $2\pi rh$:

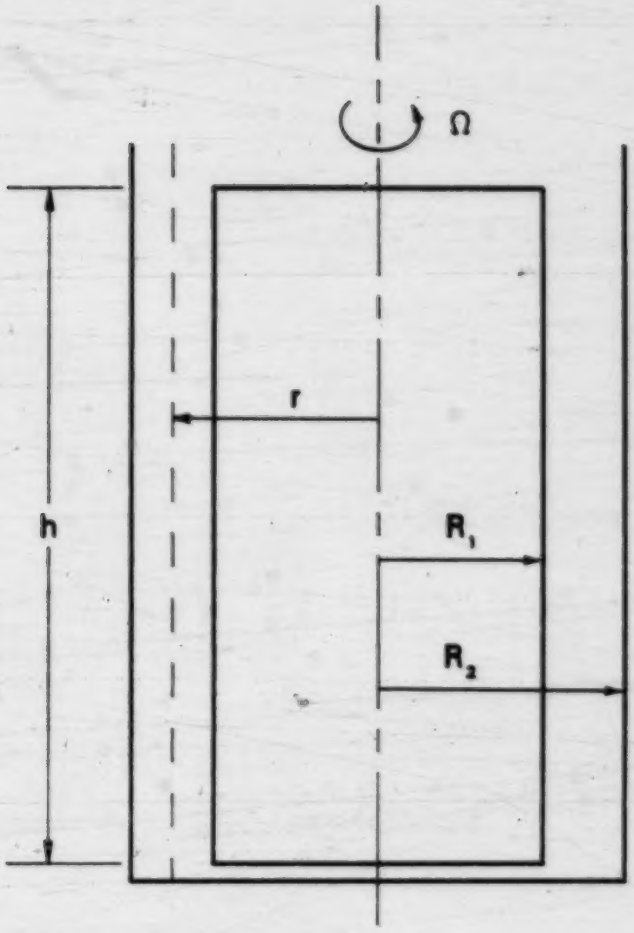

Figure A.1. Schematic of the concentric cylinder viscometer.

$$\Psi = 2\pi r^2 h\tau(r) \qquad (A.3)$$

Hence, the shear stress at r is

$$\tau(r) = \frac{\Psi}{2\pi r^2 h} \qquad (A.4)$$

which is independent of the fluid properties. The stress at the two boundaries, R_1, and R_2 are related as

$$\frac{\tau(R_2)}{\tau(R_1)} = \frac{R_1^2}{R_2^2} = \epsilon \qquad (A.5)$$

Now, combining equations A.1 and A.2 yields

$$r\frac{d\omega}{dr} = \dot{\gamma}(\tau) \qquad (A.6)$$

Differentiating equation A.4 with respect to r and substituting the result into equation A.6 obtains

$$d\omega = -\frac{\dot{\gamma}(\tau)}{2\tau}d\tau \qquad (A.7)$$

Then, integrating equation A.7 across the annulus from $r=R_1$ and $\omega(R_1)=\Omega$ to $r=R_2$ and $\omega(R_2)=0$, obtains the general solution to equation A.1:

$$\Omega = \int_{\tau_1}^{\tau} \frac{\dot{\gamma}(\tau)}{2\tau} d\tau \qquad (A.8)$$

In the case of Newtonian and plastic fluids (so long as the stresses in the annulus everywhere exceed the yield stress), the ratio of the shear stress to the shear rate is a constant, namely the apparent viscosity, η. For non-Newtonian fluids, the viscosity is a function of the shear rate, thus the actual rate of shear at any point in the annulus is unknown, except for a very narrow annulus. However, Whorlow (1980) indicates that a small annulus is not suitable for suspensions containing suspended particles which are of similar size as the gap. In such instances the flow is unlikely to be laminar, so the gap should be at least 100 times greater than the diameter of the particles.

Several approaches to solving equation A.8 may be pursued in the case of non-Newtonian fluids. If an empirical form of $\dot{\gamma}(\tau)$ is known, or can be surmised from previous studies of similar fluids, a solution is evident. An often used model is the Ostwald de Weale or power law model: $\tau = \xi \dot{\gamma}^n$.

When the form of $\dot{\gamma}(\tau)$ is unknown, equation A.8 , and hence $\dot{\gamma}$, may be represented as a converging infinite series. Krieger and Elrod obtained a rapidly converging series in 1953. Later, in a paper published in 1968, Krieger expressed this solution as a series of summable subseries in terms of the derivatives of the inverse of the flow behavior index:

$\kappa = 1/n$. His result was:

$$\dot{\gamma}(\tau_1) = \frac{2\kappa\Omega}{1-e^{\kappa}}\left[1 + \frac{\kappa'}{\kappa^2}f_1(t) + \frac{\kappa''}{\kappa^3}f_2(t) + \cdots\right] \quad (A.9)$$

where: $f_1(t) = t(e^t-1)^{-2}(te^t - 2e^t + t + 2)/2$

$f_2(t) = t^2(e^t-1)^{-3}(-te^{2t} + 3e^{2t} - 4te^t - t - 3)/6$

$t = -\kappa \ln\epsilon$

$\kappa = d\ln\Omega/d\ln\tau_1$

$\kappa' = d\kappa/d\ln\tau_1$

$\kappa'' = d^2\kappa/d(\ln\tau_1)^2$

$\tau_1 = \frac{\Psi}{2\pi h R_i^2}$

Note too, that the shear stress at the surface of the inner cylinder, τ_1, is related to the viscometer dial reading, S, through Ψ: Ψ = S x full scale torque/100, where S is a dial reading between 0 and 100.

If the equation for the power law model is re-arranged as $\dot{\gamma} = (\tau/\xi)^{1/n}$, the integral in equation A.8 is readily solved; the result is exactly the first term of equation A.9 with $\kappa = 1/n$. κ is usually called the shear thinning index, and may assume any value greater than zero with the following interpretations:

$$\kappa = \begin{cases} 0\text{-}1 \Rightarrow \text{Dilatancy (shear thickening)} \\ 1 \Rightarrow \text{Newtonian behavior} \\ 1\text{-}\infty \Rightarrow \text{Pseudoplacticity (shear thinning)} \end{cases}$$

Clearly then, equation A.9 is simply the power law model with correction terms. When κ is constant (ie. when a log-log plot of Ω versus τ, the experimental data, has constant slope), the power law alone may be used. When κ varies, equation A.9 should be used, but in a practical truncated form. In this study, the shear rate at the surface of the inner cylinder was obtained using the first two terms of equation A.9.

For viscometers with a wide annulus, that is when R_2 tends to infinity, the function f(t) tends to zero, and equation A.9 degenerates to the power law model. In practice wide annulus viscometers, such as the Brookfield Synchrolectric with the LVTD spindles, are only an approximation to an infinite sea of fluid. Again, several terms of equation A.9 may need consideration. Finally, note that if κ is set equal to one, the resulting expressions for the shear rate and viscosity are precisely those recommended by the Haake and Brookfield viscometer manufacturers.

A.3 Violation of the Assumptions

In a real viscometer, several of the idealizing assumptions listed earlier may not hold, as a result of factors such as the angular speed of the bob, the physical interaction of the fluid with the cylinder wall, and the fluid properties. Such departures have been discussed extensively in the literature and some of these potential violations are discussed below.

A.3.1 Fluid Properties

The reaction of the test fluid in the viscometer, of course, depends upon the experimental conditions imposed. However, it also depends upon factors which are difficult to control or even describe adequately (for example, inhomogeneity and previous history).

For suspensions and emulsions, the fluid is clearly inhomogeneous, and concentration gradients may be established in the rotational viscometer. The phase with the higher density will tend to migrate away from the axis of rotation. Segré and Silverberg (1961, 1962) examined this phenomena in poiseuille flow. The establishment of concentration gradients can give rise to slip at the inner (rotating) cylinder. However, the shear rate is more uniform in Couette flow, so inertial effects may be relatively more important in Poiseuille than in Couette viscometers. A crucial test for particle migration is to compare data for the same fluid using different cylinder radius ratios: Harris (1977) states the data must coincide. Porter and Johnson (1959) indicate that at sufficiently high rates of shear the material can be irreversibly degraded by such mechanical agitation.

In the theoretical development of the previous section, it was observed that the expression for the stress is independent of the fluid properties. Thus, if the fluid suffers irreversible degradation, the fluid rheology is history dependent and the stress is no longer independent of

material properties. Whorlow (1980) suggests that it is desirable to use the narrowest possible annulus in such cases. This both minimizes the uncertainty in the value of the shear stress in the gap and minimizes the difference in shear history during the test. For all non-homogeneous fluids, only the average response of the fluid at the time of measurement is obtained since any gap has finite dimensions: material in different parts of the gap will have been sheared by different stresses.

The stability of emulsions especially depends upon physical and chemical forces acting at the molecular level, and some of these are temperature dependent. Consequently, attempts to measure the rheological influence of temperature may be terminated by excessive heating. Above a certain temperature, irreversible phase separation may occur; this change in itself is interesting, but rheological measurements would be meaningless.

A.3.2 Laminar Flow and Circular Streamlines

Departure from circular streamlines and the subsequent disruption of laminar flow arises from inertial forces and therefore, can even occur in Newtonian fluids. It occurs irrespective of whether the bob or the cup rotates. When the bob rotates, the nearby fast moving fluid attempts to move outwards; since the whole layer cannot move out uniformly, it breaks into cells (Taylor Vortices) and circulates. According to Taylor (1923), when the inner cylinder rotates,

secondary motions occur above a critical transition Reynolds number,

$$Re_t = 41.3[R_2/(R_2 - R_1)]^{0.5} \qquad (A.10)$$

for Newtonian fluids the Reynolds number is:

$$Re = \Omega R_1(R_2-R_1)\rho/\eta \qquad (A.11)$$

where ρ is the fluid density. When the rotational speed of the bob is sufficient that the critical Reynolds number is surpassed, the flow is still laminar, but variable. An interesting discussion of this time varying steady flow is given by Feynman et al. (1966). As the relative velocity of the cylinders is increased further, complete turbulence eventually sets in.

Defining a Reynolds number for an inhomogeneous fluid such as an emulsion is difficult; Whorlow (1980) suggests that it is not practical to estimate the extent of secondary flow, or the magnitude of error produced in viscosity measurements. To do so, it would be necessary to establish the form of the constitutive equation for the material. Van Wazer et al. (1963), indicates that the onset of turbulence is indicated by curvature of the stress-strain curve, and that this behavior must be distinguished from dilatancy.

A.3.3 Time-Dependent Effects

When the bob is set to rotate at a particular angular velocity, an infinite (in principle) amount of time is required to establish steady flow within the fluid. Coleman et al. (1966) finds that such a time effect occurs because the flows achieved are described only approximately by equations such as those described above.

Until flow equilibrium is attained, the stress will appear to decline over time, at constant shear rate. This behavior must be distinguished from both reversible thixotropy and irreversible thixotropy.

A.3.4 Wall Adherence Condition

It is usual to assume that the fluid adjacent to the metal surface of the cylinders moves with the velocity of that surface. However, slippage may occur in several ways. True slippage occurs for rarefied gases and viscoelastic fluids (Coleman et al. 1966). Apparent slippage will occur if there is a local reduction in the concentration of the suspended particles, as discussed above, and may also occur if the metal surface affects the molecular structure of the fluid in contact with the surface (Whorlow 1980).

A.3.5 Edge and End Effects

Since the cylinders are of finite length, the torque will vary along the length of the rotating cylinder. It is less near the ends of the bob because the direction of the

maximum velocity gradient is no longer normal to the side of the cylinder. This effect is not accommodated by equation A.4, but may be corrected by letting the length, h, represent not the physical length of the cylinder, but rather the effective length of the cylinder. Rosen (1971, 1972) outlines a procedure for determining the combined edge and end effects, which are accommodated in the effective length. It is presented for use with the Brookfield viscometer LVTD spindles but is also applicable to the UL Adapter and to the Haake viscometer.

Walters (1975) explained that edge and end effects are expected to be especially important in wide gap viscometers. By using a narrow annulus viscometer, the region influenced by such effects is minimized. When a wide gap viscometer is employed, the procedure of Rosen for accommodating these effects is adequate.

A.3.6 Viscous Heating

Heating due to the dissipation of work as heat when a liquid is sheared is troublesome, especially when the viscosity is high, when high rates of shear occur, or when the shearing flow is maintained for long periods of time. The significance of this source of error depends most importantly on the temperature dependence of the material properties of the liquid (Whorlow 1980), but for suspensions, much of the viscous resistance is due to the mechanical interactions between particles. Hence, the

dependence on temperature may be primarily governed by the properties of the suspending fluid.

The amount of temperature rise depends on the temperature of the cylinders, the geometry, the shear rate, and the thermal conductivity of the fluid. For both the Haake Rotovisco and Brookfield Synchrolectric viscometers, the outer cylinder is in contact with the constant temperature (control) fluid, while the inner cylinder is thermally insulated by the test fluid. (Depending on the thermal conductivity of the test fluid, considerable time may be required for the inner cylinder to approach the temperature of the outer cylinder.) Whorlow (1980) demonstrated that for a small annulus and for a low viscosity fluid the temperature distribution in the fluid is parabolic; the location of the maximum temperature is a function of the square of the gap size, the shear rate, the shear stress and the thermal conductivity of the fluid.

Since fluid viscosity is sensitive to temperature, it is important to maintain a uniform temperature throughout the test fluid. This is most easily aproximated by using the narrowest gap possible and by obtaining the dial reading as soon as possible after switching on the viscometer (but long enough for the velocity field to be fully developed).

A.4 The Haake and Brookfield Viscometers

The use of the Haake and Brookfield viscometers is relatively simple, and provide reproducible results if used properly. The following comments apply to both viscometers unless otherwise specified.

1. When the bob is immersed in the fluid, one must ensure that no air bubbles are trapped under the cylinder, and that the sample is free of entrained air before testing.
2. The axes of the cup and bob must be coincident. This is important only for the Brookfield LVTD spindles: When the spindle is immersed into the fluid (up to the immersion mark on the spindle) ensure the spindle is centered within the cup (preferably a 600 mL beaker). Fortunately, the comparably infinite size of the cup is somewhat forgiving of slight misalignments.
3. For a mathematical treatment of the data, the guard leg, provided for use with the Brookfield LVTD spindles, is necessarily omitted.
4. The angular velocity of the bob in the Haake viscometer is not properly set by the RV3 control unit. The relationship between the speed requested n_r and the actual or true speed, n, was measured. The relationship is different if the 0.1 multiplier is used. For the primary scale, (including manual setting) the relationship is

$$n = 1.7488 n_r^{1.0132} \qquad (A.12)$$

with a standard deviation about the regression line of 0.0122. When the 0.1 multiplier is employed, the following equation applies :

$$n_i = 1.8431(n_o)^{1.0016} \qquad (A.13)$$

with a standard deviation about the regression line of 0.0285

Since the Haake Rotovisco RV3 is a wide-range instrument, it is not able to perform well at the extremes of its range. In this work, the values of n_i used were in the range $0.283 \leq n_i \leq 724$; over this range an appropriate relationship is

$$n_i = 1.7777n_o^{1.0081} \qquad (A.14)$$

This equation may be used with or without the 0.1 multiplier and has a standard deviation about the regression line of 0.0229.

The dimensions of n_i and n_o are revolutions per minute; the usual dimension of Ω is s^{-1}, hence it is related to n_i as $\Omega = 2\pi n_i/60$.

5. For both viscometers, begin the test at low values of n_i such that the dial reading , S, does not exceed 100. In fact, at no time should the dial reading exceed 100 since the torsion spring may be damaged; this is

particularly important for the Haake viscometer.

6. Particular care must be taken when handling the cup and bob assembly of the Haake viscometer. The bob axle is centered by saphire bearings which are very easily damaged or broken. Damage is most likely to occur when the cup and bob assembly is lowered into the thermally jacketed vessel containing the test fluid: the assembly must be lowered onto its seat gently, never harshly.

Appendix B

Rheological Data for Emulsions of Wainwright B, Epping, and Primrose Dewatered Crude Oils

Table B.1 Wainwright B 0.8% (dried) W/O Emulsion Rheology

Haake Rotovisco RV3
Temperature: 22.80 ±0.10°C

Shear Rate sec^{-1}		Shear Stress $dynes/cm^2$		Viscosity cP	
6.90	±0.15	58.82	±3.53	852.7	±54.4
7.80	0.17	69.41	3.53	889.5	49.1
9.67	0.22	77.65	3.53	803.4	40.7
10.85	0.14	96.47	3.53	889.2	34.6
13.75	0.13	116.47	3.53	847.0	27.0
15.64	0.19	134.12	5.88	857.5	39.0
19.63	0.23	157.65	3.53	803.0	20.4
22.19	0.25	181.18	3.53	816.5	18.4
27.74	0.33	214.12	3.53	772.0	15.7
31.19	0.30	248.24	3.53	795.9	13.7
39.01	0.38	304.71	3.53	781.1	11.9
44.35	0.47	354.12	3.54	798.5	11.6
55.62	0.57	428.24	3.54	769.9	10.2
62.75	0.61	492.95	3.54	785.6	9.5
78.65	0.75	608.25	3.55	773.3	8.6
89.22	0.86	691.78	3.55	775.4	8.5
112.00	1.09	852.96	3.57	761.5	8.1
126.96	1.25	954.13	3.58	751.5	7.9
158.81	1.59	1169.43	3.60	736.4	7.7

Table B.2 Wainwright B 0.8% (dried) W/O Emulsion Rheology

Haake Rotovisco RV3
Temperature: 40.50 ±0.05°C

Shear Rate sec^{-1}		Shear Stress $dynes/cm^2$		Viscosity cP	
19.68	±0.17	52.94	±3.53	269.0	±18.1
22.28	0.19	58.82	5.88	264.1	26.5
28.34	0.58	70.59	3.53	249.1	13.5
31.19	0.55	72.94	5.88	233.9	19.3
38.78	0.40	96.47	3.53	248.8	9.5
44.56	0.41	107.06	5.88	240.3	13.4
55.81	0.52	131.77	3.53	236.1	6.7
63.15	0.60	145.88	5.88	231.0	9.6
78.66	0.75	180.00	3.53	228.8	5.0
89.68	0.92	204.71	3.53	228.3	4.6
112.15	1.21	245.89	3.53	219.2	3.9
126.32	1.27	281.18	3.53	222.6	3.6
158.53	1.59	347.06	3.54	218.9	3.1
179.25	1.84	389.42	3.54	217.2	3.0
223.78	2.34	488.24	3.54	218.2	2.8
254.18	2.74	558.83	3.55	219.9	2.8
319.22	3.42	688.25	3.55	215.6	2.6
453.10	5.04	954.13	5.91	210.6	2.7
515.04	5.90	1063.55	5.92	206.5	2.6
568.78	6.57	1164.73	5.92	204.8	2.6

Table B.3 Wainwright B 0.8% (dried) W/O Emulsion Rheology

Haake Rotovisco RV3
Temperature: 60.00 ±0.05°C

Shear Rate sec^{-1}		Shear Stress $dynes/cm^2$		Viscosity cP	
111.70	±1.76	90.59	±2.35	81.1	±2.5
126.49	2.01	95.30	2.35	75.3	2.2
157.59	1.85	123.53	2.35	78.4	1.8
179.42	2.06	135.30	2.35	75.4	1.6
223.89	2.36	171.77	2.36	76.7	1.3
253.57	2.70	192.94	2.36	76.1	1.2
317.41	3.42	244.71	2.36	77.1	1.1
451.89	5.07	348.24	3.54	77.1	1.2
639.93	7.50	478.83	3.54	74.8	1.0
906.62	10.87	691.78	5.90	76.3	1.1
1285.60	15.93	964.72	11.78	75.0	1.3

Table B.4 Wainwright B 0.8% (dried) W/O Emulsion Rheology

Haake Rotovisco RV3
Temperature: 79.15 ±0.05°C

Shear Rate sec^{-1}		Shear Stress $dynes/cm^2$		Viscosity cP	
176.83	±1.81	48.24	±5.88	27.3	±3.3
221.43	2.32	64.12	2.35	29.0	1.1
249.76	2.66	75.30	2.35	30.1	1.0
314.36	3.54	104.12	2.35	33.1	0.8
448.50	5.00	154.12	5.88	34.4	1.4
639.72	7.61	224.71	2.36	35.1	0.6
905.81	11.31	307.06	2.36	33.9	0.5
1282.78	16.19	456.48	5.89	35.6	0.6
1845.44	25.81	635.31	5.89	34.4	0.6
2616.87	37.62	810.60	5.90	31.0	0.5

Table B.5 Wainwright B 4.8% W/O Emulsion Rheology

Haake Rotovisco RV3
Temperature: 22.65 ±0.05°C

Shear Rate sec^{-1}		Shear Stress $dynes/cm^2$		Viscosity cP	
9.57	±0.08	72.94	±1.18	762.3	±13.8
10.83	0.09	84.71	1.18	782.1	12.7
13.58	0.12	111.41	2.00	820.6	16.3
15.45	0.13	127.88	2.35	827.8	16.8
19.34	0.17	161.53	2.00	835.3	12.8
21.94	0.21	188.59	1.18	859.5	9.8
27.47	0.26	233.77	1.18	850.9	9.2
31.14	0.31	273.30	2.01	877.7	10.8
39.02	0.37	336.48	1.19	862.4	8.8
44.14	0.41	389.42	1.20	882.3	8.7
55.23	0.53	487.07	1.21	881.9	8.7
62.60	0.62	565.89	1.22	903.9	9.1
78.43	0.76	702.37	1.25	895.5	8.8
89.00	0.88	808.25	1.27	908.2	9.1
111.59	1.10	1000.02	1.32	896.2	8.9
126.02	1.27	1140.02	1.36	904.6	9.2
128.83	1.30	1160.02	5.92	900.4	10.2

Table B.6 Wainwright B 4.8% W/O Emulsion Rheology

Haake Rotovisco RV3
Temperature: 39.95 ±0.05°C

Shear Rate sec^{-1}		Shear Stress $dynes/cm^2$		Viscosity cP	
38.57	±0.35	85.77	±0.24	222.4	±2.1
43.73	0.40	101.18	0.59	231.4	2.5
54.94	0.52	133.77	0.36	243.5	2.4
62.53	0.58	152.12	0.36	243.3	2.3
78.29	0.75	193.77	0.72	247.5	2.5
88.80	0.86	219.18	0.38	246.8	2.4
111.16	1.09	278.83	0.39	250.8	2.5
126.27	1.24	316.01	0.40	250.3	2.5
157.48	1.63	394.12	2.01	250.3	2.9
178.37	1.85	456.48	1.21	255.9	2.7
224.21	2.34	574.13	1.23	256.1	2.7
253.99	2.68	645.89	1.24	254.3	2.7
317.66	3.41	810.60	1.27	255.2	2.8
450.55	5.00	1155.31	1.36	256.4	2.9

Table B.7 Wainwright B 4.8% W/O Emulsion Rheology

Haake Rotovisco RV3
Temperature: 59.90 ±0.05°C

Shear Rate sec^{-1}		Shear Stress $dynes/cm^2$		Viscosity cP	
77.68	±0.74	55.06	±0.24	70.9	±0.7
88.08	0.85	64.82	0.36	73.6	0.8
110.67	1.10	84.71	0.24	76.5	0.8
125.10	1.27	96.35	0.24	77.0	0.8
156.44	1.61	127.41	1.18	81.4	1.1
178.32	1.82	145.53	1.18	81.6	1.1
223.49	2.33	185.53	1.18	83.0	1.0
253.04	2.68	210.24	1.18	83.1	1.0
317.67	3.51	268.24	1.19	84.4	1.0
387.35	4.34	321.54	5.89	83.0	1.8
447.73	5.05	378.48	2.01	84.5	1.1
526.49	6.14	458.83	5.89	87.1	1.5
638.74	7.35	554.13	2.38	86.8	1.1
759.57	8.88	663.54	5.90	87.4	1.3
906.92	10.78	791.78	3.56	87.3	1.1
1120.67	13.70	974.14	5.91	86.9	1.2
1299.57	16.36	1103.55	3.59	84.9	1.1
1415.41	17.96	1176.49	5.92	83.1	1.1

Table B.8 Wainwright B 4.8% W/O Emulsion Rheology

Haake Rotovisco RV3
Temperature: 79.45 ±0.05°C

Shear Rate sec^{-1}		Shear Stress $dynes/cm^2$		Viscosity cP	
156.21	±1.65	49.06	±0.59	31.4	±0.5
177.13	1.89	58.71	0.59	33.1	0.5
222.72	2.32	75.65	0.47	34.0	0.4
251.74	2.66	87.06	0.59	34.6	0.4
315.99	3.47	113.77	0.83	36.0	0.5
384.29	4.40	139.18	5.88	36.2	1.6
446.93	5.11	169.41	2.00	37.9	0.6
526.79	5.95	201.18	5.88	38.2	1.2
636.54	7.32	247.06	1.19	38.8	0.5
758.08	8.88	298.01	5.89	39.3	0.9
904.13	10.76	357.65	3.54	39.6	0.6
1112.41	13.53	447.07	5.89	40.2	0.7
1286.02	17.47	523.54	3.54	40.7	0.6
1432.09	18.71	565.89	5.89	39.5	0.7
1599.27	20.20	635.31	11.77	39.7	0.9
1839.37	26.55	729.42	11.77	39.7	0.9
2240.58	28.75	835.31	11.78	37.3	0.7
2641.16	34.42	941.19	11.78	35.6	0.6

Table B.9 Wainwright B 10.4% W/O Emulsion Rheology

Haake Rotovisco RV3
Temperature: 22.85 ±0.05°C

Shear Rate sec^{-1}		Shear Stress $dynes/cm^2$		Viscosity cP	
9.63	±0.09	91.77	±3.53	953.4	±37.8
10.89	0.10	108.24	3.53	993.5	33.8
13.66	0.13	134.12	1.18	981.7	12.5
15.68	0.26	156.47	2.35	997.9	22.6
19.41	0.37	178.83	2.36	921.2	21.4
21.85	0.30	221.18	2.36	1012.1	17.8
27.61	0.32	264.71	2.36	958.8	14.1
31.27	0.37	310.59	2.36	993.2	14.0
39.00	0.50	370.59	2.36	950.1	13.6
44.15	0.52	442.36	2.37	1002.0	13.1
55.48	0.61	535.30	2.37	964.9	11.4
62.71	0.66	624.72	1.23	996.2	10.7
78.48	0.83	763.54	2.40	972.9	10.7
89.05	0.96	889.43	1.29	998.8	10.9
111.91	1.17	1083.55	3.59	968.2	10.6
118.66	1.17	1176.49	5.92	991.5	11.0
138.55	1.38	1403.55	5.94	1013.0	11.0

Table B.10 Wainwright B 10.4% W/O Emulsion Rheology

Haake Rotovisco RV3
Temperature: 40.40 ±0.05°C

Shear Rate sec^{-1}		Shear Stress $dynes/cm^2$		Viscosity cP	
27.27	±0.45	81.18	±2.35	297.7	±9.9
30.88	0.51	83.53	1.18	270.5	5.9
38.54	0.48	117.65	2.35	305.3	7.2
44.44	0.53	127.06	1.18	285.9	4.3
55.45	0.54	161.18	1.18	290.7	3.5
62.83	0.62	178.83	1.18	284.6	3.4
78.31	0.74	225.89	2.36	288.5	4.1
89.36	0.89	257.65	1.19	288.3	3.2
111.72	1.17	314.12	1.19	281.2	3.1
126.05	1.27	361.18	1.20	286.5	3.0
157.92	1.59	449.42	2.37	284.6	3.2
180.28	1.96	511.77	1.22	283.9	3.2
224.35	2.86	615.30	1.23	274.3	3.5
251.31	2.72	723.54	2.39	287.9	3.3
279.88	3.00	807.07	5.90	288.4	3.7
317.78	3.43	917.66	2.42	288.8	3.2
347.50	4.27	1011.78	5.91	291.2	4.0
384.29	4.76	1176.49	11.79	306.1	4.9

Table B.11 Wainwright B 10.4% W/O Emulsion Rheology

Haake Rotovisco RV3
Temperature: 59.05 ±0.05°C

Shear Rate sec^{-1}		Shear Stress $dynes/cm^2$		Viscosity cP	
77.69	±1.21	74.71	±0.59	96.2	±1.7
88.09	1.38	95.30	1.18	108.2	2.2
111.99	1.38	113.41	0.59	101.3	1.4
125.52	1.26	131.77	2.35	105.0	2.2
157.78	1.63	167.06	1.18	105.9	1.3
179.71	1.83	187.06	1.18	104.1	1.2
224.46	2.35	231.77	1.18	103.3	1.2
255.14	2.78	263.53	1.19	103.3	1.2
316.39	3.97	320.01	5.89	101.1	2.3
384.60	5.02	415.30	5.89	108.0	2.1
454.69	5.28	468.24	5.89	103.0	1.8
529.35	6.01	544.72	5.89	102.9	1.6
637.04	7.37	661.19	5.90	103.8	1.5
758.53	9.01	802.37	5.90	105.8	1.5
912.35	11.03	952.96	5.91	104.5	1.4
1167.68	14.44	1176.49	5.92	100.8	1.3

Table B.12 Wainwright B 10.4% W/O Emulsion Rheology

Haake Rotovisco RV3
Temperature: 79.65 ±0.05°C

Shear Rate sec^{-1}		Shear Stress $dynes/cm^2$		Viscosity cP	
223.09	±2.54	92.35	±0.59	41.4	±0.5
252.62	2.91	102.35	2.35	40.5	1.0
315.92	3.44	134.12	2.35	42.5	0.9
449.65	5.03	195.30	2.36	43.4	0.7
526.68	6.12	228.24	5.88	43.3	1.2
635.20	7.35	284.71	3.53	44.8	0.8
758.18	8.88	343.54	0.62	45.3	0.5
904.43	10.76	411.77	5.89	45.5	0.8
1116.09	13.64	514.13	5.89	46.1	0.8
1295.84	16.39	588.25	11.77	45.4	1.1
1523.03	19.43	670.60	11.77	44.0	1.0
1854.73	30.86	800.01	11.77	43.1	1.0
2235.27	34.35	882.37	11.78	39.5	0.8
2656.67	41.29	1011.78	11.78	38.1	0.7

Table B.13 Wainwright B 18.0% W/O Emulsion Rheology

Haake Rotovisco RV3
Temperature: 23.10 ±0.05°C

Shear Rate sec^{-1}		Shear Stress $dynes/cm^2$		Viscosity cP	
6.76	±0.06	65.30	±0.59	965.4	±12.0
7.65	0.07	76.47	1.18	999.6	17.6
9.60	0.08	97.65	1.18	1017.5	15.1
10.90	0.10	114.47	0.83	1050.0	12.4
13.70	0.12	142.00	0.83	1036.4	10.7
15.49	0.13	162.36	1.18	1047.8	11.8
19.50	0.17	202.00	0.83	1036.2	9.8
21.88	0.20	226.71	0.38	1036.4	9.7
27.55	0.39	296.48	1.19	1076.0	15.8
31.21	0.44	314.12	1.19	1006.3	14.8
38.87	0.39	409.42	1.20	1053.3	11.1
44.28	0.43	454.13	1.21	1025.5	10.3
54.87	0.56	576.48	1.23	1050.6	11.0
62.77	0.99	695.31	1.25	1107.6	17.6
79.35	1.03	811.78	1.27	1023.1	13.4
89.48	0.98	934.13	1.30	1043.9	11.5
112.05	1.25	1121.20	1.35	1000.6	11.2

Table B.14 Wainwright B 18.0% W/O Emulsion Rheology

Haake Rotovisco RV3
Temperature: 40.10 ±0.05°C

Shear Rate sec^{-1}		Shear Stress $dynes/cm^2$		Viscosity cP	
19.26	±0.19	49.41	±1.18	256.6	±6.6
21.80	0.21	59.41	0.59	272.6	3.8
27.55	0.25	75.30	0.59	273.3	3.3
31.16	0.29	84.00	0.59	269.5	3.1
39.08	0.41	107.06	0.24	274.0	2.9
43.83	0.50	117.30	0.25	267.6	3.1
54.92	0.67	160.36	0.37	292.0	3.6
62.86	0.74	173.77	0.37	276.4	3.3
78.26	0.76	222.36	0.38	284.1	2.8
88.86	0.86	250.59	0.38	282.0	2.8
110.85	1.10	318.48	0.40	287.3	2.9
126.18	1.35	369.42	0.42	292.8	3.1
158.13	1.65	452.95	1.21	286.4	3.1
178.94	1.85	520.01	1.22	290.6	3.1
224.59	2.33	645.89	1.24	287.6	3.0
254.33	2.67	729.42	1.25	286.8	3.1
317.34	3.56	905.90	1.29	285.5	3.2
352.10	4.38	1023.55	5.91	290.7	4.0
416.04	5.24	1176.49	5.92	282.8	3.8

Table B.15 Wainwright B 18.0% W/O Emulsion Rheology

Haake Rotovisco RV3
Temperature: 59.70 ±0.05°C

Shear Rate sec^{-1}		Shear Stress $dynes/cm^2$		Viscosity cP	
62.37	±0.58	52.94	±1.18	84.9	±2.0
78.02	0.74	68.24	1.18	87.5	1.7
88.59	0.85	78.24	0.59	88.3	1.1
111.13	1.10	100.00	0.59	90.0	1.0
125.49	1.28	112.83	0.36	89.9	1.0
156.72	1.59	146.71	0.83	93.6	1.1
178.74	1.83	168.24	0.37	94.1	1.0
224.14	2.33	210.59	0.83	94.0	1.0
254.51	2.69	238.83	0.38	93.8	1.0
319.66	3.43	294.48	0.84	92.1	1.0
386.09	4.69	350.59	5.89	90.8	1.9
448.77	5.34	423.54	1.20	94.4	1.2
528.50	6.09	491.77	5.89	93.1	1.5
636.16	7.32	603.54	2.38	94.9	1.2
757.72	8.91	731.78	5.90	96.6	1.4
906.44	10.79	876.49	2.41	96.7	1.2
1067.66	12.97	1025.90	5.91	96.1	1.3
1243.56	15.33	1176.49	5.92	94.6	1.3

Table B.16 Wainwright B 18.0% W/O Emulsion Rheology

Haake Rotovisco RV3
Temperature: 79.20 ±0.05°C

Shear Rate sec^{-1}		Shear Stress $dynes/cm^2$		Viscosity cP	
157.16	±1.61	59.41	±0.35	37.8	±0.4
178.20	1.85	67.18	0.24	37.7	0.4
223.13	2.36	86.71	0.24	38.9	0.4
252.39	2.72	98.00	0.24	38.8	0.4
315.74	3.41	127.41	1.18	40.4	0.6
385.10	4.22	158.00	5.88	41.0	1.6
449.54	5.02	186.71	1.18	41.5	0.5
526.64	6.02	219.65	5.88	41.7	1.2
636.45	7.40	272.59	2.36	42.8	0.6
756.58	8.98	325.54	5.89	43.0	0.9
901.49	10.80	400.01	5.89	44.4	0.8
1111.75	13.57	500.01	11.77	45.0	1.2
1280.40	16.18	588.25	11.77	45.9	1.1
1438.35	19.83	647.07	11.77	45.0	1.0
1605.30	23.21	705.89	11.77	44.0	1.0
1835.76	27.54	817.66	8.25	44.5	0.8
2208.32	33.54	935.31	11.78	42.4	0.8

Table B.17 Wainwright B 26.5% W/O Emulsion Rheology

Haake Rotovisco RV3
Temperature: 22.80 ±0.15°C

Shear Rate sec^{-1}		Shear Stress $dynes/cm^2$		Viscosity cP	
3.37	±0.03	58.24	±0.24	1728.3	±15.7
4.76	0.04	85.88	0.13	1802.6	14.9
6.80	0.06	125.53	2.00	1845.9	33.4
7.71	0.07	139.18	2.00	1805.4	30.4
9.67	0.09	176.83	1.42	1828.4	21.8
11.03	0.09	196.12	1.18	1778.5	18.3
13.78	0.12	240.00	1.19	1741.9	16.9
15.57	0.13	269.42	2.01	1730.4	19.4
19.53	0.17	331.77	1.19	1698.8	15.7
22.03	0.19	372.95	1.20	1693.2	15.6
27.70	0.28	467.07	1.21	1686.3	17.4
31.28	0.32	510.60	1.22	1632.4	17.4
38.69	0.38	647.07	1.24	1672.6	16.7
44.19	0.56	774.13	1.26	1752.0	22.4
55.87	0.56	928.25	1.30	1661.3	16.7
62.65	0.58	1052.96	1.33	1680.6	15.8
69.48	0.67	1170.61	1.37	1684.8	16.4
78.59	0.77	1311.79	1.41	1669.2	16.4

Table B.18 Wainwright B 26.5% W/O Emulsion Rheology

Haake Rotovisco RV3
Temperature: 39.95 ±0.05°C

Shear Rate sec^{-1}		Shear Stress $dynes/cm^2$		Viscosity cP	
13.74	±0.15	62.94	±0.59	458.2	±6.5
15.54	0.17	68.24	0.59	439.2	6.1
19.42	0.17	87.06	0.59	448.2	5.0
22.18	0.19	97.06	0.59	437.6	4.6
27.54	0.29	118.24	0.59	429.4	5.0
30.94	0.28	138.47	1.18	447.5	5.5
38.77	0.35	178.00	0.83	459.1	4.6
43.99	0.40	205.89	1.18	468.0	5.0
55.21	0.51	263.53	0.84	477.3	4.7
62.78	0.58	298.83	1.19	476.0	4.8
78.30	0.77	372.59	0.85	475.9	4.8
88.78	0.88	431.77	1.20	486.3	5.0
111.42	1.09	538.83	1.22	483.6	4.9
126.23	1.25	614.13	1.23	486.5	4.9
157.76	1.61	763.54	1.26	484.0	5.0
179.46	1.92	876.49	1.29	488.4	5.3
225.24	2.37	1070.61	2.44	475.3	5.1
255.05	2.72	1211.79	11.79	475.1	6.9

Table B.19 Wainwright B 26.5% W/O Emulsion Rheology

Haake Rotovisco RV3
Temperature: 59.00 ±0.05°C

Shear Rate sec^{-1}		Shear Stress $dynes/cm^2$		Viscosity cP	
39.08	±0.40	61.30	±0.24	156.8	±1.7
44.31	0.45	67.41	0.24	152.1	1.6
55.28	0.51	85.77	0.36	155.2	1.6
62.34	0.60	97.06	0.59	155.7	1.8
77.90	0.75	126.71	1.18	162.7	2.2
88.77	0.85	145.06	1.18	163.4	2.1
111.22	1.08	183.18	1.18	164.7	1.9
125.85	1.24	208.59	1.18	165.8	1.9
157.98	1.68	264.36	1.19	167.3	1.9
180.13	1.86	293.30	1.19	162.8	1.8
224.40	2.38	362.01	1.20	161.3	1.8
253.28	2.67	414.13	1.20	163.5	1.8
318.39	3.47	521.19	2.37	163.7	1.9
385.40	4.69	623.54	5.89	161.8	2.5
448.39	5.47	758.84	2.40	169.2	2.1
527.45	6.24	878.84	5.91	166.6	2.3
635.57	7.42	1094.14	3.59	172.1	2.1
685.15	8.06	1176.49	5.92	171.7	2.2

Table B.20 Wainwright B 26.5% W/O Emulsion Rheology

Haake Rotovisco RV3
Temperature: 79.15 ±0.05°C

Shear Rate sec^{-1}		Shear Stress $dynes/cm^2$		Viscosity cP	
88.56	±0.86	58.47	±0.35	66.0	±0.8
110.90	1.09	74.24	0.24	66.9	0.7
126.01	1.30	85.88	0.24	68.2	0.7
157.02	1.78	106.47	0.36	67.8	0.8
177.50	1.91	126.71	0.83	71.4	0.9
223.02	2.34	161.18	0.37	72.3	0.8
251.92	2.66	186.24	1.18	73.9	0.9
318.84	4.45	241.18	2.01	75.6	1.2
388.77	5.97	274.95	5.88	70.7	1.9
448.58	5.23	331.42	1.19	73.9	0.9
526.99	6.10	387.07	5.89	73.4	1.4
636.04	7.38	481.18	2.37	75.7	1.0
757.54	8.88	576.48	5.89	76.1	1.2
905.04	10.90	700.01	4.72	77.3	1.1
1117.69	13.58	858.84	5.90	76.8	1.1
1291.45	17.36	992.96	5.91	76.9	1.1
1434.61	19.43	1070.61	11.78	74.6	1.3
1579.28	21.55	1176.49	11.79	74.5	1.3

Table B.21 Wainwright B 28.0% W/O/W Emulsion Rheology

Haake Rotovisco RV3
Temperature: 24.70 ±0.05°C

Shear Rate sec^{-1}		Shear Stress $dynes/cm^2$		Viscosity cP	
10.29	±0.08	56.00	±0.59	544.4	±7.1
11.64	0.09	59.41	0.59	510.3	6.5
14.72	0.18	66.12	0.36	449.1	5.9
16.18	0.25	69.06	0.24	426.8	6.9
20.18	0.21	80.00	0.24	396.5	4.3
23.29	0.19	85.06	0.36	365.2	3.4
29.27	0.26	95.18	0.24	325.1	3.0
32.93	0.33	100.59	0.36	305.4	3.2
40.47	0.48	113.53	0.36	280.6	3.5
45.41	0.42	124.71	0.36	274.7	2.7
56.90	0.53	144.71	0.36	254.3	2.4
64.66	0.64	158.47	0.37	245.1	2.5
81.03	0.78	182.00	0.37	224.6	2.2
91.37	0.86	198.47	0.37	217.2	2.1
114.35	1.10	231.42	0.38	202.4	2.0
128.93	1.26	252.59	0.38	195.9	1.9
161.03	1.60	298.01	0.40	185.1	1.9
183.64	1.91	327.42	0.40	178.3	1.9
228.90	2.70	380.01	0.85	166.0	2.0
257.28	2.75	423.54	1.20	164.6	1.8
326.11	4.17	504.71	1.21	154.8	2.0
397.13	5.57	564.72	5.89	142.2	2.5
458.91	5.37	641.19	1.24	139.7	1.7
540.53	6.13	716.48	5.90	132.6	1.9
651.47	7.44	825.90	3.56	126.8	1.5
771.00	9.18	941.19	5.91	122.1	1.6
918.82	11.22	1094.14	5.92	119.1	1.6
1016.55	12.53	1176.49	5.92	115.7	1.5

Table B.22 Wainwright B 28.0% W/O/W Emulsion Rheology

Haake Rotovisco RV3
Temperature: 40.90 ±0.30°C

Shear Rate sec^{-1}		Shear Stress $dynes/cm^2$		Viscosity cP	
38.89	±0.35	64.71	±0.59	166.4	±2.1
44.10	0.40	74.12	0.59	168.1	2.0
55.00	0.53	94.12	0.36	171.1	1.8
62.38	0.63	111.18	0.36	178.2	1.9
79.00	0.91	139.18	0.83	176.2	2.3
89.77	1.02	150.94	0.36	168.1	2.0
111.60	1.09	187.42	0.83	167.9	1.8
126.52	1.25	212.59	0.38	168.0	1.7
157.00	1.85	262.00	0.39	166.9	2.0
162.83	8.19	313.77	2.01	192.7	9.8
201.40	6.47	223.53	3.88	111.0	4.1
278.58	7.50	238.83	1.19	85.7	2.3
330.18	9.88	254.95	7.88	77.2	3.3
385.08	5.02	302.01	7.88	78.4	2.3
448.42	6.13	372.59	11.77	83.1	2.9
531.83	6.33	423.54	5.89	79.6	1.5
653.60	18.41	511.77	3.54	78.3	2.3
801.65	24.82	535.30	11.77	66.8	2.5
927.17	10.96	605.89	5.89	65.3	1.0
1151.42	16.50	705.89	11.77	61.3	1.3
1347.29	19.23	758.84	11.77	56.3	1.2
1464.28	19.37	805.90	11.77	55.0	1.1
1624.21	21.68	876.49	11.78	54.0	1.0
1855.39	29.99	982.37	11.78	52.9	1.1
2031.14	31.93	1017.67	11.78	50.1	1.0
2190.01	28.28	1082.37	11.78	49.4	0.8
2374.04	30.89	1147.08	23.54	48.3	1.2

Table B.23 Wainwright B 28.0% W/O/W Emulsion Rheology

Haake Rotovisco RV3
Temperature: 59.25 ±0.10°C

Shear Rate sec^{-1}		Shear Stress $dynes/cm^2$		Viscosity cP	
55.15	±0.51	70.00	±0.59	126.9	±1.6
62.45	0.58	79.88	0.36	127.9	1.3
78.17	0.75	102.35	0.36	130.9	1.3
88.33	0.87	116.36	0.36	131.7	1.4
109.96	1.11	152.94	1.18	139.1	1.8
125.63	1.61	184.36	3.88	146.7	3.6
155.49	2.34	223.53	3.88	143.8	3.3
176.07	2.46	293.30	2.01	166.6	2.6
224.09	2.39	363.54	1.20	162.2	1.8
254.05	2.77	417.65	2.37	164.4	2.0
318.84	3.43	514.13	1.22	161.2	1.8
385.75	4.35	623.54	5.89	161.6	2.4
448.66	5.06	744.72	1.26	166.0	1.9
527.53	5.97	877.66	5.91	166.4	2.2
638.09	7.42	1075.31	0.73	168.5	2.0
702.08	8.24	1176.49	5.92	167.6	2.1

Table B.24 Wainwright B 28.0% W/O/W Emulsion Rheology

Haake Rotovisco RV3
Temperature: 78.20 ±0.05°C

Shear Rate sec^{-1}		Shear Stress $dynes/cm^2$		Viscosity cP	
112.90	±4.08	71.30	±0.24	63.1	±2.3
127.85	4.63	86.12	0.24	67.4	2.4
165.07	6.63	91.18	0.36	55.2	2.2
177.43	1.89	103.18	0.13	58.2	0.6
221.56	2.32	137.30	0.36	62.0	0.7
252.62	2.74	160.00	0.83	63.3	0.8
317.74	3.42	201.53	0.83	63.4	0.7
384.28	4.54	244.71	5.88	63.7	1.7
446.52	5.16	300.01	1.19	67.2	0.8
525.40	5.99	356.12	5.89	67.8	1.4
635.61	7.44	445.89	1.21	70.2	0.8
755.48	9.06	532.95	5.89	70.5	1.2
900.84	10.92	661.19	2.39	73.4	0.9
1112.94	13.56	823.54	5.90	74.0	1.0
1282.25	16.24	964.72	5.91	75.2	1.1
1421.16	18.08	1058.84	5.92	74.5	1.0
1564.48	20.07	1176.49	11.79	75.2	1.2

Table B.25 Wainwright B 34.4% W/O/W Emulsion Rheology

Haake Rotovisco RV3
Temperature: 22.75 ±0.05°C

Shear Rate sec^{-1}		Shear Stress $dynes/cm^2$		Viscosity cP	
20.15	±0.22	58.24	±0.35	289.1	±3.6
22.80	0.25	61.88	0.59	271.4	3.9
28.62	0.36	71.88	0.59	251.2	3.8
32.12	0.44	75.88	0.36	236.2	3.4
39.66	0.36	89.77	0.24	226.3	2.1
45.36	0.50	99.77	0.24	219.9	2.5
56.65	0.69	114.83	0.25	202.7	2.5
64.60	1.03	128.59	0.83	199.1	3.4
79.59	1.58	144.71	0.36	181.8	3.6
89.74	1.36	169.41	0.37	188.8	2.9
113.91	1.26	196.47	0.37	172.5	1.9
128.21	1.29	218.47	0.38	170.4	1.7
160.91	1.60	258.48	0.39	160.6	1.6
185.68	2.41	283.89	0.39	152.9	2.0
232.15	3.20	320.36	0.40	138.0	1.9
260.41	2.90	352.95	0.85	135.5	1.5
326.43	3.58	408.24	1.20	125.1	1.4
395.19	4.29	470.60	5.89	119.1	2.0
457.71	5.17	527.07	2.37	115.2	1.4
534.32	6.02	602.36	5.89	112.7	1.7
646.18	7.42	709.42	2.39	109.8	1.3
769.39	8.96	817.66	5.90	106.3	1.5
917.21	10.85	948.25	3.57	103.4	1.3
1118.81	14.61	1111.78	5.92	99.4	1.4
1227.99	16.16	1176.49	82.36	95.8	6.8

Table B.26 Wainwright B 34.4% W/O/W Emulsion Rheology

Haake Rotovisco RV3
Temperature: 39.50 ±0.05°C

Shear Rate sec^{-1}		Shear Stress $dynes/cm^2$		Viscosity cP	
19.63	±0.21	70.59	±5.88	359.5	±30.2
22.22	0.23	76.35	0.24	343.6	3.8
27.87	0.33	94.35	0.36	338.6	4.2
31.29	0.39	101.18	0.24	323.3	4.1
39.04	0.41	129.41	0.36	331.5	3.6
44.59	0.44	142.00	0.83	318.5	3.6
55.64	0.51	175.65	0.83	315.7	3.3
63.05	0.58	196.83	0.37	312.2	2.9
79.53	1.04	242.36	0.38	304.8	4.0
91.01	1.12	258.83	0.39	284.4	3.5
113.59	1.19	309.77	2.01	272.7	3.4
127.84	1.44	335.30	2.01	262.3	3.4
160.07	1.93	409.42	1.20	255.8	3.2
185.80	1.86	441.18	35.30	237.5	19.1
227.47	3.68	505.89	3.54	222.4	3.9
254.66	2.91	582.36	3.55	228.7	3.0
321.80	3.48	705.89	35.30	219.4	11.2
391.22	4.42	823.54	5.90	210.5	2.8
457.68	5.89	947.08	11.78	206.9	3.7
545.32	6.09	1052.96	47.06	193.1	8.9
648.00	7.36	1176.49	23.54	181.6	4.2

Table B.27 Wainwright B 34.4% W/O/W Emulsion Rheology

Haake Rotovisco RV3
Temperature: 59.70 ±0.05°C

Shear Rate sec^{-1}		Shear Stress $dynes/cm^2$		Viscosity cP	
39.13	±0.36	56.12	±0.47	143.4	±1.8
44.37	0.42	62.35	0.24	140.5	1.4
55.10	0.55	78.24	0.36	142.0	1.6
62.41	0.63	92.24	0.36	147.8	1.6
78.02	0.81	115.30	0.25	147.8	1.6
88.35	0.91	136.83	0.36	154.9	1.6
110.84	1.12	172.94	0.37	156.0	1.6
125.28	1.26	202.00	0.37	161.2	1.6
157.22	1.59	258.48	0.39	164.4	1.7
179.58	1.86	294.12	0.39	163.8	1.7
224.84	2.38	360.83	0.41	160.5	1.7
253.97	2.68	410.60	1.20	161.7	1.8
319.18	3.45	510.60	1.22	160.0	1.8
387.16	4.49	608.25	5.89	157.1	2.4
450.12	5.18	722.37	2.39	160.5	1.9
529.02	6.05	838.84	5.90	158.6	2.1
639.31	7.45	1023.55	5.91	160.1	2.1
742.63	8.78	1176.49	5.92	158.4	2.0

Table B.28 Wainwright B 34.4% W/O/W Emulsion Rheology

Haake Rotovisco RV3
Temperature: 79.20 ±0.05°C

Shear Rate sec^{-1}		Shear Stress $dynes/cm^2$		Viscosity cP	
79.41	±1.17	54.59	±0.24	68.7	±1.1
90.04	1.33	63.18	0.24	70.2	1.1
113.09	1.58	73.06	0.24	64.6	0.9
126.31	1.27	83.53	0.24	66.1	0.7
157.11	1.80	103.18	0.24	65.7	0.8
178.58	2.22	122.71	0.36	68.7	0.9
224.57	2.58	149.06	0.36	66.4	0.8
252.93	2.72	172.59	0.37	68.2	0.7
318.57	3.48	216.83	0.83	68.1	0.8
386.13	4.61	258.83	0.39	67.0	0.8
448.73	5.25	311.77	2.01	69.5	0.9
527.12	6.12	363.54	1.20	69.0	0.8
635.73	7.35	451.77	3.54	71.1	1.0
756.71	8.87	543.54	5.89	71.8	1.1
903.02	10.79	662.36	2.39	73.4	0.9
1109.72	13.92	823.54	5.90	74.2	1.1
1274.97	16.51	988.25	5.91	77.5	1.1
1442.36	21.02	1088.25	5.92	75.4	1.2
1624.20	23.86	1176.49	11.79	72.4	1.3

Table B.29 Wainwright B 42.0% W/O/W Emulsion Rheology

Haake Rotovisco RV3
Temperature: 22.95 ±0.05°C

Shear Rate sec^{-1}		Shear Stress $dynes/cm^2$		Viscosity cP	
80.16	±0.96	58.82	±0.35	73.4	±1.0
90.89	1.10	62.94	0.24	69.3	0.9
112.99	1.09	75.53	0.36	66.8	0.7
128.16	1.25	83.41	0.36	65.1	0.7
161.10	1.73	99.41	0.83	61.7	0.8
183.75	1.89	107.65	0.36	58.6	0.6
221.37	3.93	126.24	0.36	57.0	1.0
251.86	6.66	165.06	0.37	65.5	1.7
347.84	3.65	179.65	0.37	51.6	0.6
400.69	9.28	194.12	5.88	48.4	1.8
459.66	6.04	221.53	1.18	48.2	0.7
540.08	6.81	244.71	5.88	45.3	1.2
647.43	7.40	285.53	1.19	44.1	0.5
773.65	9.30	329.42	5.89	42.6	0.9
919.98	11.44	373.30	0.85	40.6	0.5
1127.23	13.62	447.07	5.89	39.7	0.7
1308.19	19.75	505.89	2.37	38.7	0.6
1537.87	53.01	535.30	5.89	34.8	1.3
1668.52	48.86	552.95	23.53	33.1	1.7
1868.14	27.46	611.78	11.77	32.7	0.8
1984.45	39.67	635.31	11.77	32.0	0.9
2128.49	28.30	694.13	23.53	32.6	1.2
2317.71	32.45	764.72	23.53	33.0	1.1
2583.82	36.50	841.19	23.54	32.6	1.0

Table B.30 Wainwright B 42.0% W/O/W Emulsion Rheology

Haake Rotovisco RV3
Temperature: 40.55 ±0.05°C

Shear Rate sec^{-1}		Shear Stress $dynes/cm^2$		Viscosity cP	
28.94	±0.33	60.00	±5.88	207.3	±20.5
40.99	0.47	70.59	5.88	172.2	14.5
56.28	0.74	87.06	5.88	154.7	10.6
79.33	0.85	121.18	5.88	152.7	7.6
113.25	1.21	156.47	5.88	138.2	5.4
119.37	19.14	176.47	5.88	147.8	24.2
129.02	1.73	160.00	5.88	124.0	4.9
187.61	15.05	152.94	5.88	81.5	7.3
230.68	2.36	177.65	5.88	77.0	2.7
264.59	3.10	192.94	5.88	72.9	2.4
331.48	3.75	217.65	5.88	65.7	1.9
354.10	14.47	245.89	5.88	69.4	3.3
411.90	12.34	164.71	5.88	40.0	1.9
545.94	9.80	176.47	5.88	32.3	1.2
622.79	9.60	204.71	11.77	32.9	2.0
738.88	9.92	324.71	23.53	43.9	3.2
868.14	61.64	400.01	29.41	46.1	4.7
925.66	11.59	329.42	11.77	35.6	1.3
1025.93	12.86	265.89	17.65	25.9	1.8
1101.39	45.39	227.06	23.53	20.6	2.3
1173.25	48.38	241.18	23.53	20.6	2.2

Table B.31 Wainwright B 42.0% W/O/W Emulsion Rheology

Haake Rotovisco RV3
Temperature: 60.00 ±0.05°C

Shear Rate sec^{-1}		Shear Stress $dynes/cm^2$		Viscosity cP	
39.46	±0.51	52.94	±5.88	134.2	±15.0
56.03	0.74	65.88	5.88	117.6	10.6
79.40	1.09	94.12	5.88	118.5	7.6
115.55	1.10	116.47	5.88	100.8	5.2
130.62	1.26	125.88	5.88	96.4	4.6
162.53	1.73	144.71	5.88	89.0	3.7
184.90	2.12	158.83	5.88	85.9	3.3
233.73	2.40	181.18	5.88	77.5	2.6
287.45	21.01	194.12	5.88	67.5	5.3
388.94	21.61	200.00	5.88	51.4	3.2
401.47	12.70	211.77	5.88	52.7	2.2
446.90	5.62	243.53	5.88	54.5	1.5
527.10	7.88	304.71	5.89	57.8	1.4
657.35	8.31	350.59	11.77	53.3	1.9
803.80	12.97	388.24	11.77	48.3	1.7
928.27	21.37	429.42	11.77	46.3	1.7
1036.79	12.94	308.24	17.65	29.7	1.7
1114.28	15.55	236.47	17.65	21.2	1.6
1258.36	48.16	220.00	23.53	17.5	2.0
1394.53	18.51	264.71	23.53	19.0	1.7
1570.34	21.06	305.89	23.53	19.5	1.5

Table B.32 Wainwright B 42.0% W/O/W Emulsion Rheology

Haake Rotovisco RV3
Temperature: 79.50 ±0.05°C

Shear Rate sec^{-1}		Shear Stress $dynes/cm^2$		Viscosity cP	
56.42	±0.53	47.06	±5.88	83.4	±10.5
79.92	0.78	62.35	5.88	78.0	7.4
113.69	1.11	80.00	5.88	70.4	5.2
160.05	1.66	104.71	11.77	65.4	7.4
184.41	3.29	117.65	5.88	63.8	3.4
233.22	3.42	131.77	5.88	56.5	2.7
262.29	3.20	144.71	5.88	55.2	2.3
328.94	3.75	164.71	5.88	50.1	1.9
401.13	5.18	188.24	5.88	46.9	1.6
483.10	7.13	203.53	5.88	42.1	1.4
581.81	6.57	216.47	5.88	37.2	1.1
647.92	16.04	231.77	5.88	35.8	1.3
770.61	20.57	283.53	5.88	36.8	1.2
1008.59	22.75	298.83	5.89	29.6	0.9
1085.96	17.80	411.77	11.77	37.9	1.2
1308.05	20.56	423.54	11.77	32.4	1.0
1364.55	22.56	436.48	11.77	32.0	1.0
1509.00	25.08	458.83	17.65	30.4	1.3

Table B.33 Wainwright B 46.4% W/O/W Emulsion Rheology

Haake Rotovisco RV3
Temperature: 22.60 ±0.10°C

Shear Rate sec^{-1}		Shear Stress $dynes/cm^2$		Viscosity cP	
55.90	±0.70	65.06	±0.24	116.4	±1.5
63.30	0.79	69.77	0.24	110.2	1.4
78.95	0.84	87.06	0.24	110.3	1.2
90.27	0.89	95.30	0.24	105.6	1.1
112.14	1.16	115.06	0.14	102.6	1.1
126.05	1.24	130.94	0.36	103.9	1.1
159.31	2.41	164.36	0.37	103.2	1.6
182.02	2.70	174.12	0.37	95.7	1.4
225.35	2.35	212.95	0.83	94.5	1.1
256.41	2.82	240.00	0.84	93.6	1.1
323.05	3.46	287.06	1.19	88.9	1.0
391.59	4.51	333.30	1.19	85.1	1.0
453.83	5.04	383.54	1.20	84.5	1.0
534.87	6.07	441.18	5.89	82.5	1.4
667.44	26.61	514.13	3.54	77.0	3.1
803.16	35.43	527.07	11.77	65.6	3.2
918.66	11.28	600.01	3.55	65.3	0.9
1130.87	13.99	720.01	5.90	63.7	0.9
1309.20	16.54	800.01	11.77	61.1	1.2
1442.66	18.38	864.72	11.78	59.9	1.1
1622.28	20.27	952.96	11.78	58.7	1.0
1851.34	23.62	1058.84	5.92	57.2	0.8
1991.03	30.11	1117.67	5.92	56.1	0.9
2118.79	32.18	1176.49	11.79	55.5	1.0

Table B.34 Wainwright B 46.4% W/O/W Emulsion Rheology

Haake Rotovisco RV3
Temperature: 40.15 ±0.10°C

Shear Rate sec^{-1}		Shear Stress $dynes/cm^2$		Viscosity cP	
158.41	±1.59	54.24	±0.24	34.2	±0.4
179.61	1.82	61.06	0.12	34.0	0.4
223.60	2.50	75.53	0.24	33.8	0.4
251.64	2.67	88.24	0.24	35.1	0.4
315.73	3.40	114.24	0.24	36.2	0.4
384.73	4.22	142.36	5.88	37.0	1.6
450.20	5.13	168.59	0.37	37.4	0.4
535.91	6.84	196.12	5.88	36.6	1.2
663.55	9.86	223.89	1.54	33.7	0.6
781.98	13.37	243.53	5.88	31.1	0.9
915.11	10.92	281.53	1.19	30.8	0.4
1130.47	14.25	339.18	5.89	30.0	0.6
1297.35	18.29	375.65	5.89	29.0	0.6
1419.86	17.68	417.65	11.77	29.4	0.9
1597.53	20.12	470.60	5.89	29.5	0.5
1807.64	23.90	541.19	3.54	29.9	0.4
1925.59	24.80	598.83	5.89	31.1	0.5
2110.17	28.34	682.36	11.77	32.3	0.7
2296.90	30.81	747.07	5.90	32.5	0.5
2477.04	35.26	823.54	11.78	33.2	0.7
2586.73	47.20	847.07	35.30	32.7	1.5
2680.39	48.99	882.37	58.83	32.9	2.3

Table B.35 Wainwright B 46.4% W/O/W Emulsion Rheology

Haake Rotovisco RV3
Temperature: 59.25 ±0.15°C

Shear Rate sec^{-1}		Shear Stress $dynes/cm^2$		Viscosity cP	
110.63	±1.14	55.18	±0.24	49.9	±0.6
125.27	1.30	65.18	0.24	52.0	0.6
157.21	1.59	82.59	0.24	52.5	0.6
179.28	1.93	95.18	0.24	53.1	0.6
225.42	2.34	116.47	0.25	51.7	0.5
252.92	2.73	130.94	0.36	51.8	0.6
316.67	3.45	168.59	0.83	53.2	0.6
386.75	4.23	205.53	5.88	53.1	1.6
460.04	10.56	240.00	1.19	52.2	1.2
530.30	10.92	255.30	5.88	48.1	1.5
633.59	7.47	325.54	7.88	51.4	1.4
759.66	8.97	392.12	7.89	51.6	1.2
908.14	10.78	464.71	58.83	51.2	6.5
1110.70	14.37	570.60	17.65	51.4	1.7
1266.06	15.66	688.25	29.42	54.4	2.4
1394.50	17.50	794.13	29.42	56.9	2.2
1574.35	20.32	958.84	35.30	60.9	2.4
1793.13	23.41	1129.43	23.54	63.0	1.5

Table B.36 Wainwright B 46.4% W/O/W Emulsion Rheology

Haake Rotovisco RV3
Temperature: 79.60 ±0.10°C

Shear Rate sec^{-1}		Shear Stress $dynes/cm^2$		Viscosity cP	
110.78	±1.36	59.53	±0.24	53.7	±0.7
125.45	1.55	71.88	0.24	57.3	0.7
157.55	1.80	88.00	0.24	55.9	0.7
176.66	1.81	103.53	0.24	58.6	0.6
221.00	2.32	138.83	0.83	62.8	0.8
251.93	2.84	165.06	0.37	65.5	0.8
316.93	3.42	208.24	0.37	65.7	0.7
384.55	4.25	257.65	5.88	67.0	1.7
448.53	5.09	308.59	0.84	68.8	0.8
525.46	6.10	363.18	5.89	69.1	1.4
634.29	7.38	457.66	1.21	72.2	0.9
750.83	9.25	552.95	5.89	73.6	1.2
896.37	11.33	715.31	3.56	79.8	1.1
1113.23	13.52	894.13	5.91	80.3	1.1
1282.54	15.89	1041.20	3.58	81.2	1.0
1418.31	17.74	1149.43	5.92	81.0	1.1

Table B.37 Wainwright B 54.0% W/O/W Emulsion Rheology

Brookfield Sychrolectric LVTD
Temperature: 22.90 ±0.10°C

Shear Rate sec^{-1}	Shear Stress $dynes/cm^2$	Viscosity cP
0.39 ± 0.01	0.63 ± 0.01	163.0 ± 3.6
0.77 0.01	0.93 0.01	120.8 1.8
1.93 0.02	1.86 0.01	96.2 1.1
3.87 0.04	2.83 0.02	73.2 0.8
7.74 0.07	4.11 0.02	53.1 0.6

Table B.38 Wainwright B 54.0% W/O/W Emulsion Rheology

Brookfield Sychrolectric LVTD
Temperature: 40.00 ±0.10°C

Shear Rate sec^{-1}	Shear Stress $dynes/cm^2$	Viscosity cP
0.77 ± 0.01	0.49 ± 0.01	63.0 ± 1.3
1.94 0.02	0.95 0.01	49.1 0.6
3.87 0.04	1.55 0.01	39.9 0.4
7.74 0.08	2.49 0.01	32.1 0.3
15.49 0.15	3.40 0.01	22.0 0.2
38.72 0.38	6.01 0.02	15.5 0.2

Table B.39 Wainwright B 54.0% W/O/W Emulsion Rheology

Brookfield Sychrolectric LVTD
Temperature: 60.00 ±0.10°C

Shear Rate sec^{-1}	Shear Stress $dynes/cm^2$	Viscosity cP
1.94 ± 0.02	0.52 ± 0.01	26.9 ± 0.5
3.89 0.04	0.78 0.01	20.1 0.3
7.78 0.08	1.13 0.01	14.5 0.2
15.55 0.16	1.59 0.01	10.2 0.1
38.88 0.41	3.06 0.01	7.9 0.1
77.75 0.81	5.32 0.01	6.8 0.1

Table B.40 Wainwright B 54.0% W/O/W Emulsion Rheology

Brookfield Sychrolectric LVTD
Temperature: 79.00 ±0.10°C

Shear Rate sec^{-1}	Shear Stress $dynes/cm^2$	Viscosity cP
3.77 ± 0.03	0.44 ± 0.01	11.5 ± 0.2
7.55 0.07	0.71 0.01	9.5 0.1
15.10 0.13	1.27 0.02	8.4 0.1
37.74 0.33	2.60 0.02	6.9 0.1
75.48 0.66	4.48 0.02	5.9 0.1

Table B.41 Wainwright B 95.6% O/W Emulsion Rheology

Haake Rotovisco RV3
Temperature: 23.90 ±0.05°C

Shear Rate sec^{-1}		Shear Stress $dynes/cm^2$		Viscosity cP	
524.25	±6.56	52.94	±5.88	10.1	±1.1
633.55	8.04	63.53	5.88	10.0	0.9
738.89	9.36	81.18	8.24	11.0	1.1
878.79	10.69	125.88	5.88	14.3	0.7
1090.00	13.63	189.42	11.77	17.4	1.1
1258.93	15.84	231.77	5.88	18.4	0.5
1396.88	19.57	277.65	11.77	19.9	0.9
1537.75	21.70	305.89	11.77	19.9	0.8

Table B.42 Wainwright B 95.6% O/W Emulsion Rheology

Haake Rotovisco RV3
Temperature: 39.70 ±0.10°C

Shear Rate sec^{-1}		Shear Stress $dynes/cm^2$		Viscosity cP	
313.75	±3.46	60.00	±3.53	19.1	±1.1
381.96	4.29	78.82	5.88	20.6	1.6
441.70	5.42	94.12	5.88	21.3	1.4
515.39	5.88	127.06	5.88	24.7	1.2
622.89	7.23	178.83	5.88	28.7	1.0
740.36	8.74	247.06	11.77	33.4	1.6
882.68	10.60	344.71	11.77	39.1	1.4
1090.39	13.48	510.60	23.53	46.8	2.2
1264.67	16.00	632.95	35.30	50.0	2.9
1418.10	18.61	714.13	35.30	50.4	2.6
1596.88	21.17	796.48	35.30	49.9	2.3

Table B.43 Wainwright B 95.6% O/W Emulsion Rheology

Haake Rotovisco RV3
Temperature: 59.30 ±0.10°C

Shear Rate sec^{-1}		Shear Stress $dynes/cm^2$		Viscosity cP	
312.07	±3.39	61.18	±2.35	19.6	±0.8
379.91	4.20	82.35	3.53	21.7	1.0
442.97	4.96	102.35	5.88	23.1	1.4
517.74	5.95	129.41	5.88	25.0	1.2
624.90	7.26	178.83	5.88	28.6	1.0
742.77	8.79	236.47	11.77	31.8	1.6
884.16	10.61	323.54	11.77	36.6	1.4
1093.35	13.75	470.60	11.77	43.0	1.2
1277.90	17.80	564.72	35.30	44.2	2.8
1462.89	22.62	611.78	41.18	41.8	2.9
1647.31	25.66	652.95	41.18	39.6	2.6

Table B.44 Wainwright B 95.6% O/W Emulsion Rheology

Haake Rotovisco RV3
Temperature: 79.10 ±0.15°C

Shear Rate sec^{-1}		Shear Stress $dynes/cm^2$		Viscosity cP	
311.23	±3.42	63.53	±2.35	20.4	±0.8
378.89	4.24	84.71	5.88	22.4	1.6
443.39	5.63	110.59	11.77	24.9	2.7
522,11	6.34	130.59	17.65	25.0	3.4
627.08	7.26	172.94	17.65	27.6	2.8
739.27	9.11	225.89	23.53	30.6	3.2
882.64	11.21	341.18	23.53	38.7	2.7
1100.66	13.67	463.54	29.41	42.1	2.7
1284.56	18.28	547.07	35.30	42.6	2.8
1432.71	19.66	588.25	35.30	41.1	2.5
1613.33	22.34	662.36	35.30	41.1	2.3

Table B.45 Wainwright B 97.6% O/W Emulsion Rheology

Brookfield Synchrolectric LVTD
Temperature: 22.20 ±0.10°C

Shear Rate sec^{-1}	Shear Stress $dynes/cm^2$	Viscosity cP
7.38 ± 0.07	0.09 ± 0.01	1.2 ± 0.1
14.76 0.13	0.17 0.01	1.1 0.1
36.90 0.33	0.41 0.01	1.1 0.0
73.80 0.66	0.81 0.01	1.1 0.0

Table B.46 Wainwright B 97.6% O/W Emulsion Rheology

Brookfield Synchrolectric LVTD
Temperature: 40.30 ±0.10°C

Shear Rate sec^{-1}	Shear Stress $dynes/cm^2$	Viscosity cP
7.40 ± 0.08	0.07 ± 0.01	1.0 ± 0.1
14.79 0.15	0.12 0.01	0.8 0.1
36.98 0.38	0.30 0.01	0.8 0.0
73.95 0.77	0.62 0.01	0.8 0.0

Table B.47 Wainwright B 97.6% O/W Emulsion Rheology

Brookfield Synchrolectric LVTD
Temperature: 59.60 ±0.10°C

Shear Rate sec^{-1}	Shear Stress $dynes/cm^2$	Viscosity cP
7.34 ± 0.08	0.06 ± 0.01	0.8 ± 0.2
14.68 0.17	0.09 0.01	0.6 0.1
36.70 0.42	0.24 0.01	0.6 0.0
73.41 0.84	0.59 0.01	0.8 0.0

Table B.48 Wainwright B 97.6% O/W Emulsion Rheology

Brookfield Synchrolectric LVTD
Temperature: 74.50 ±0.20°C

Shear Rate sec^{-1}	Shear Stress $dynes/cm^2$	Viscosity cP
7.34 ± 0.10	0.06 ± 0.01	0.8 ± 0.2
14.68 0.21	0.08 0.01	0.6 0.1
36.70 0.51	0.21 0.01	0.6 0.0
73.40 1.03	0.57 0.01	0.8 0.0

Table B.49 Epping 0.9% (dried) W/O Emulsion Rheology

Haake Rotovisco RV3
Temperature: 23.05 ±0.05°C

Shear Rate sec^{-1}	Shear Stress $dynes/cm^2$	Viscosity cP
0.33 ± 0.00	48.82 ± 0.59	14603.8 ±219.7
0.47 0.00	65.88 0.36	13937.4 143.7
0.67 0.01	92.24 0.47	13677.7 144.4
0.96 0.01	121.18 0.83	12620.6 137.9
1.35 0.01	164.36 1.53	12134.4 150.5
1.92 0.02	225.53 0.83	11749.6 104.5
2.72 0.02	309.77 0.84	11382.5 96.7
3.40 0.03	378.48 2.36	11133.8 117.1
3.84 0.03	430.60 2.37	11224.7 111.0
4.80 0.04	531.77 2.37	11078.3 102.6
5.45 0.04	603.54 2.38	11082.8 99.9
6.83 0.06	751.78 2.40	11014.2 96.4
7.73 0.06	844.72 2.41	10929.9 94.4
9.70 0.08	1048.25 2.43	10808.7 92.4
10.98 0.09	1176.49 2.46	10717.7 91.4

Table B.50 Epping 0.9% (dried) W/O Emulsion Rheology

Haake Rotovisco RV3
Temperature: 40.55 ±0.10°C

Shear Rate sec^{-1}	Shear Stress $dynes/cm^2$	Viscosity cP
1.92 ± 0.02	47.65 ± 0.47	2481.3 ± 31.9
2.72 0.02	64.71 1.18	2377.4 47.4
3.41 0.03	80.00 1.77	2349.4 55.3
3.85 0.03	88.83 1.77	2305.1 49.5
4.67 0.06	109.41 1.18	2343.3 40.8
5.32 0.12	160.83 3.88	3020.7 100.7
7.76 0.08	172.59 3.88	2225.5 54.7
7.85 0.15	178.47 2.00	2273.8 50.3
9.71 0.08	219.65 2.00	2262.6 27.8
10.98 0.09	247.42 1.42	2253.9 22.7
13.75 0.11	305.53 1.19	2222.6 20.5
15.53 0.13	343.89 2.01	2214.4 22.7
19.47 0.17	428.24 1.20	2199.9 19.8
22.03 0.19	484.71 1.21	2200.5 19.7
27.58 0.24	603.54 1.23	2188.1 19.6
31.21 0.27	683.54 1.25	2190.2 19.7
39.06 0.35	854.13 1.28	2186.7 19.8
44.38 0.40	964.72 1.31	2174.0 19.8
55.57 0.51	1194.14 2.46	2148.9 20.2

Table B.51 Epping 0.9% (dried) W/O Emulsion Rheology

Haake Rotovisco RV3
Temperature: 59.80 ±0.05°C

Shear Rate sec^{-1}	Shear Stress $dynes/cm^2$	Viscosity cP
9.74 ± 0.12	62.35 ± 1.18	640.0 ± 14.6
11.03 0.14	66.47 0.24	602.8 8.0
13.72 0.12	83.53 0.59	608.6 6.8
15.61 0.13	92.94 0.59	595.3 6.3
19.42 0.20	113.77 0.59	585.9 6.7
22.01 0.23	133.30 2.00	605.7 11.2
27.65 0.27	161.53 0.83	584.3 6.5
31.29 0.31	185.89 0.83	594.0 6.4
39.36 0.35	225.53 0.83	573.0 5.5
44.43 0.40	252.12 0.84	567.4 5.5
55.58 0.51	312.59 0.84	562.4 5.4
62.87 0.58	351.42 0.85	558.9 5.4
78.53 0.74	437.65 1.21	557.3 5.5
89.20 0.86	497.66 1.21	557.9 5.5
111.58 1.11	614.13 1.23	550.4 5.6
126.47 1.29	702.37 1.25	555.4 5.7
158.26 1.63	861.19 1.28	544.1 5.7
179.83 1.92	983.55 1.31	546.9 5.9
225.19 2.45	1194.14 2.46	530.3 5.9

Table B.52 Epping 0.9% (dried) W/O Emulsion Rheology

Haake Rotovisco RV3
Temperature: 79.35 ±0.10°C

Shear Rate sec^{-1}	Shear Stress $dynes/cm^2$	Viscosity cP
27.80 ± 0.24	62.94 ± 0.59	226.4 ± 2.9
31.48 0.28	70.59 1.18	224.2 4.2
39.47 0.35	85.18 0.59	215.8 2.4
44.70 0.40	94.47 0.36	211.3 2.1
55.27 0.65	114.71 0.25	207.5 2.5
62.81 0.86	136.47 0.83	217.3 3.3
79.04 0.95	161.53 0.37	204.4 2.5
89.42 1.01	186.71 0.37	208.8 2.4
112.28 1.20	223.89 0.38	199.4 2.2
126.54 1.27	254.95 0.84	201.5 2.1
159.03 1.62	312.95 0.40	196.8 2.0
180.15 1.86	347.06 0.41	192.6 2.0
224.88 2.34	428.24 1.20	190.4 2.1
254.10 2.67	483.54 1.21	190.3 2.1
318.41 3.42	603.54 1.23	189.5 2.1
387.87 4.24	728.25 5.90	187.8 2.6
450.87 5.02	844.72 2.41	187.4 2.2
530.69 6.13	995.31 5.91	187.6 2.4
641.33 7.54	1176.49 3.60	183.4 2.2

Table B.53 Epping 14.4% W/O Emulsion Rheology

Brookfield Synchrolectric LVTD
Temperature: 23.80 ±0.20°C

Shear Rate sec^{-1}		Shear Stress $dynes/cm^2$		Viscosity cP	
0.06	±0.00	4.10	±0.02	6494.7	±107.4
0.13	0.00	8.54	0.02	6762.7	57.5
0.06	0.01	4.00	0.06	6326.0	510.6
0.13	0.01	7.64	0.07	6034.0	473.4
0.32	0.02	19.55	0.08	6180.0	480.5
0.63	0.05	39.87	0.13	6301.6	489.4
0.31	0.03	18.73	0.25	5981.9	490.7
0.63	0.05	38.97	0.30	6224.9	505.8
1.25	0.10	79.58	0.45	6355.8	515.3
2.50	0.20	159.52	0.80	6369.8	516.1
1.25	0.10	78.76	1.30	6312.9	532.3
2.50	0.21	154.78	1.76	6203.3	517.8
6.24	0.52	382.31	3.58	6128.8	510.0
12.48	1.03	761.89	6.88	6106.9	508.0

Table B.54 Epping 14.4% W/O Emulsion Rheology

Brookfield Synchrolectric LVTD
Temperature: 37.00 ±0.20°C

Shear Rate sec^{-1}		Shear Stress $dynes/cm^2$		Viscosity cP	
0.07	±0.00	1.10	±0.02	1694.6	±36.5
0.13	0.00	2.24	0.02	1724.9	18.8
0.33	0.00	5.71	0.02	1755.2	8.5
0.65	0.00	11.58	0.02	1781.8	5.6
0.31	0.00	6.56	0.06	2097.1	22.6
0.63	0.00	13.08	0.07	2092.2	13.6
1.25	0.00	25.74	0.09	2057.8	10.0
2.50	0.01	48.15	0.63	1924.8	25.9
0.62	0.00	13.23	0.24	2138.0	41.0
1.24	0.01	25.98	0.27	2100.2	24.3
2.47	0.01	52.20	0.34	2109.6	17.9
6.19	0.03	128.74	2.42	2081.3	40.7
2.46	0.03	59.07	1.21	2397.3	55.0
6.16	0.06	141.66	1.67	2299.6	35.8
12.32	0.13	281.68	2.74	2286.3	32.2

Table B.55 Epping 14.4% W/O Emulsion Rheology

Brookfield Synchrolectric LVTD
Temperature: 58.00 ±0.20°C

Shear Rate sec^{-1}		Shear Stress $dynes/cm^2$		Viscosity cP	
0.32	±0.00	1.58	±0.02	489.2	±5.3
0.65	0.00	3.25	0.02	502.6	3.0
1.29	0.00	6.60	0.02	510.5	2.1
2.59	0.01	13.43	0.03	519.0	1.8
0.62	0.00	3.39	0.06	544.7	10.3
1.24	0.00	6.90	0.06	554.6	5.6
2.49	0.01	13.61	0.07	547.2	3.6
6.22	0.02	33.53	0.11	539.3	2.8
2.45	0.02	15.68	0.25	639.5	11.0
6.13	0.04	36.05	0.29	587.9	6.3
12.26	0.09	71.74	0.42	585.1	5.4

Table B.56 Epping 14.4% W/O Emulsion Rheology

Brookfield Synchrolectric LVTD
Temperature: 74.00 ±0.20°C

Shear Rate sec^{-1}		Shear Stress $dynes/cm^2$		Viscosity cP	
0.67	±0.00	1.36	±0.02	202.9	±2.7
1.34	0.01	2.68	0.02	200.0	1.7
2.68	0.02	5.23	0.02	195.0	1.3
6.71	0.04	13.16	0.03	196.1	1.2
1.30	0.01	2.74	0.06	211.5	5.0
2.59	0.02	5.97	0.31	230.6	12.0
6.48	0.04	12.68	0.07	195.9	1.7
12.95	0.09	26.08	0.09	201.3	1.5
6.45	0.03	16.15	0.25	250.5	4.0
12.89	0.06	30.31	0.28	235.1	2.4

Table B.57 Epping 17.0% W/O Emulsion Rheology

Brookfield Synchrolectric LVTD
Temperature: 22.30 ±0.10°C

Shear Rate sec^{-1}		Shear Stress $dynes/cm^2$		Viscosity cP	
0.06	±0.00	5.08	±0.02	7935.5	±130.0
0.13	0.00	10.45	0.02	8156.6	68.7
0.05	0.01	3.94	0.06	7192.2	1403.6
0.11	0.02	8.56	0.07	7810.3	1516.5
0.27	0.05	22.72	0.09	8293.5	1608.3
0.55	0.11	46.37	0.14	8462.0	1640.7
0.27	0.06	22.00	0.26	8175.0	1684.1
0.54	0.11	45.53	0.32	8457.6	1740.4
1.08	0.22	91.99	0.50	8544.6	1757.8
2.15	0.44	184.33	0.92	8560.9	1761.1
1.07	0.23	89.15	1.35	8341.2	1778.4
2.14	0.45	176.12	1.91	8238.8	1754.4
5.34	1.14	435.91	4.03	8156.9	1736.3
10.69	2.27	843.93	7.60	7896.0	1680.7

Table B.58 Epping 17.0% W/O Emulsion Rheology

Brookfield Synchrolectric LVTD
Temperature: 38.80 ±0.10°C

Shear Rate sec^{-1}		Shear Stress $dynes/cm^2$		Viscosity cP	
0.07	±0.00	1.23	±0.02	1886.6	±39.9
0.13	0.00	2.53	0.02	1941.1	22.2
0.33	0.00	6.44	0.02	1978.5	13.3
0.65	0.00	12.86	0.02	1976.1	11.4
0.13	0.00	2.65	0.06	2114.7	53.9
0.31	0.00	8.07	0.07	2577.0	27.6
0.63	0.00	15.86	0.08	2532.7	20.3
1.25	0.01	31.53	0.11	2518.0	18.0
0.62	0.00	17.44	0.25	2816.2	46.0
1.24	0.01	33.47	0.28	2702.8	31.2
2.48	0.02	51.26	0.34	2069.6	21.2
6.19	0.05	126.87	0.65	2048.8	19.1
2.45	0.03	55.79	1.20	2280.5	56.0
6.12	0.07	136.74	1.64	2235.7	37.6
12.23	0.14	259.80	2.56	2124.0	32.6

Table B.59 Epping 17.0% W/O Emulsion Rheology

Brookfield Synchrolectric LVTD
Temperature: 57.50 ±0.10°C

Shear Rate sec^{-1}		Shear Stress $dynes/cm^2$		Viscosity cP	
0.33	±0.00	1.62	±0.02	494.4	±5.3
0.66	0.00	3.29	0.02	501.6	2.9
1.31	0.00	6.60	0.02	502.8	2.0
2.62	0.01	13.28	0.03	506.4	1.6
0.63	0.00	4.43	0.06	702.0	10.3
1.26	0.00	8.93	0.07	706.9	5.9
2.53	0.01	17.55	0.08	694.7	4.0
6.32	0.02	33.80	0.11	535.3	2.6
1.25	0.01	10.77	0.24	861.5	19.8
2.50	0.01	20.13	0.25	805.3	11.1
6.25	0.03	39.79	0.30	636.8	6.0
12.50	0.07	73.73	0.43	590.0	4.7
12.33	0.12	113.76	1.49	922.7	15.2

Table B.60 Epping 17.0% W/O Emulsion Rheology

Brookfield Synchrolectric LVTD
Temperature: 73.00 ±0.50°C

Shear Rate sec^{-1}		Shear Stress $dynes/cm^2$		Viscosity cP	
0.33	±0.00	0.76	±0.02	228.6	±4.9
0.66	0.00	1.53	0.02	231.0	2.5
1.32	0.00	3.05	0.02	231.0	1.4
2.64	0.01	6.11	0.02	231.0	0.9
6.61	0.02	15.20	0.03	229.9	0.7
0.64	0.00	2.71	0.06	425.3	9.9
1.27	0.00	4.77	0.06	374.5	5.1
2.55	0.01	8.93	0.07	350.4	2.9
6.37	0.02	20.63	0.08	323.8	1.7
12.74	0.04	40.85	0.13	320.7	1.5
2.51	0.02	10.30	0.24	410.7	9.9
6.27	0.04	19.66	0.25	313.7	4.5
12.54	0.08	34.64	0.29	276.3	2.9

Table B.61 Epping 20.0% W/O Emulsion Rheology

Brookfield Synchrolectric LVTD
Temperature: 24.40 ±0.10°C

Shear Rate sec^{-1}		Shear Stress $dynes/cm^2$		Viscosity cP	
0.07	±0.00	5.46	±0.02	8253.0	±134.7
0.13	0.00	10.92	0.02	8253.0	69.2
0.06	0.01	4.43	0.06	7732.2	1146.5
0.11	0.02	9.73	0.07	8483.9	1248.1
0.29	0.04	24.97	0.09	8709.4	1278.7
0.57	0.08	50.34	0.15	8779.2	1288.6
0.28	0.04	24.34	0.26	8621.0	1337.7
0.56	0.09	49.74	0.33	8807.6	1364.4
1.13	0.17	99.83	0.53	8838.6	1368.7
2.26	0.35	197.21	0.98	8729.9	1351.7
1.12	0.18	94.62	1.38	8426.9	1348.9
2.25	0.36	192.52	2.03	8573.1	1369.6
5.61	0.89	464.90	4.28	8280.8	1322.2
11.23	1.79	884.95	7.96	7881.4	1258.3

Table B.62 Epping 20.0% W/O Emulsion Rheology

Brookfield Synchrolectric LVTD
Temperature: 40.00 ±0.15°C

Shear Rate sec^{-1}		Shear Stress $dynes/cm^2$		Viscosity cP	
0.06	±0.00	1.29	±0.02	1990.5	±50.6
0.13	0.00	2.79	0.02	2154.3	39.6
0.32	0.01	6.92	0.02	2133.7	34.3
0.65	0.01	13.81	0.03	2130.0	33.5
0.13	0.01	3.23	0.06	2561.8	137.4
0.32	0.02	8.00	0.07	2537.4	127.3
0.63	0.03	15.73	0.08	2493.5	123.8
1.26	0.06	30.66	0.10	2430.1	120.4
2.52	0.12	59.48	0.18	2356.9	116.7
0.62	0.01	19.43	0.25	3150.6	72.1
1.23	0.02	35.46	0.29	2875.4	58.9
2.47	0.05	68.47	0.40	2775.8	54.6
6.17	0.12	168.18	0.84	2727.4	53.0
2.42	0.08	83.14	1.32	3438.8	132.5
6.04	0.21	185.96	1.99	3076.9	112.9
12.09	0.42	351.68	3.32	2909.4	105.8

Table B.63 Epping 20.0% W/O Emulsion Rheology

Brookfield Synchrolectric LVTD
Temperature: 60.60 ±0.15°C

Shear Rate sec^{-1}		Shear Stress $dynes/cm^2$		Viscosity cP	
0.14	±0.00	0.81	±0.02	589.9	±18.4
0.34	0.01	1.71	0.02	497.1	12.5
0.69	0.02	3.42	0.02	498.2	11.8
1.37	0.03	6.90	0.02	502.3	11.7
2.75	0.06	13.78	0.03	501.4	11.6
0.68	0.03	3.88	0.06	571.4	23.4
1.36	0.05	7.82	0.07	575.9	22.2
2.72	0.10	15.27	0.07	562.3	21.4
6.79	0.26	37.38	0.12	550.5	20.8
1.35	0.05	11.24	1.17	834.0	92.9
2.69	0.11	19.43	0.25	721.1	29.7
6.74	0.26	41.66	0.31	618.6	24.6
13.47	0.53	82.04	0.46	609.0	24.0

Table B.64 Epping 20.0% W/O Emulsion Rheology

Brookfield Synchrolectric LVTD
Temperature: 76.00 ±0.50°C

Shear Rate sec^{-1}		Shear Stress $dynes/cm^2$		Viscosity cP	
0.34	±0.00	0.90	±0.02	263.6	±4.8
0.68	0.00	1.75	0.02	256.6	2.5
1.36	0.00	3.40	0.02	249.7	1.5
2.72	0.01	6.71	0.02	246.5	1.1
2.63	0.01	7.33	0.06	278.3	2.7
6.58	0.02	16.99	0.08	258.2	1.6
13.16	0.06	33.25	0.11	252.6	1.4
6.56	0.03	18.73	0.25	285.4	4.0
13.12	0.05	34.64	0.29	264.0	2.4

Table B.65 Epping 20.4% W/O Emulsion Rheology

Brookfield Synchrolectric LVTD
Temperature: 23.40 ±0.10°C

Shear Rate sec^{-1}		Shear Stress $dynes/cm^2$		Viscosity cP	
0.07	±0.00	6.14	±0.02	9232.3	±150.2
0.13	0.00	12.23	0.02	9196.8	76.8
0.06	0.01	4.99	0.06	8470.6	1552.9
0.12	0.02	10.16	0.07	8627.5	1574.4
0.29	0.05	25.71	0.09	8732.0	1591.5
0.59	0.11	50.74	0.15	8617.0	1570.2
0.29	0.06	24.81	0.26	8544.6	1638.3
0.58	0.11	49.86	0.34	8584.9	1644.4
1.16	0.22	97.96	0.53	8433.8	1615.0
2.32	0.44	187.96	0.93	8091.2	1549.3
1.16	0.23	90.79	1.36	7857.6	1547.1
2.31	0.45	181.58	1.95	7857.6	1544.9
5.78	1.13	435.37	4.03	7535.7	1481.0
11.55	2.27	819.32	7.38	7090.8	1393.5

Table B.66 Epping 20.4% W/O Emulsion Rheology

Brookfield Synchrolectric LVTD
Temperature: 40.00 ±0.15°C

Shear Rate sec^{-1}		Shear Stress $dynes/cm^2$		Viscosity cP	
0.07	±0.00	1.54	±0.02	2282.9	±56.0
0.14	0.00	2.86	0.02	2114.0	38.8
0.34	0.01	7.24	0.03	2143.1	34.8
0.68	0.01	14.36	0.03	2124.5	33.4
0.13	0.00	3.20	0.06	2452.6	66.7
0.33	0.01	8.00	0.07	2452.5	47.6
0.65	0.01	15.92	0.08	2438.4	44.0
1.31	0.02	31.86	0.11	2440.8	43.1
0.65	0.01	20.25	0.25	3130.6	69.6
1.29	0.02	35.93	0.29	2777.8	55.6
2.59	0.05	67.76	0.40	2619.4	50.4
6.47	0.12	159.17	0.80	2461.1	46.7
2.61	0.10	70.01	1.26	2684.7	110.9
6.52	0.24	161.89	1.81	2483.3	96.4
13.04	0.48	309.57	2.97	2374.3	91.1

Table B.67 Epping 20.4% W/O Emulsion Rheology

Brookfield Synchrolectric LVTD
Temperature: 57.90 ±0.20°C

Shear Rate sec^{-1}		Shear Stress $dynes/cm^2$		Viscosity cP	
0.33	±0.00	1.72	±0.02	527.7	±5.3
0.65	0.00	3.50	0.02	536.2	3.0
1.31	0.00	7.08	0.02	542.2	2.1
2.61	0.01	14.25	0.03	545.2	1.7
0.63	0.00	4.56	0.06	724.8	10.4
1.26	0.00	8.31	0.07	661.1	5.8
2.51	0.01	14.78	0.07	587.7	3.7
6.29	0.02	36.39	0.12	578.9	2.8
2.48	0.01	17.44	0.25	703.5	10.8
6.20	0.03	40.38	0.30	651.6	6.1
12.39	0.07	77.95	0.44	628.9	5.0

Table B.68 Epping 20.4% W/O Emulsion Rheology

Brookfield Synchrolectric LVTD
Temperature: 75.00 ±0.20°C

Shear Rate sec^{-1}		Shear Stress $dynes/cm^2$		Viscosity cP	
0.35	±0.01	0.82	±0.02	236.9	±6.2
0.69	0.01	1.45	0.02	209.5	4.3
1.38	0.02	2.82	0.02	203.8	3.8
2.76	0.05	5.52	0.02	199.9	3.5
6.91	0.12	13.82	0.03	200.0	3.5
1.37	0.04	3.51	0.06	255.3	8.0
2.75	0.07	6.03	0.06	219.5	6.2
6.87	0.18	13.67	0.07	198.9	5.3
13.75	0.36	26.66	0.10	193.9	5.1
7.65	0.01	15.45	0.25	202.1	3.2
15.29	0.03	29.14	0.27	190.6	1.8

Table B.69 Epping 43.2% W/O/W Emulsion Rheology

Brookfield Synchrolectric LVTD
Temperature: 22.50 ±0.10°C

Shear Rate sec^{-1}		Shear Stress $dynes/cm^2$		Viscosity cP	
0.12	±0.00	6.83	±0.02	5749.8	±92.9
0.24	0.00	9.87	0.02	4153.4	34.3
0.12	0.02	4.31	0.06	3667.3	562.0
0.24	0.04	6.37	0.06	2711.2	412.8
0.59	0.09	10.93	0.07	1859.8	282.5
1.18	0.18	16.26	0.08	1383.1	210.0
2.35	0.36	23.89	0.09	1016.4	154.3
4.70	0.71	28.32	0.32	602.5	91.7
11.75	1.78	52.25	0.34	444.5	67.5
0.55	0.13	13.69	0.24	2482.2	605.3
1.10	0.27	18.49	0.25	1676.0	408.2
2.21	0.54	25.28	0.26	1145.6	278.9
4.41	1.07	36.75	0.29	832.7	202.6
11.03	2.68	53.84	1.20	487.9	119.2
22.07	5.37	88.95	1.25	403.1	98.2
11.84	0.00	52.51	5.49	443.5	46.4
23.68	0.00	83.14	2.31	351.1	9.8

Table B.70 Epping 43.2% W/O/W Emulsion Rheology

Brookfield Synchrolectric LVTD
Temperature: 39.50 ±0.50°C

Shear Rate sec^{-1}		Shear Stress $dynes/cm^2$		Viscosity cP	
0.08	±0.00	1.62	±0.02	2016.6	±56.1
0.16	0.00	2.66	0.02	1654.4	37.9
0.40	0.01	5.70	0.02	1417.5	29.9
0.80	0.02	10.11	0.02	1257.9	26.1
0.08	0.02	2.96	0.12	3499.2	731.5
0.17	0.03	4.19	0.06	2478.6	507.9
0.42	0.09	9.54	0.07	2259.9	461.9
0.84	0.17	18.23	0.08	2157.8	440.8
1.69	0.34	33.96	0.11	2010.2	410.6
0.42	0.09	14.04	0.24	3334.8	693.7
0.84	0.17	26.92	0.27	3195.8	663.1
1.68	0.35	47.40	0.33	2813.7	583.5
3.37	0.70	81.46	0.46	2417.7	501.3
8.42	1.75	152.15	1.38	1806.3	374.7
1.57	0.04	55.79	1.20	3554.2	111.3
3.14	0.07	106.65	1.45	3397.4	90.0
7.85	0.18	245.03	2.44	3122.1	77.5
15.70	0.36	415.68	6.61	2648.2	73.4

Table B.71 Epping 43.2% W/O/W Emulsion Rheology

Brookfield Synchrolectric LVTD
Temperature: 59.90 ±0.50°C

Shear Rate sec^{-1}		Shear Stress $dynes/cm^2$		Viscosity cP	
0.13	±0.00	0.99	±0.02	750.2	±14.7
0.33	0.00	2.41	0.02	728.8	8.1
0.66	0.01	4.93	0.02	745.4	6.8
1.32	0.01	9.90	0.02	749.0	6.4
0.32	0.00	3.26	0.06	1024.8	22.0
0.64	0.01	6.77	0.06	1063.4	14.3
1.27	0.01	13.36	0.07	1048.9	11.4
2.55	0.02	26.05	0.09	1022.3	10.3
1.26	0.01	12.76	0.24	1011.7	22.0
2.52	0.03	24.23	0.26	960.7	14.5
6.30	0.07	58.63	0.37	930.1	11.4
12.61	0.13	111.77	0.59	886.4	10.4
6.50	0.05	69.46	1.26	1069.3	20.9
12.99	0.10	131.27	1.60	1010.4	14.4

Table B.72 Epping 53.2% W/O/W Emulsion Rheology

Brookfield Synchrolectric LVTD
Temperature: 22.90 ±0.10°C

Shear Rate sec^{-1}		Shear Stress $dynes/cm^2$		Viscosity cP	
0.10	±0.00	1.68	±0.02	1699.5	±47.6
0.20	0.00	2.42	0.02	1223.0	28.7
0.50	0.01	4.53	0.02	913.3	19.7
0.99	0.02	7.04	0.02	710.8	15.1
1.98	0.04	11.20	0.02	565.0	11.9
0.20	0.00	2.56	0.06	1296.4	39.7
0.49	0.01	4.46	0.06	905.9	20.2
0.99	0.02	6.96	0.06	706.0	13.7
1.97	0.03	11.02	0.07	559.2	10.1
3.94	0.07	16.78	0.08	425.6	7.5
9.86	0.17	24.88	0.20	252.4	4.7
19.71	0.33	40.21	0.33	204.0	3.8
1.99	0.07	9.60	0.24	481.8	20.3
3.98	0.14	15.33	0.25	384.9	14.5
9.96	0.34	20.48	0.71	205.7	10.0
19.92	0.68	30.66	0.72	154.0	6.4

Table B.73 Epping 53.2% W/O/W Emulsion Rheology

Brookfield Synchrolectric LVTD
Temperature: 39.80 ±0.10°C

Shear Rate sec^{-1}		Shear Stress $dynes/cm^2$		Viscosity cP	
0.47	±0.01	1.09	±0.02	232.3	±7.3
0.93	0.03	1.87	0.02	200.3	5.8
1.87	0.05	3.02	0.02	161.6	4.6
3.74	0.10	4.79	0.02	128.2	3.6
9.35	0.26	8.36	0.05	89.4	2.5
0.93	0.03	2.71	0.06	292.8	10.8
1.85	0.05	4.28	0.06	231.3	7.5
3.70	0.11	6.96	0.06	188.0	5.7
9.25	0.27	8.13	0.19	87.8	3.2
18.50	0.54	13.95	0.07	75.4	2.2
8.00	0.01	9.71	0.47	121.4	5.9
16.00	0.02	15.57	0.25	97.3	1.5

Table B.74 Epping 53.2% W/O/W Emulsion Rheology

Brookfield Synchrolectric LVTD -
Temperature: 59.20 ±0.10°C

Shear Rate sec^{-1}		Shear Stress $dynes/cm^2$		Viscosity cP	
0.38	±0.00	0.84	±0.02	224.3	±4.4
0.75	0.00	1.54	0.02	205.5	2.4
1.50	0.01	2.86	0.02	190.3	1.4
3.00	0.01	5.12	0.02	170.4	1.0
7.51	0.04	11.22	0.02	149.5	0.8
1.46	0.01	4.68	0.06	321.3	5.0
2.91	0.02	8.87	0.07	304.4	3.3
7.28	0.06	19.70	0.08	270.6	2.4
14.56	0.11	25.55	0.09	175.5	1.5
0.37	0.01	0.56	0.01	149.5	3.8
0.74	0.01	0.68	0.01	91.4	1.8
1.86	0.03	0.88	0.01	47.5	0.8
3.72	0.05	1.28	0.02	34.6	0.6
7.43	0.11	2.03	0.02	27.3	0.4
14.86	0.22	3.63	0.02	24.4	0.4

Table B.75 Epping 64.0% W/O/W Emulsion Rheology

Brookfield Synchrolectric LVTD
Temperature: 22.60 ±0.10°C

Shear Rate sec^{-1}		Shear Stress $dynes/cm^2$		Viscosity cP	
0.39	±0.01	0.80	±0.01	206.8	±4.9
0.78	0.01	1.34	0.01	172.5	3.1
1.94	0.03	2.74	0.01	140.9	2.2
3.89	0.06	3.72	0.01	95.8	1.5
7.77	0.12	4.84	0.01	62.3	0.9

Table B.76 Epping 64.0% W/O/W Emulsion Rheology

Brookfield Synchrolectric LVTD
Temperature: 40.00 ±0.10°C

Shear Rate sec^{-1}		Shear Stress $dynes/cm^2$		Viscosity cP	
0.40	±0.01	0.50	±0.01	126.0	±3.4
0.80	0.01	0.65	0.01	80.9	1.7
2.00	0.03	0.81	0.01	40.6	0.8
3.99	0.06	1.16	0.01	29.0	0.5
7.99	0.13	1.75	0.01	21.9	0.4
15.97	0.26	2.74	0.01	17.2	0.3
39.93	0.64	5.34	0.01	13.4	0.2

Table B.77 Epping 64.0% W/O/W Emulsion Rheology

Brookfield Synchrolectric LVTD
Temperature: 59.80 ±0.10°C

Shear Rate sec^{-1}		Shear Stress $dynes/cm^2$		Viscosity cP	
0.38	±0.01	0.09	±0.01	23.7	±2.0
0.76	0.01	0.16	0.01	20.7	1.0
1.90	0.02	0.30	0.01	16.0	0.4
3.80	0.03	0.46	0.01	12.1	0.2
7.61	0.07	0.77	0.01	10.2	0.1
15.21	0.13	1.34	0.01	8.8	0.1
38.04	0.33	2.80	0.01	7.4	0.1
76.07	0.67	4.43	0.01	5.8	0.1

Table B.78 Epping 66.8% W/O/W Emulsion Rheology

Brookfield Synchrolectric LVTD
Temperature: 21.60 ±0.10°C

Shear Rate sec^{-1}		Shear Stress $dynes/cm^2$		Viscosity cP	
0.20	±0.01	0.94	±0.02	461.9	±17.8
0.51	0.02	1.78	0.02	348.0	12.2
1.02	0.03	2.95	0.02	288.7	9.9
2.04	0.07	4.05	0.02	197.8	6.7
4.09	0.14	5.82	0.02	142.4	4.8
10.22	0.35	11.31	0.02	110.6	3.8
1.03	0.06	2.68	0.06	260.8	15.3
2.05	0.11	4.40	0.06	214.4	12.0
4.11	0.22	6.93	0.06	168.6	9.3
10.27	0.56	9.33	0.07	90.8	5.0
20.54	1.11	12.87	0.07	62.7	3.4

Table B.79 Epping 66.8% W/O/W Emulsion Rheology

Brookfield Synchrolectric LVTD
Temperature: 38.00 ±0.20°C

Shear Rate sec^{-1}		Shear Stress $dynes/cm^2$		Viscosity cP	
0.94	±0.01	0.88	±0.02	93.7	±2.1
1.88	0.03	1.46	0.02	77.8	1.4
3.76	0.05	2.26	0.02	60.0	0.9
9.41	0.13	4.12	0.02	43.8	0.6
18.82	0.26	6.85	0.02	36.4	0.5
8.61	0.01	3.88	0.06	45.0	0.7
17.23	0.01	6.16	0.06	35.7	0.4

Table B.80 Epping 66.8% W/O/W Emulsion Rheology

Brookfield Synchrolectric LVTD
Temperature: 59.70 ±0.20°C

Shear Rate sec^{-1}		Shear Stress $dynes/cm^2$		Viscosity cP	
0.79	±0.01	0.33	±0.01	42.0	±1.1
1.97	0.02	0.63	0.01	32.1	0.5
3.94	0.04	1.03	0.01	26.1	0.3
7.87	0.09	1.43	0.01	18.2	0.2
15.74	0.17	2.17	0.01	13.8	0.2
39.35	0.43	2.94	0.01	7.5	0.1
78.70	0.86	5.11	0.01	6.5	0.1

Table B.81 Epping 70.4% W/O/W Emulsion Rheology

Brookfield Synchrolectric LVTD
Temperature: 22.65 ±0.05°C

Shear Rate sec^{-1}		Shear Stress $dynes/cm^2$		Viscosity cP	
0.39	±0.01	0.75	±0.01	194.5	±4.2
0.77	0.01	1.08	0.01	139.6	2.1
1.93	0.02	2.04	0.01	105.6	1.2
3.86	0.04	3.54	0.01	91.6	1.0
7.72	0.08	4.91	0.01	63.6	0.7

Table B.82 Epping 70.4% W/O/W Emulsion Rheology

Brookfield Synchrolectric LVTD
Temperature: 39.75 ±0.10°C

Shear Rate sec^{-1}		Shear Stress $dynes/cm^2$		Viscosity cP	
0.39	±0.01	0.30	±0.01	76.1	±2.4
0.78	0.01	0.50	0.01	64.6	1.3
1.95	0.02	1.00	0.01	51.3	0.7
3.90	0.04	1.55	0.01	39.7	0.5
7.79	0.09	2.18	0.01	27.9	0.3
15.58	0.17	2.73	0.01	17.5	0.2
38.96	0.43	5.29	0.01	13.6	0.2

Table B.83 Epping 70.4% W/O/W Emulsion Rheology

Brookfield Synchrolectric LVTD
Temperature: 59.30 ±0.10°C

Shear Rate sec^{-1}		Shear Stress $dynes/cm^2$		Viscosity cP	
0.39	±0.01	0.16	±0.01	41.4	±2.1
0.78	0.01	0.24	0.01	31.3	1.0
1.95	0.02	0.47	0.01	24.3	0.4
3.90	0.04	0.73	0.01	18.7	0.3
7.79	0.07	1.09	0.01	14.0	0.2
15.58	0.14	1.48	0.01	9.5	0.1
38.95	0.35	2.66	0.01	6.8	0.1
77.90	0.69	4.41	0.01	5.7	0.1

Table B.84 Epping 70.4% W/O/W Emulsion Rheology

Brookfield Synchrolectric LVTD
Temperature: 75.50 ±0.10°C

Shear Rate sec^{-1}		Shear Stress $dynes/cm^2$		Viscosity cP	
0.39	±0.01	0.09	±0.01	23.3	±2.0
0.77	0.01	0.16	0.01	20.4	1.0
1.94	0.02	0.29	0.01	14.7	0.4
3.87	0.04	0.40	0.01	10.3	0.2
7.75	0.07	0.60	0.01	7.8	0.1
15.49	0.14	0.92	0.01	5.9	0.1
38.73	0.35	1.70	0.01	4.4	0.0
77.47	0.71	3.04	0.01	3.9	0.0

Table B.85 Epping 96.8% O/W Emulsion Rheology

Brookfield Synchrolectric LVTD
Temperature: 23.80 ±0.10°C

Shear Rate sec^{-1}		Shear Stress $dynes/cm^2$		Viscosity cP	
3.73	±0.04	0.08	±0.01	2.0	±0.2
7.46	0.08	0.11	0.01	1.4	0.1
14.91	0.17	0.19	0.01	1.3	0.1
37.28	0.41	0.47	0.01	1.3	0.0
74.56	0.83	0.94	0.01	1.3	0.0

Table B.86 Epping 96.8% O/W Emulsion Rheology

Brookfield Synchrolectric LVTD
Temperature: 39.00 ±0.20°C

Shear Rate sec^{-1}		Shear Stress $dynes/cm^2$		Viscosity cP	
3.77	±0.06	0.08	±0.01	2.0	±0.2
7.54	0.12	0.10	0.01	1.3	0.1
15.09	0.23	0.14	0.01	0.9	0.1
37.72	0.58	0.35	0.01	0.9	0.0
75.44	1.16	0.69	0.01	0.9	0.0

Table B.87 Epping 96.8% O/W Emulsion Rheology

Brookfield Synchrolectric LVTD
Temperature: 59.40 ±0.20°C

Shear Rate sec^{-1}		Shear Stress $dynes/cm^2$		Viscosity cP	
7.41	±0.10	0.08	±0.01	1.1	±0.1
14.82	0.21	0.12	0.01	0.8	0.1
37.05	0.52	0.29	0.01	0.8	0.0
74.10	1.03	0.66	0.01	0.9	0.0

Table B.88 Epping 96.8% O/W Emulsion Rheology

Brookfield Synchrolectric LVTD
Temperature: 75.40 ±0.20°C

Shear Rate sec^{-1}		Shear Stress $dynes/cm^2$		Viscosity cP	
7.39	±0.10	0.08	±0.01	1.0	±0.1
14.78	0.20	0.11	0.01	0.8	0.1
36.96	0.50	0.26	0.01	0.7	0.0
73.91	1.00	0.65	0.01	0.9	0.0

Table B.89 Epping 98.0% O/W Emulsion Rheology

Brookfield Synchrolectric LVTD
Temperature: 25.20 ±0.10°C

Shear Rate sec^{-1}		Shear Stress $dynes/cm^2$		Viscosity cP	
3.73	±0.04	0.07	±0.01	1.8	±0.2
7.47	0.08	0.10	0.01	1.4	0.1
14.93	0.15	0.18	0.01	1.2	0.1
37.33	0.38	0.44	0.01	1.2	0.0
74.66	0.76	0.85	0.01	1.1	0.0

Table B.90 Epping 98.0% O/W Emulsion Rheology

Brookfield Synchrolectric LVTD
Temperature: 39.70 ±0.20°C

Shear Rate sec^{-1}		Shear Stress $dynes/cm^2$		Viscosity cP	
3.76	±0.04	0.06	±0.01	1.6	±0.3
7.51	0.08	0.09	0.01	1.1	0.1
15.02	0.16	0.15	0.01	1.0	0.1
37.55	0.40	0.34	0.01	0.9	0.0
75.10	0.80	0.66	0.01	0.9	0.0

Table B.91 Epping 98.0% O/W Emulsion Rheology

Brookfield Synchrolectric LVTD
Temperature: 60.00 ±0.20°C

Shear Rate sec^{-1}		Shear Stress $dynes/cm^2$		Viscosity cP	
7.36	±0.08	0.06	±0.01	0.8	±0.2
14.73	0.15	0.12	0.01	0.8	0.1
36.82	0.38	0.26	0.01	0.7	0.0
73.64	0.77	0.62	0.01	0.8	0.0

Table B.92 Epping 98.0% O/W Emulsion Rheology

Brookfield Synchrolectric LVTD
Temperature: 74.50 ±0.20°C

Shear Rate sec^{-1}		Shear Stress $dynes/cm^2$		Viscosity cP	
7.33	±0.08	0.05	±0.01	0.7	±0.2
14.65	0.16	0.09	0.01	0.6	0.1
36.63	0.40	0.23	0.01	0.6	0.0
73.27	0.80	0.60	0.01	0.8	0.0

Table B.93 Epping 98.4% O/W Emulsion Rheology

Brookfield Synchrolectric LVTD
Temperature: 22.65 ±0.10°C

Shear Rate sec^{-1}		Shear Stress $dynes/cm^2$		Viscosity cP	
7.41	±0.07	0.10	±0.01	1.3	±0.1
14.81	0.13	0.18	0.01	1.2	0.1
37.03	0.34	0.43	0.01	1.2	0.0
74.06	0.67	0.84	0.01	1.1	0.0

Table B.94 Epping 98.4% O/W Emulsion Rheology

Brookfield Synchrolectric LVTD
Temperature: 39.75 ±0.10°C

Shear Rate sec^{-1}		Shear Stress $dynes/cm^2$		Viscosity cP	
7.41	±0.07	0.07	±0.01	1.0	±0.1
14.82	0.13	0.14	0.01	1.0	0.1
37.06	0.33	0.32	0.01	0.9	0.0
74.11	0.67	0.62	0.01	0.8	0.0

Table B.95 Epping 98.4% O/W Emulsion Rheology

Brookfield Synchrolectric LVTD
Temperature: 59.30 ±0.10°C

Shear Rate sec^{-1}		Shear Stress $dynes/cm^2$		Viscosity cP	
7.39	±0.09	0.07	±0.01	0.9	±0.1
14.78	0.18	0.12	0.01	0.8	0.1
36.95	0.44	0.25	0.01	0.7	0.0
73.90	0.88	0.62	0.01	0.8	0.0

Table B.96 Epping 98.4% O/W Emulsion Rheology

Brookfield Synchrolectric LVTD
Temperature: 75.60 ±0.10°C

Shear Rate sec^{-1}		Shear Stress $dynes/cm^2$		Viscosity cP	
7.38	±0.12	0.06	±0.01	0.9	±0.1
14.76	0.24	0.11	0.01	0.7	0.1
36.90	0.61	0.20	0.01	0.5	0.0
73.80	1.22	0.60	0.01	0.8	0.0

Table B.97 Primrose 3.6% (dried) W/O Emulsion Rheology

Brookfield Synchrolectric LVTD
Temperature: 22.00 ±0.10°C

Shear Rate sec^{-1}		Shear Stress $dynes/cm^2$		Viscosity cP	
0.06	±0.00	49.62	±0.33	80137.3	±1448.2
0.12	0.00	100.65	0.54	81271.4	889.4
0.33	0.01	233.54	2.35	71356.4	2296.9
0.65	0.02	472.56	4.35	72191.9	2296.5
1.31	0.04	945.66	8.50	72233.8	2291.1

Table B.98 Primrose 3.6% (dried) W/O Emulsion Rheology

Brookfield Synchrolectric LVTD
Temperature: 40.00 ±0.20°C

Shear Rate sec^{-1}		Shear Stress $dynes/cm^2$		Viscosity cP	
0.08	±0.01	11.55	±0.19	14357.1	±1472.9
0.16	0.02	17.61	0.19	10949.7	1105.3
0.40	0.04	39.90	0.22	9923.6	994.7
0.40	0.04	32.54	0.28	8121.3	830.6
0.80	0.08	62.50	0.38	7799.9	796.0
1.60	0.16	117.86	0.61	7354.4	750.1
1.60	0.16	142.20	1.67	8882.0	916.1
3.20	0.33	281.68	2.74	8796.6	905.4
8.01	0.82	702.82	6.36	8779.5	903.1

Table B.99 Primrose 3.6% (dried) W/O Emulsion Rheology

Brookfield Synchrolectric LVTD
Temperature: 59.60 ±0.50°C

Shear Rate sec^{-1}		Shear Stress $dynes/cm^2$		Viscosity cP	
0.14	±0.00	2.42	±0.02	1728.4	±33.5
0.35	0.01	5.57	0.02	1589.2	27.0
0.70	0.01	10.92	0.02	1557.8	25.9
0.30	0.07	8.56	0.19	2818.9	608.6
0.61	0.13	14.16	0.07	2332.2	501.0
1.21	0.26	25.80	0.09	2124.3	456.3
2.43	0.52	50.09	0.19	2062.2	443.0
1.35	0.03	33.24	0.49	2463.0	59.3
2.70	0.05	61.44	0.38	2276.5	45.2
6.75	0.13	149.81	0.76	2220.1	43.4

Table B.100 Primrose 22.8% W/O Emulsion Rheology

Brookfield Synchrolectric LVTD
Temperature: 23.80 ±0.10°C

Shear Rate sec^{-1}		Shear Stress $dynes/cm^2$		Viscosity cP	
0.06	±0.00	96.20	±0.52	156474.9	±2764.1
0.12	0.00	196.15	0.97	159520.9	1729.7
0.07	0.00	100.64	2.36	153128.8	9929.3
0.13	0.01	184.32	1.97	140229.4	8387.1
0.33	0.02	462.71	4.27	140811.8	8323.9
0.66	0.04	898.63	8.08	136733.9	8069.3

Table B.101 Primrose 22.8% W/O Emulsion Rheology

Brookfield Synchrolectric LVTD
Temperature: 44.80 ±0.20°C

Shear Rate sec^{-1}		Shear Stress $dynes/cm^2$		Viscosity cP	
0.07	±0.00	10.96	±0.07	16788.1	±305.9
0.13	0.00	21.37	0.09	16363.7	178.4
0.33	0.00	52.65	0.16	16127.9	123.5
0.13	0.01	24.46	0.26	18990.4	1354.2
0.32	0.02	57.82	0.36	17954.5	1264.0
0.64	0.05	96.55	0.52	14992.4	1053.6
1.29	0.09	167.60	0.84	13011.6	913.8
0.64	0.05	111.58	1.48	17380.0	1263.7
1.28	0.09	219.87	2.24	17124.4	1236.5
2.57	0.18	421.15	3.91	16400.2	1182.1
6.42	0.46	916.13	8.24	14270.3	1028.0

Table B.102 Primrose 22.8% W/O Emulsion Rheology

Brookfield Synchrolectric LVTD
Temperature: 54.20 ±0.20°C

Shear Rate sec^{-1}		Shear Stress $dynes/cm^2$		Viscosity cP	
0.06	±0.00	5.85	±0.06	9311.6	±259.2
0.13	0.00	12.44	0.07	9899.7	221.1
0.31	0.01	31.68	0.11	10085.9	207.9
0.63	0.01	60.53	0.18	9635.1	196.1
0.30	0.01	43.54	0.31	14438.2	292.1
0.60	0.01	82.86	0.46	13739.5	268.1
1.21	0.02	94.56	0.51	7840.1	152.3
1.24	0.03	98.45	1.40	7950.9	216.7
2.48	0.06	189.24	2.01	7641.7	195.2
6.19	0.14	449.04	4.15	7253.0	181.3
12.38	0.29	846.67	7.62	6837.8	170.3

Table B.103 Primrose 22.8% W/O Emulsion Rheology

Brookfield Synchrolectric LVTD
Temperature: 62.00 ±0.20°C

Shear Rate sec^{-1}		Shear Stress $dynes/cm^2$		Viscosity cP	
0.31	±0.00	15.95	±0.08	5191.8	±34.0
0.61	0.00	32.82	0.11	5342.2	26.2
0.64	0.08	29.73	0.27	4641.4	579.1
1.28	0.16	57.35	0.36	4476.9	557.7
2.56	0.32	110.25	0.58	4303.3	535.9
2.55	0.32	141.11	1.67	5526.1	702.9
6.38	0.81	317.23	3.03	4969.2	631.1
12.77	1.62	580.85	5.29	4549.3	577.6

Table B.104 Primrose 32.0% W/O Emulsion Rheology

Brookfield Synchrolectric LVTD
Temperature: 22.80 ±0.10°C

Shear Rate sec^{-1}		Shear Stress $dynes/cm^2$		Viscosity cP	
0.06	±0.00	122.52	±1.55	193848.6	±5830.6
0.13	0.00	251.59	2.49	199041.1	5089.8
0.32	0.01	609.29	5.54	192809.9	4663.5

Table B.105 Primrose 32.0% W/O Emulsion Rheology

Brookfield Synchrolectric LVTD
Temperature: 43.20 ±0.20°C

Shear Rate sec^{-1}		Shear Stress $dynes/cm^2$		Viscosity cP	
0.08	±0.00	17.86	±0.19	21585.2	±414.6
0.17	0.00	30.29	0.15	18310.2	172.2
0.16	0.00	30.43	0.49	18524.7	359.4
0.41	0.00	72.09	0.58	17555.7	199.2
0.82	0.01	138.10	0.81	16814.7	159.9
0.82	0.01	140.02	2.52	17061.1	332.9
1.64	0.01	257.06	3.17	15661.6	225.4
3.28	0.02	492.25	4.52	14995.1	176.9

Table B.106 Primrose 32.0% W/O Emulsion Rheology

Brookfield Synchrolectric LVTD
Temperature: 53.50 ±0.20°C

Shear Rate sec^{-1}		Shear Stress $dynes/cm^2$		Viscosity cP	
0.08	±0.01	9.85	±0.07	12216.7	±1113.0
0.16	0.01	15.21	0.13	9429.8	850.6
0.40	0.04	34.05	0.11	8444.8	756.3
0.40	0.04	36.28	0.50	9030.0	832.0
0.80	0.07	67.88	0.57	8447.4	772.5
1.61	0.15	127.57	0.77	7937.7	724.4

Table B.107 Primrose 32.0% W/O Emulsion Rheology

Brookfield Synchrolectric LVTD
Temperature: 64.00 ±0.30°C

Shear Rate sec^{-1}		Shear Stress $dynes/cm^2$		Viscosity cP	
0.14	±0.00	6.50	±0.06	4730.2	±119.7
0.34	0.01	14.29	0.07	4160.7	94.5
0.69	0.02	27.59	0.10	4017.3	89.4
1.37	0.03	54.49	0.19	3968.0	88.1
0.70	0.02	25.75	0.48	3666.7	123.1
1.40	0.04	83.80	0.62	5966.7	171.4
2.80	0.08	125.80	2.46	4487.6	154.3
7.01	0.20	289.88	2.80	4136.4	123.7
14.02	0.40	565.54	5.49	4035.0	120.7

Table B.108 Primrose 44.8% W/O/W Emulsion Rheology

Brookfield Synchrolectric LVTD
Temperature: 22.00 ±0.10°C

Shear Rate sec^{-1}		Shear Stress $dynes/cm^2$		Viscosity cP	
0.23	±0.02	20.94	±0.14	9160.4	±988.1
0.46	0.05	21.86	0.14	4782.3	511.6
1.14	0.12	29.56	0.15	2586.5	275.9
2.29	0.24	34.79	0.16	1522.3	162.3
4.57	0.49	45.57	0.18	996.9	106.2
0.17	0.03	14.04	0.47	8281.1	1328.0
0.34	0.05	18.26	0.48	5382.7	852.3
0.85	0.13	24.34	0.26	2870.8	448.9
1.70	0.26	30.66	0.28	1808.0	282.5
3.39	0.53	37.45	0.50	1104.2	172.9
6.78	1.06	49.16	0.52	724.6	113.3
16.96	2.65	72.56	0.58	427.9	66.8
33.92	5.29	102.76	0.86	303.0	47.3
10.22	3.49	76.57	5.51	748.9	260.9
25.56	8.71	86.42	2.32	338.1	115.6
51.12	17.43	103.92	5.55	203.3	70.1

Table B.109 Primrose 44.8% W/O/W Emulsion Rheology

Brookfield Synchrolectric LVTD
Temperature: 44.00 ±0.20°C

Shear Rate sec^{-1}		Shear Stress $dynes/cm^2$		Viscosity cP	
0.25	±0.03	13.85	±0.19	5498.7	±684.1
0.50	0.06	14.41	0.13	2859.3	352.3
1.26	0.15	17.49	0.19	1388.1	171.0
2.52	0.31	20.01	0.19	794.3	97.7
5.04	0.62	24.63	0.14	488.8	60.0
10.08	1.24	33.56	0.15	333.0	40.9
3.12	0.35	18.26	0.48	585.5	67.2
6.24	0.70	21.53	0.26	345.3	38.8
12.47	1.39	27.15	0.49	217.7	24.6
31.19	3.48	40.96	0.73	131.4	14.9
62.37	6.97	55.01	0.54	88.2	9.9

Table B.110 Primrose 44.8% W/O/W Emulsion Rheology

Brookfield Synchrolectric LVTD
Temperature: 56.00 ±0.20°C

Shear Rate sec^{-1}		Shear Stress $dynes/cm^2$		Viscosity cP	
0.21	±0.05	13.55	±0.31	6543.8	±1491.4
0.41	0.09	12.01	0.31	2900.1	660.7
1.04	0.23	14.16	0.19	1368.3	310.1
2.07	0.47	14.90	0.13	719.8	162.9
4.14	0.94	17.67	0.19	426.8	96.7
8.28	1.87	24.81	0.20	299.7	67.8
20.70	4.68	42.49	0.33	205.2	46.5
4.48	1.68	16.39	1.17	365.7	140.0
8.96	3.37	18.26	0.48	203.8	76.8
17.92	6.74	22.24	0.48	124.1	46.7
44.80	16.84	36.75	0.50	82.0	30.9
89.60	33.68	52.67	0.75	58.8	22.1

Table B.111 Primrose 44.8% W/O/W Emulsion Rheology

Brookfield Synchrolectric LVTD
Temperature: 63.50 ±0.50°C

Shear Rate sec^{-1}		Shear Stress $dynes/cm^2$		Viscosity cP	
0.17	±0.01	7.76	±0.13	4664.1	±162.8
0.42	0.01	14.47	0.19	3479.5	112.8
0.83	0.02	25.43	0.14	3057.6	91.9
1.66	0.05	44.03	0.22	2646.7	79.2
1.71	0.09	13.81	2.34	808.8	143.2
3.41	0.17	20.60	1.17	603.2	46.0
8.54	0.43	117.04	2.41	1370.9	75.1

Table B.112 Primrose 48.0% W/O/W Emulsion Rheology

Brookfield Synchrolectric LVTD
Temperature: 22.00 ±0.10°C

Shear Rate sec^{-1}		Shear Stress $dynes/cm^2$		Viscosity cP	
0.19	±0.02	28.09	±0.49	15015.6	±1660.1
0.37	0.04	32.30	0.49	8634.0	944.4
0.94	0.10	38.86	0.30	4154.3	450.1
1.87	0.20	45.64	0.52	2440.0	265.1
3.74	0.40	50.33	0.53	1345.2	146.0
7.48	0.81	64.60	0.56	863.4	93.6
18.71	2.02	109.31	0.70	584.4	63.2
37.41	4.04	160.34	0.90	428.6	46.4
5.99	0.14	60.16	5.50	1004.3	94.6
11.98	0.28	65.63	5.50	547.8	47.6
29.95	0.69	86.42	3.37	288.5	13.1
59.91	1.38	121.42	2.44	202.7	6.2

Table B.113 Primrose 48.0% W/O/W Emulsion Rheology

Brookfield Synchrolectric LVTD
Temperature: 43.50 ±0.10°C

Shear Rate sec^{-1}		Shear Stress $dynes/cm^2$		Viscosity cP	
0.36	±0.03	34.11	±0.32	9526.6	±848.3
0.72	0.06	36.64	0.32	5115.8	449.7
1.79	0.16	43.84	0.22	2448.7	213.8
3.58	0.31	50.37	0.34	1406.6	122.9
61.00	0.01	112.59	0.72	184.6	1.2
122.00	0.01	148.64	1.00	121.8	0.8

Table B.114 Primrose 48.0% W/O/W Emulsion Rheology

Brookfield Synchrolectric LVTD
Temperature: 52.00 ±0.20°C

Shear Rate sec^{-1}		Shear Stress $dynes/cm^2$		Viscosity cP	
0.22	±0.03	22.23	±0.31	9898.1	±1182.9
0.45	0.05	23.40	0.20	5209.5	615.6
1.12	0.13	29.37	0.20	2615.7	308.3
2.25	0.26	39.41	0.16	1754.8	206.5
4.49	0.53	47.66	0.33	1061.1	125.0
0.22	0.02	19.66	0.25	9085.0	763.9
0.43	0.04	22.70	0.26	5245.5	434.0
1.08	0.09	29.96	0.27	2768.8	227.4
2.16	0.18	38.62	0.50	1784.6	147.4
4.33	0.35	49.39	0.53	1141.0	93.9
8.66	0.71	60.86	0.55	703.0	57.7
21.64	1.77	89.65	0.64	414.2	33.9
43.28	3.53	111.42	0.88	257.4	21.1

Table B.115 Primrose 48.0% W/O/W Emulsion Rheology

Brookfield Synchrolectric LVTD
Temperature: 64.00 ±0.30°C

Shear Rate sec^{-1}		Shear Stress $dynes/cm^2$		Viscosity cP	
0.19	±0.03	17.49	±0.31	9044.2	±1201.6
0.39	0.05	16.99	0.19	4394.7	577.5
0.97	0.13	21.30	0.19	2203.7	288.8
1.93	0.25	28.82	0.15	1490.4	194.9
3.87	0.51	37.19	0.21	961.7	125.8
7.73	1.01	50.68	0.19	655.2	85.7
0.97	0.13	22.94	0.48	2372.8	314.2
1.93	0.25	30.90	0.49	1598.0	210.4
3.87	0.51	47.05	0.52	1216.7	159.6
7.73	1.01	62.50	0.56	808.1	105.9
19.34	2.53	95.03	0.65	491.5	64.3
38.67	5.05	117.04	1.30	302.6	39.7

Table B.116 Primrose 62.4% W/O/W Emulsion Rheology

Brookfield Synchrolectric LVTD
Temperature: 22.50 ±0.10°C

Shear Rate sec^{-1}		Shear Stress $dynes/cm^2$		Viscosity cP	
0.38	±0.01	3.72	±0.01	981.5	±17.9
0.76	0.01	6.26	0.01	824.2	9.8

Table B.117 Primrose 62.4% W/O/W Emulsion Rheology

Brookfield Synchrolectric LVTD
Temperature: 42.00 ±0.10°C

Shear Rate sec^{-1}		Shear Stress $dynes/cm^2$		Viscosity cP	
0.38	±0.01	1.78	±0.01	467.6	± 8.7
0.76	0.01	2.98	0.01	391.7	4.7
1.90	0.02	5.77	0.01	303.3	2.9

Table B.118 Primrose 62.4% W/O/W Emulsion Rheology

Brookfield Synchrolectric LVTD
Temperature: 56.00 ±0.20°C

Shear Rate sec^{-1}		Shear Stress $dynes/cm^2$		Viscosity cP	
0.40	±0.02	0.87	±0.01	218.1	± 9.9
0.80	0.03	1.53	0.01	191.8	8.1
2.00	0.08	3.04	0.01	152.3	6.3
3.99	0.17	2.43	0.01	60.7	2.5
7.99	0.33	3.70	0.01	46.4	1.9

Table B.119 Primrose 62.4% W/O/W Emulsion Rheology

Brookfield Synchrolectric LVTD
Temperature: 66.00 ±0.30°C

Shear Rate sec^{-1}		Shear Stress $dynes/cm^2$		Viscosity cP	
1.86	±0.02	0.81	±0.01	43.7	± 0.6
3.73	0.04	1.57	0.01	42.1	0.5
7.46	0.07	2.94	0.01	39.4	0.4
14.91	0.14	5.00	0.01	33.5	0.3

Table B.120 Primrose 64.4% W/O/W Emulsion Rheology

Brookfield Synchrolectric LVTD
Temperature: 22.80 ±0.10°C

Shear Rate sec^{-1}		Shear Stress $dynes/cm^2$		Viscosity cP	
2.67	±0.03	1.52	±0.02	56.8	± 0.9
6.68	0.08	3.82	0.02	57.2	0.7
13.37	0.16	7.44	0.02	55.6	0.7
1.84	0.02	0.95	0.01	51.8	0.6
3.69	0.03	1.95	0.01	53.0	0.5
7.37	0.07	3.98	0.01	54.0	0.5

Table B.121 Primrose 64.4% W/O/W Emulsion Rheology

Brookfield Synchrolectric LVTD
Temperature: 44.50 ±0.10°C

Shear Rate sec^{-1}		Shear Stress $dynes/cm^2$		Viscosity cP	
1.85	±0.02	0.68	±0.01	36.5	± 0.6
3.70	0.04	1.14	0.01	30.8	0.4
7.40	0.07	2.31	0.01	31.2	0.3
14.81	0.15	4.68	0.01	31.6	0.3

Table B.122 Primrose 64.4% W/O/W Emulsion Rheology

Brookfield Synchrolectric LVTD
Temperature: 55.00 ±0.20°C

Shear Rate sec^{-1}		Shear Stress $dynes/cm^2$		Viscosity cP	
3.68	±0.03	0.81	±0.01	22.0	± 0.3
7.36	0.07	1.64	0.01	22.2	0.2
14.72	0.13	3.26	0.01	22.1	0.2

Table B.123 Primrose 64.4% W/O/W Emulsion Rheology

Brookfield Synchrolectric LVTD
Temperature: 64.50 ±0.30°C

Shear Rate sec^{-1}		Shear Stress $dynes/cm^2$		Viscosity cP	
7.46	±0.08	1.14	±0.01	15.3	± 0.2
14.91	0.17	2.28	0.01	15.3	0.2
37.28	0.42	4.70	0.02	12.6	0.2

Table B.124 Primrose 78.5% O/W Emulsion Rheology

Brookfield Synchrolectric LVTD
Temperature: 23.50 ±0.10°C

Shear Rate sec^{-1}		Shear Stress $dynes/cm^2$		Viscosity cP	
14.77	±0.13	0.50	±0.01	3.4	± 0.1
36.93	0.33	1.18	0.01	3.2	0.0
73.87	0.66	2.35	0.01	3.2	0.0

Table B.125 Primrose 78.5% O/W Emulsion Rheology

Brookfield Synchrolectric LVTD
Temperature: 41.50 ±0.10°C

Shear Rate sec^{-1}		Shear Stress $dynes/cm^2$		Viscosity cP	
14.78	±0.13	0.36	±0.02	2.4	± 0.1
36.94	0.33	0.87	0.01	2.4	0.0
73.88	0.66	1.68	0.01	2.3	0.0

Table B.126 Primrose 78.5% O/W Emulsion Rheology

Brookfield Synchrolectric LVTD
Temperature: 51.50 ±0.20°C

Shear Rate sec^{-1}		Shear Stress $dynes/cm^2$		Viscosity cP	
14.79	±0.13	0.31	±0.02	2.1	± 0.1
36.98	0.33	0.73	0.01	2.0	0.0
73.95	0.66	1.43	0.01	1.9	0.0

Table B.127 Primrose 78.5% O/W Emulsion Rheology

Brookfield Synchrolectric LVTD
Temperature: 60.50 ±0.30°C

Shear Rate sec^{-1}		Shear Stress $dynes/cm^2$		Viscosity cP	
36.87	±0.33	0.64	±0.01	1.7	± 0.0
73.75	0.66	1.26	0.01	1.7	0.0

Table B.128 Primrose 82.4% O/W Emulsion Rheology

Brookfield Sychrolectric LVTD
Temperature: 23.00 ±0.10°C

Shear Rate sec^{-1}		Shear Stress $dynes/cm^2$		Viscosity cP	
7.36	±0.07	0.59	±0.01	8.0	± 0.1
14.72	0.13	1.16	0.01	7.9	0.1
36.79	0.33	2.92	0.01	7.9	0.1
73.59	0.66	5.93	0.01	8.1	0.1

Table B.129 Primrose 82.4% O/W Emulsion Rheology

Brookfield Sychrolectric LVTD
Temperature: 41.50 ±0.10°C

Shear Rate sec^{-1}		Shear Stress $dynes/cm^2$		Viscosity cP	
7.39	±0.07	0.41	±0.01	5.6	± 0.1
14.77	0.14	0.82	0.01	5.5	0.1
36.93	0.34	2.07	0.01	5.6	0.1
73.85	0.67	3.77	0.01	5.1	0.0

Table B.130 Primrose 82.4% O/W Emulsion Rheology

Brookfield Sychrolectric LVTD
Temperature: 50.10 ±0.20°C

Shear Rate sec^{-1}		Shear Stress $dynes/cm^2$		Viscosity cP	
14.88	±0.18	0.65	±0.01	4.3	± 0.1
37.21	0.45	1.61	0.01	4.3	0.1
74.41	0.90	2.68	0.01	3.6	0.0

Table B.131 Primrose 82.4% O/W Emulsion Rheology

Brookfield Sychrolectric LVTD
Temperature: 60.00 ±0.20°C

Shear Rate sec^{-1}		Shear Stress $dynes/cm^2$		Viscosity cP	
14.76	±0.13	0.45	±0.01	3.1	± 0.1
36.91	0.33	1.07	0.01	2.9	0.0
73.81	0.67	2.16	0.01	2.9	0.0

Table B.132 Primrose 88.8% O/W Emulsion Rheology

Brookfield Synchrolectric LVTD
Temperature: 22.00 ±0.10°C

Shear Rate sec^{-1}		Shear Stress $dynes/cm^2$		Viscosity cP	
3.71	±0.03	0.14	±0.02	3.7	± 0.4
7.42	0.07	0.24	0.01	3.2	0.1
14.84	0.14	0.46	0.01	3.1	0.1
37.09	0.34	1.08	0.01	2.9	0.0
74.18	0.68	2.18	0.01	2.9	0.0

Table B.133 Primrose 88.8% O/W Emulsion Rheology

Brookfield Synchrolectric LVTD
Temperature: 44.00 ±0.10°C

Shear Rate sec^{-1}		Shear Stress $dynes/cm^2$		Viscosity cP	
3.72	±0.03	0.09	±0.02	2.5	± 0.4
7.43	0.07	0.17	0.01	2.2	0.1
14.86	0.13	0.31	0.01	2.1	0.1
37.15	0.34	0.71	0.01	1.9	0.0
74.31	0.67	1.42	0.01	1.9	0.0

Table B.134 Primrose 88.8% O/W Emulsion Rheology

Brookfield Synchrolectric LVTD
Temperature: 51.00 ±0.10°C

Shear Rate sec^{-1}		Shear Stress $dynes/cm^2$		Viscosity cP	
3.73	±0.03	0.09	±0.02	2.4	± 0.4
7.45	0.07	0.16	0.01	2.1	0.1
14.91	0.14	0.28	0.01	1.9	0.1
37.26	0.34	0.63	0.01	1.7	0.0
74.53	0.69	1.27	0.01	1.7	0.0

Table B.135 Primrose 88.8% O/W Emulsion Rheology

Brookfield Synchrolectric LVTD
Temperature: 60.00 ±0.10°C

Shear Rate sec^{-1}		Shear Stress $dynes/cm^2$		Viscosity cP	
3.74	±0.04	0.08	±0.02	2.0	± 0.4
7.48	0.07	0.13	0.01	1.7	0.1
14.95	0.14	0.22	0.01	1.5	0.1
37.38	0.35	0.50	0.01	1.3	0.0
74.76	0.70	0.97	0.01	1.3	0.0

Table B.136 Primrose 95.2% O/W Emulsion Rheology

Brookfield Synchrolectric LVTD
Temperature: 22.80 ±0.10°C

Shear Rate sec^{-1}		Shear Stress $dynes/cm^2$		Viscosity cP	
3.71	±0.03	0.13	±0.02	3.4	± 0.4
7.42	0.07	0.23	0.01	3.0	0.1
14.85	0.13	0.42	0.01	2.8	0.1
37.12	0.34	0.98	0.01	2.6	0.0
74.25	0.67	1.97	0.01	2.6	0.0

Table B.137 Primrose 95.2% O/W Emulsion Rheology

Brookfield Synchrolectric LVTD
Temperature: 45.00 ±0.10°C

Shear Rate sec^{-1}		Shear Stress $dynes/cm^2$		Viscosity cP	
3.73	±0.04	0.09	±0.02	2.4	± 0.4
7.45	0.07	0.15	0.01	2.0	0.1
14.90	0.14	0.27	0.01	1.8	0.1
37.26	0.35	0.62	0.01	1.7	0.0
74.52	0.70	1.25	0.01	1.7	0.0

Table B.138 Primrose 95.2% O/W Emulsion Rheology

Brookfield Synchrolectric LVTD
Temperature: 55.00 ±0.20°C

Shear Rate sec^{-1}		Shear Stress $dynes/cm^2$		Viscosity cP	
3.73	±0.04	0.08	±0.02	2.2	± 0.4
7.46	0.07	0.13	0.01	1.8	0.1
14.92	0.15	0.23	0.01	1.5	0.1
37.30	0.37	0.55	0.01	1.5	0.0
74.59	0.75	1.09	0.01	1.5	0.0

Table B.139 Primrose 95.2% O/W Emulsion Rheology

Brookfield Synchrolectric LVTD
Temperature: 65.00 ±0.20°C

Shear Rate sec^{-1}		Shear Stress $dynes/cm^2$		Viscosity cP	
3.75	±0.04	0.08	±0.02	2.0	± 0.4
7.49	0.08	0.11	0.01	1.5	0.1
14.98	0.15	0.20	0.01	1.3	0.1
37.45	0.39	0.45	0.01	1.2	0.0
74.90	0.77	0.89	0.01	1.2	0.0

Table B.140 Primrose 98.6% O/W Emulsion Rheology

Brookfield Synchrolectric LVTD
Temperature: 23.00 ±0.10°C

Shear Rate sec^{-1}		Shear Stress $dynes/cm^2$		Viscosity cP	
14.71	±0.13	0.17	±0.02	1.1	± 0.1
36.79	0.33	0.42	0.01	1.1	0.0
73.57	0.66	0.84	0.01	1.1	0.0

Table B.141 Primrose 98.6% O/W Emulsion Rheology

Brookfield Synchrolectric LVTD
Temperature: 45.00 ±0.10°C

Shear Rate sec^{-1}		Shear Stress $dynes/cm^2$		Viscosity cP	
14.61	±0.13	0.11	±0.02	0.7	± 0.2
36.53	0.33	0.29	0.02	0.8	0.0
73.07	0.67	0.61	0.01	0.8	0.0

Table B.142 Primrose 98.6% O/W Emulsion Rheology

Brookfield Synchrolectric LVTD
Temperature: 55.00 ±0.20°C

Shear Rate sec^{-1}		Shear Stress $dynes/cm^2$		Viscosity cP	
36.01	±0.33	0.24	±0.01	0.7	± 0.0
72.02	0.66	0.60	0.01	0.8	0.0

Table B.143 Primrose 98.6% O/W Emulsion Rheology

Brookfield Synchrolectric LVTD
Temperature: 64.20 ±0.20°C

Shear Rate sec^{-1}		Shear Stress $dynes/cm^2$		Viscosity cP	
35.96	±0.33	0.23	±0.01	0.6	± 0.0
71.91	0.66	0.59	0.01	0.8	0.0

Appendix C

Droplet Size Distribution Data for Emulsions of Wainwright B, Epping, and Primrose Dewatered Crude Oils

Table C.1 Wainwright B 0.8% W/O Emulsion
Primary Distribution

Particle size range (microns)	Number frequency in range	Percentage in range	Percentage per micron	Cumulative percentage less than
0.7 - 1.2	3	16.7	34.2	16.7
1.2 - 1.9	7	38.9	53.2	55.6
1.9 - 3.0	4	22.2	20.3	77.8
3.0 - 3.7	2	11.1	18.3	88.9
3.7 - 3.9	2	11.1	45.6	100.0
	18			

Geometric mean particle size: 1.9 microns
Dispersity: 1.6

Table C.2 Wainwright B 4.8% W/O Emulsion
Primary Distribution

Particle size range (microns)	Number frequency in range	Percentage in range	Percentage per micron	Cumulative percentage less than
0.0 - 0.5	3	3.3	6.8	3.3
0.5 - 0.7	3	3.3	13.7	6.7
0.7 - 1.0	5	5.6	22.8	12.2
1.0 - 1.2	12	13.3	54.8	25.6
1.2 - 1.7	19	21.1	43.3	46.7
1.7 - 1.9	13	14.4	59.3	61.1
1.9 - 2.3	7	7.8	21.3	68.9
2.3 - 2.4	7	7.8	63.9	76.7
2.4 - 2.9	6	6.7	13.7	83.3
2.9 - 3.2	6	6.7	27.4	90.0
3.4 - 3.9	4	4.4	9.1	94.4
3.9 - 4.4	3	3.3	6.8	97.8
4.4 - 4.6	2	2.2	9.1	100.0
	90			

Geometric mean particle size: 1.7 microns
Dispersity: 1.8

Table C.3 Wainwright B 10.4% W/O Emulsion
Primary Distribution

Particle size range (microns)	Number frequency in range	Percentage in range	Percentage per micron	Cumulative percentage less than
0.0 - 0.2	5	1.3	5.3	1.3
0.2 - 0.5	16	4.2	17.1	5.5
0.5 - 0.7	60	15.6	64.2	21.1
0.7 - 1.0	86	22.4	92.0	43.5
1.0 - 1.2	89	23.2	95.2	66.7
1.2 - 1.5	51	13.3	54.5	79.9
1.5 - 1.7	25	6.5	26.7	86.5
1.7 - 2.3	29	7.6	12.4	94.0
2.3 - 2.4	8	2.1	17.1	96.1
2.4 - 2.7	8	2.1	8.6	98.2
2.7 - 3.2	4	1.0	2.1	99.2
3.4 - 3.7	2	0.5	2.1	99.7
3.9 - 4.1	1	0.3	1.1	100.0
	384			

Geometric mean particle size: 1.0 microns
Dispersity: 1.7

Table C.4 Wainwright B 18.0% W/O Emulsion
Primary Distribution

Particle size range (microns)	Number frequency in range	Percentage in range	Percentage per micron	Cumulative percentage less than
0.2 - 0.5	2	1.7	7.1	1.7
0.5 - 0.7	8	6.9	28.3	8.6
0.7 - 1.0	13	11.2	46.0	19.8
1.0 - 1.2	12	10.3	42.5	30.2
1.2 - 1.8	15	12.9	21.2	43.1
1.8 - 2.4	17	14.7	24.1	57.8
2.4 - 3.0	10	8.6	14.2	66.4
3.0 - 3.7	17	14.7	24.1	81.0
3.7 - 4.9	8	6.9	5.7	87.9
4.9 - 6.1	7	6.0	5.0	94.0
6.7 - 7.3	2	1.7	2.8	95.7
7.3 - 7.9	2	1.7	2.8	97.4
9.1 - 9.7	1	0.9	1.4	98.3
9.7 - 10.3	2	1.7	2.8	100.0
	116			

Geometric mean particle size: 2.0 microns
Dispersity: 2.1

Table C.5 Wainwright B 26.5% W/O Emulsion
Primary Distribution

Particle size range (microns)	Number frequency in range	Percentage in range	Percentage per micron	Cumulative percentage less than
0.0 - 0.2	5	3.0	12.2	3.0
0.2 - 0.6	13	7.7	21.2	10.7
0.6 - 0.7	25	14.9	122.2	25.6
0.7 - 1.0	12	7.1	29.3	32.7
1.0 - 1.2	17	10.1	41.6	42.9
1.2 - 1.7	15	8.9	18.3	51.8
1.7 - 1.9	10	6.0	24.4	57.7
1.9 - 2.4	19	11.3	23.2	69.0
2.4 - 3.0	13	7.7	12.7	76.8
3.0 - 3.7	11	6.5	10.8	83.3
3.7 - 4.3	4	2.4	3.9	85.7
4.3 - 4.9	5	3.0	4.9	88.7
4.9 - 5.5	5	3.0	4.9	91.7
5.5 - 6.7	4	2.4	2.0	94.0
6.7 - 7.3	4	2.4	3.9	96.4
7.3 - 8.6	3	1.8	1.3	98.2
8.6 - 9.7	1	0.6	0.5	98.8
9.7 - 10.3	2	1.2	2.0	100.0
	168			

Geometric mean particle size: 1.5 microns
Dispersity: 2.5

Table C.6 Wainwright B 28.0% W/O/W Emulsion
Primary Distribution

Particle size range (microns)	Number frequency in range	Percentage in range	Percentage per micron	Cumulative percentage less than
0.6 - 1.2	1	2.8	4.6	2.8
1.2 - 1.8	1	2.8	4.6	5.6
1.8 - 2.4	3	8.3	13.7	13.9
2.4 - 3.0	3	8.3	13.7	22.2
3.0 - 3.7	4	11.1	18.3	33.3
3.7 - 5.5	6	16.7	9.1	50.0
5.5 - 6.1	5	13.9	22.8	63.9
6.1 - 6.7	3	8.3	13.7	72.2
6.7 - 7.3	4	11.1	18.3	83.3
8.5 - 11.0	4	11.1	4.6	94.4
14.6 - 17.0	1	2.8	1.1	97.2
48.7 - 51.3	1	2.8	1.1	100.0
	36			

Geometric mean particle size: 4.9 microns
Dispersity: 2.0

Table C.7 Wainwright B 28.0% W/O/W Emulsion
Secondary Distribution

Particle size range (microns)	Number frequency in range	Percentage in range	Percentage per micron	Cumulative percentage less than
0.0 - 2.4	1	8.3	3.4	8.3
2.4 - 4.9	4	33.3	13.7	41.7
4.9 - 7.3	3	25.0	10.3	66.7
7.3 - 9.7	1	8.3	3.4	75.0
9.7 - 12.2	1	8.3	3.4	83.3
14.6 - 17.0	1	8.3	3.4	91.7
19.5 - 21.9	1	8.3	3.4	100.0
	12			

Geometric mean particle size: 5.8 microns
Dispersity: 2.2

Table C.8 Wainwright B 34.4% W/O/W Emulsion
Primary Distribution

Particle size range (microns)	Number frequency in range	Percentage in range	Percentage per micron	Cumulative percentage less than
0.2 - 1.2	4	10.5	10.8	10.5
1.7 - 2.4	5	13.2	18.0	23.7
2.4 - 6.1	8	21.1	5.8	44.7
6.7 - 12.2	7	18.4	3.4	63.2
12.2 - 18.3	6	15.8	2.6	78.9
18.3 - 24.4	4	10.5	1.7	89.5
31.0 - 36.5	3	7.9	1.4	97.4
36.5 - 42.6	1	2.6	0.4	100.0
	38			

Geometric mean particle size: 6.7 microns
Dispersity: 3.2

Table C.9 Wainwright B 34.4% W/O/W Emulsion
Secondary Distribution

Particle size range (microns)	Number frequency in range	Percentage in range	Percentage per micron	Cumulative percentage less than
0.0 - 0.7	14	35.9	49.1	35.9
0.7 - 1.0	11	28.2	115.8	64.1
1.0 - 1.2	6	15.4	63.2	79.5
1.5 - 1.7	3	7.7	31.6	87.2
1.7 - 1.9	1	2.6	10.5	89.7
1.9 - 2.2	1	2.6	10.5	92.3
2.2 - 2.4	1	2.6	10.5	94.9
2.4 - 2.8	1	2.6	7.0	97.4
3.4 - 3.7	1	2.6	10.5	100.0
	39			

Geometric mean particle size: 0.8 microns
Dispersity: 1.9

Table C.10 Wainwright B 46.4% W/O/W Emulsion
Primary Distribution

Particle size range (microns)	Number frequency in range	Percentage in range	Percentage per micron	Cumulative percentage less than
1.0 - 1.8	5	12.2	14.3	12.2
1.8 - 4.3	11	26.8	11.0	39.0
4.3 - 5.5	6	14.6	12.0	53.7
5.5 - 9.9	7	17.1	3.9	70.7
9.9 - 12.2	3	7.3	3.2	78.0
12.2 - 14.6	2	4.9	2.0	82.9
19.5 - 24.4	3	7.3	1.5	90.2
30.4 - 36.5	3	7.3	1.2	97.6
36.5 - 42.6	1	2.4	0.4	100.0
	41			

Geometric mean particle size: 6.0 microns
Dispersity: 2.6

Table C.11 Wainwright B 46.4% W/O/W Emulsion
Secondary Distribution

Particle size range (microns)	Number frequency in range	Percentage in range	Percentage per micron	Cumulative percentage less than
0.5 - 1.0	6	11.5	23.7	11.5
1.0 - 1.5	5	9.6	19.7	21.2
1.5 - 1.9	8	15.4	31.6	36.5
1.9 - 2.4	9	17.3	35.5	53.8
2.4 - 2.9	7	13.5	27.6	67.3
2.9 - 3.4	7	13.5	27.6	80.8
3.4 - 3.9	6	11.5	23.7	92.3
3.9 - 4.4	1	1.9	3.9	94.2
4.4 - 4.9	2	3.8	7.9	98.1
7.8 - 8.3	1	1.9	3.9	100.0
	52			

Geometric mean particle size: 2.1 microns
Dispersity: 1.7

Table C.12 Wainwright B 54.0% W/O/W Emulsion
Primary Distribution

Particle size range (microns)	Number frequency in range	Percentage in range	Percentage per micron	Cumulative percentage less than
0.0 - 0.2	2	3.6	14.9	3.6
0.2 - 0.5	6	10.9	44.8	14.5
0.7 - 1.7	8	14.5	14.9	29.1
1.7 - 6.1	7	12.7	2.9	41.8
6.1 - 8.5	7	12.7	5.2	54.5
8.5 - 11.0	7	12.7	5.2	67.3
11.0 - 12.2	6	10.9	9.0	78.2
12.2 - 13.4	2	3.6	3.0	81.8
13.4 - 18.3	3	5.5	1.1	87.3
18.3 - 19.5	2	3.6	3.0	90.9
19.5 - 24.4	2	3.6	0.7	94.5
36.5 - 42.6	2	3.6	0.6	98.2
42.6 - 48.5	1	1.8	0.3	100.0
	55			

Geometric mean particle size: 4.4 microns
Dispersity: 4.4

Table C.13 Wainwright B 54.0% W/O/W Emulsion
Secondary Distribution

Particle size range (microns)	Number frequency in range	Percentage in range	Percentage per micron	Cumulative percentage less than
0.5 - 1.0	5	8.1	16.6	8.1
1.0 - 1.5	10	16.1	33.1	24.2
1.5 - 1.9	10	16.1	33.1	40.3
1.9 - 2.4	18	29.0	59.6	69.4
2.4 - 2.9	6	9.7	19.9	79.0
2.9 - 3.4	4	6.5	13.2	85.5
3.4 - 3.9	5	8.1	16.6	93.5
3.9 - 4.4	3	4.8	9.9	98.4
4.4 - 4.7	1	1.6	4.4	100.0
	62			

Geometric mean particle size: 2.0 microns
Dispersity: 1.6

Table C.14 Wainwright B 95.6% O/W Emulsion
Primary Distribution

Particle size range (microns)	Number frequency in range	Percentage in range	Percentage per micron	Cumulative percentage less than
0.0 - 0.2	15	2.0	8.3	2.0
0.2 - 0.6	31	4.2	11.5	6.2
0.6 - 0.7	83	11.2	92.0	17.4
0.7 - 1.0	98	13.2	54.3	30.6
1.0 - 1.3	86	11.6	31.8	42.2
1.3 - 1.6	100	13.5	55.4	55.7
1.6 - 1.7	48	6.5	53.2	62.2
1.7 - 1.9	51	6.9	28.3	69.1
1.9 - 2.2	63	8.5	34.9	77.6
2.2 - 2.4	23	3.1	12.7	80.7
2.4 - 2.7	22	3.0	12.2	83.7
2.7 - 2.9	27	3.6	15.0	87.3
2.9 - 3.2	17	2.3	9.4	89.6
3.2 - 3.4	9	1.2	5.0	90.8
3.4 - 3.7	14	1.9	7.8	92.7
3.7 - 3.9	16	2.2	8.9	94.9
3.9 - 4.1	6	0.8	3.3	95.7
4.1 - 4.4	7	0.9	3.9	96.6
4.4 - 4.6	5	0.7	2.8	97.3
4.6 - 4.9	4	0.5	2.2	97.8
4.9 - 5.1	4	0.5	2.2	98.4
5.1 - 5.4	5	0.7	2.8	99.1
5.4 - 6.6	3	0.4	0.3	99.5
6.6 - 6.8	2	0.3	1.1	99.7
7.3 - 8.5	1	0.1	0.1	99.9
8.5 - 9.1	1	0.1	0.2	100.0
	741			

Geometric mean particle size: 1.4 microns
Dispersity: 2.0

Table C.15 Wainwright B 97.6% O/W Emulsion
Primary Distribution

Particle size range (microns)	Number frequency in range	Percentage in range	Percentage per micron	Cumulative percentage less than
0.0 - 0.1	5	2.4	20.0	2.4
0.1 - 0.5	14	6.8	18.7	9.3
0.5 - 0.7	22	10.7	44.1	20.0
0.7 - 1.0	27	13.2	54.1	33.2
1.0 - 1.2	32	15.6	64.1	48.8
1.2 - 1.5	28	13.7	56.1	62.4
1.5 - 1.7	23	11.2	46.1	73.7
1.7 - 2.1	23	11.2	30.7	84.9
2.1 - 2.2	10	4.9	40.1	89.8
2.2 - 2.7	10	4.9	10.0	94.6
2.7 - 3.4	9	4.4	6.0	99.0
3.4 - 4.1	1	0.5	0.7	99.5
4.1 - 4.4	1	0.5	2.0	100.0
	205			

Geometric mean particle size: 1.1 microns
Dispersity: 2.1

Table C.16 Epping 0.9% W/O Emulsion
Primary Distribution

Particle size range (microns)	Number frequency in range	Percentage in range	Percentage per micron	Cumulative percentage less than
0.0 - 0.5	1	0.6	1.3	0.6
0.5 - 0.7	42	26.8	109.9	27.4
0.7 - 1.0	35	22.3	91.5	49.7
1.0 - 1.2	17	10.8	44.5	60.5
1.2 - 1.5	15	9.6	39.2	70.1
1.5 - 1.7	11	7.0	28.8	77.1
1.7 - 1.9	10	6.4	26.2	83.4
1.9 - 2.2	10	6.4	26.2	89.8
2.2 - 2.4	8	5.1	20.9	94.9
2.4 - 2.7	3	1.9	7.8	96.8
2.7 - 3.2	3	1.9	3.9	98.7
3.2 - 4.1	2	1.3	1.3	100.0
	157			

Geometric mean particle size: 1.1 microns
Dispersity: 1.7

Table C.17 Epping 14.4% W/O Emulsion
Primary Distribution

Particle size range (microns)	Number frequency in range	Percentage in range	Percentage per micron	Cumulative percentage less than
0.0 - 0.1	44	6.3	51.3	6.3
0.1 - 0.2	39	5.5	45.5	11.8
0.2 - 0.4	122	17.3	142.3	29.1
0.4 - 0.5	72	10.2	84.0	39.3
0.5 - 0.6	122	17.3	142.3	56.7
0.6 - 0.7	126	17.9	147.0	74.6
0.7 - 0.9	111	15.8	129.5	90.3
0.9 - 1.0	32	4.5	37.3	94.9
1.0 - 1.1	26	3.7	30.3	98.6
1.1 - 1.2	8	1.1	9.3	99.7
1.2 - 1.5	2	0.3	1.2	100.0
	704			

Geometric mean particle size: 0.5 microns
Dispersity: 2.0

Table C.18 Epping 17.0% W/O Emulsion
Primary Distribution

Particle size range (microns)	Number frequency in range	Percentage in range	Percentage per micron	Cumulative percentage less than
0.0 - 0.2	1	0.3	1.1	0.3
0.2 - 0.5	65	16.8	68.8	17.0
0.5 - 0.7	192	49.5	203.2	66.5
0.7 - 1.0	44	11.3	46.6	77.8
1.0 - 1.2	19	4.9	20.1	82.7
1.2 - 1.5	7	1.8	7.4	84.5
1.5 - 1.7	14	3.6	14.8	88.1
1.7 - 1.9	7	1.8	7.4	89.9
1.9 - 2.2	6	1.5	6.4	91.5
2.2 - 2.4	6	1.5	6.4	93.0
2.7 - 2.9	10	2.6	10.6	95.6
2.9 - 3.2	4	1.0	4.2	96.6
3.2 - 3.7	4	1.0	2.1	97.7
3.7 - 4.1	4	1.0	2.1	98.7
4.1 - 5.8	4	1.0	0.6	99.7
6.3 - 6.6	1	0.3	1.1	100.0
	388			

Geometric mean particle size: 0.7 microns
Dispersity: 1.8

Table C.19 Epping 20.0% W/O Emulsion
Primary Distribution

Particle size range (microns)	Number frequency in range	Percentage in range	Percentage per micron	Cumulative percentage less than
0.2 - 0.5	27	10.5	43.1	10.5
0.5 - 0.7	119	46.3	190.1	56.8
0.7 - 1.0	35	13.6	55.9	70.4
1.0 - 1.2	15	5.8	24.0	76.3
1.2 - 1.5	15	5.8	24.0	82.1
1.5 - 1.7	13	5.1	20.8	87.2
1.7 - 1.9	8	3.1	12.8	90.3
1.9 - 2.2	10	3.9	16.0	94.2
2.2 - 2.4	3	1.2	4.8	95.3
2.7 - 2.9	5	1.9	8.0	97.3
3.2 - 3.4	3	1.2	4.8	98.4
3.4 - 4.4	3	1.2	1.2	99.6
4.4 - 4.6	1	0.4	1.6	100.0
	257			

Geometric mean particle size: 0.8 microns
Dispersity: 1.7

Table C.20 Epping 20.4% W/O Emulsion
Primary Distribution

Particle size range (microns)	Number frequency in range	Percentage in range	Percentage per micron	Cumulative percentage less than
0.0 - 0.2	2	0.4	1.8	0.4
0.2 - 0.5	108	23.9	98.3	24.4
0.5 - 0.7	213	47.2	193.9	71.6
0.7 - 1.0	53	11.8	48.3	83.4
1.0 - 1.2	27	6.0	24.6	89.4
1.2 - 1.5	12	2.7	10.9	92.0
1.5 - 1.7	18	4.0	16.4	96.0
1.7 - 1.9	9	2.0	8.2	98.0
1.9 - 2.2	5	1.1	4.6	99.1
2.2 - 2.4	2	0.4	1.8	99.6
2.4 - 2.7	1	0.2	0.9	99.8
2.9 - 3.2	1	0.2	0.9	100.0
	451			

Geometric mean particle size: 0.6 microns
Dispersity: 1.6

Table C.21 Epping 43.2% W/O/W Emulsion
Primary Distribution

Particle size range (microns)	Number frequency in range	Percentage in range	Percentage per micron	Cumulative percentage less than
1.2 - 2.4	4	8.9	7.3	8.9
2.4 - 4.9	5	11.1	4.6	20.0
4.9 - 8.5	4	8.9	2.4	28.9
8.5 - 9.7	4	8.9	7.3	37.8
9.7 - 10.3	4	8.9	14.6	46.7
10.3 - 11.0	5	11.1	18.3	57.8
11.0 - 12.2	6	13.3	11.0	71.1
12.2 - 13.4	3	6.7	5.5	77.8
13.4 - 15.2	4	8.9	4.9	86.7
15.2 - 16.4	3	6.7	5.5	93.3
16.4 - 19.5	2	4.4	1.5	97.8
19.5 - 42.6	1	2.2	0.1	100.0
	45			

Geometric mean particle size: 8.6 microns
Dispersity: 2.0

Table C.22 Epping 43.2% W/O/W Emulsion
Secondary Distribution

Particle size range (microns)	Number frequency in range	Percentage in range	Percentage per micron	Cumulative percentage less than
0.2 - 0.5	2	6.1	24.9	6.1
0.5 - 0.7	11	33.3	136.9	39.4
0.7 - 1.0	6	18.2	74.7	57.6
1.0 - 1.5	2	6.1	12.4	63.6
1.5 - 1.7	6	18.2	74.7	81.8
1.7 - 2.4	3	9.1	12.4	90.9
2.4 - 2.9	1	3.0	6.2	93.9
2.9 - 3.2	1	3.0	12.4	97.0
4.1 - 4.4	1	3.0	12.4	100.0
	33			

Geometric mean particle size: 1.0 microns
Dispersity: 1.9

Table C.23 Epping 53.2% W/O/W Emulsion
Primary Distribution

Particle size range (microns)	Number frequency in range	Percentage in range	Percentage per micron	Cumulative percentage less than
0.0 - 0.6	30	11.3	18.6	11.3
0.6 - 1.2	93	35.1	57.6	46.4
1.2 - 1.8	32	12.1	19.8	58.5
1.8 - 2.4	26	9.8	16.1	68.3
2.4 - 3.0	17	6.4	10.5	74.7
3.0 - 3.7	9	3.4	5.6	78.1
3.7 - 4.3	8	3.0	5.0	81.1
4.3 - 6.7	22	8.3	3.4	89.4
6.7 - 7.3	5	1.9	3.1	91.3
7.3 - 8.5	6	2.3	1.9	93.6
8.5 - 9.7	4	1.5	1.2	95.1
9.7 - 11.0	1	0.4	0.3	95.5
11.0 - 12.2	5	1.9	1.5	97.4
14.0 - 15.8	4	1.5	0.8	98.9
21.9 - 31.7	2	0.8	0.1	99.6
31.7 - 32.3	1	0.4	0.6	100.0
	265			

Geometric mean particle size: 1.6 microns
Dispersity: 2.7

Table C.24 Epping 53.2% W/O/W Emulsion
Secondary Distribution

Particle size range (microns)	Number frequency in range	Percentage in range	Percentage per micron	Cumulative percentage less than
0.0 - 0.2	3	12.5	51.3	12.5
0.2 - 0.5	5	20.8	85.6	33.3
0.5 - 0.7	3	12.5	51.3	45.8
0.7 - 1.0	4	16.7	68.4	62.5
1.0 - 1.2	4	16.7	68.4	79.2
1.2 - 2.2	3	12.5	12.8	91.7
2.2 - 2.6	2	8.3	22.8	100.0
	24			

Geometric mean particle size: 0.7 microns
Dispersity: 2.4

Table C.25 Epping 64.0% W/O/W Emulsion
Primary Distribution

Particle size range (microns)	Number frequency in range	Percentage in range	Percentage per micron	Cumulative percentage less than
0.0 - 0.6	3	1.5	2.5	1.5
0.6 - 1.2	39	19.9	32.7	21.4
1.2 - 1.8	45	23.0	37.7	44.4
1.8 - 2.4	29	14.8	24.3	59.2
2.4 - 3.0	19	9.7	15.9	68.9
3.0 - 3.7	10	5.1	8.4	74.0
3.7 - 4.3	9	4.6	7.5	78.6
4.3 - 4.9	9	4.6	7.5	83.2
4.9 - 5.5	4	2.0	3.4	85.2
5.5 - 6.1	3	1.5	2.5	86.7
6.1 - 7.3	5	2.6	2.1	89.3
7.3 - 9.7	5	2.6	1.0	91.8
9.7 - 11.0	3	1.5	1.3	93.4
11.0 - 20.7	5	2.6	0.3	95.9
20.7 - 22.5	4	2.0	1.1	98.0
22.5 - 24.4	2	1.0	0.6	99.0
24.4 - 44.4	2	1.0	0.1	100.0
	196			

Geometric mean particle size: 2.4 microns
Dispersity: 2.4

Table C.26 Epping 64.0% W/O/W Emulsion
Secondary Distribution

Particle size range (microns)	Number frequency in range	Percentage in range	Percentage per micron	Cumulative percentage less than
0.5 - 1.0	5	9.1	18.7	9.1
1.0 - 1.5	13	23.6	48.5	32.7
1.5 - 1.9	8	14.5	29.9	47.3
1.9 - 2.4	8	14.5	29.9	61.8
2.4 - 2.9	3	5.5	11.2	67.3
2.9 - 3.4	8	14.5	29.9	81.8
3.4 - 3.9	1	1.8	3.7	83.6
3.9 - 4.4	2	3.6	7.5	87.3
4.4 - 4.9	1	1.8	3.7	89.1
5.4 - 5.8	1	1.8	3.7	90.9
5.8 - 6.3	3	5.5	11.2	96.4
6.3 - 6.8	1	1.8	3.7	98.2
6.8 - 7.3	1	1.8	3.7	100.0
	55			

Geometric mean particle size: 2.1 microns
Dispersity: 1.8

Table C.27 Epping 66.8% W/O/W Emulsion
Primary Distribution

Particle size range (microns)	Number frequency in range	Percentage in range	Percentage per micron	Cumulative percentage less than
0.0 - 0.6	6	2.9	4.7	2.9
0.6 - 1.2	49	23.6	38.7	26.4
1.2 - 1.8	44	21.2	34.7	47.6
1.8 - 2.3	23	11.1	22.7	58.7
2.3 - 3.0	30	14.4	19.7	73.1
3.0 - 3.7	17	8.2	13.4	81.3
3.7 - 4.3	7	3.4	5.5	84.6
4.3 - 4.9	4	1.9	3.2	86.5
4.9 - 5.5	6	2.9	4.7	89.4
5.5 - 6.1	2	1.0	1.6	90.4
6.1 - 6.7	5	2.4	3.9	92.8
6.7 - 7.3	3	1.4	2.4	94.2
7.3 - 7.9	1	0.5	0.8	94.7
8.5 - 9.7	3	1.4	1.2	96.2
9.7 - 17.0	2	1.0	0.1	97.1
17.0 - 20.7	3	1.4	0.4	98.6
20.7 - 25.6	1	0.5	0.1	99.0
25.6 - 26.2	1	0.5	0.8	99.5
26.2 - 57.2	1	0.5	0.0	100.0
	208			

Geometric mean particle size: 2.1 microns
Dispersity: 2.3

Table C.28 Epping 66.8% W/O/W Emulsion
Secondary Distribution

Particle size range (microns)	Number frequency in range	Percentage in range	Percentage per micron	Cumulative percentage less than
0.0 - 0.4	8	13.3	36.5	13.3
0.4 - 0.5	7	11.7	95.8	25.0
0.5 - 0.7	8	13.3	54.8	38.3
0.7 - 1.2	8	13.3	27.4	51.7
1.2 - 1.5	7	11.7	47.9	63.3
1.5 - 1.9	7	11.7	24.0	75.0
1.9 - 2.2	7	11.7	47.9	86.7
2.2 - 2.4	2	3.3	13.7	90.0
2.4 - 2.9	3	5.0	10.3	95.0
2.9 - 3.4	1	1.7	3.4	96.7
3.4 - 3.8	2	3.3	9.1	100.0
	60			

Geometric mean particle size: 0.9 microns
Dispersity: 2.4

Table C.29 Epping 70.4% W/O/W Emulsion
Primary Distribution

Particle size range (microns)	Number frequency in range	Percentage in range	Percentage per micron	Cumulative percentage less than
0.0 - 1.0	4	3.3	3.3	3.3
1.0 - 1.5	13	10.6	21.7	13.8
1.5 - 1.9	14	11.4	23.4	25.2
1.9 - 2.4	20	16.3	33.4	41.5
2.4 - 2.9	11	8.9	18.4	50.4
2.9 - 3.4	9	7.3	15.0	57.7
3.4 - 3.9	13	10.6	21.7	68.3
3.9 - 4.4	8	6.5	13.4	74.8
4.4 - 4.9	3	2.4	5.0	77.2
4.9 - 5.8	5	4.1	4.2	81.3
5.8 - 6.8	3	2.4	2.5	83.7
6.8 - 7.8	3	2.4	2.5	86.2
7.8 - 9.7	3	2.4	1.3	88.6
10.7 - 12.2	5	4.1	2.8	92.7
12.2 - 15.1	3	2.4	0.8	95.1
18.5 - 19.6	2	1.6	1.5	96.7
24.8 - 25.3	2	1.6	3.3	98.4
25.3 - 33.2	1	0.8	0.1	99.2
33.2 - 37.5	1	0.8	0.2	100.0
	123			

Geometric mean particle size: 3.2 microns
Dispersity: 2.3

Table C.30 Epping 70.4% W/O/W Emulsion
Secondary Distribution

Particle size range (microns)	Number frequency in range	Percentage in range	Percentage per micron	Cumulative percentage less than
0.0 - 1.0	3	13.6	14.0	13.6
1.0 - 1.9	7	31.8	32.7	45.5
1.9 - 2.9	5	22.7	23.3	68.2
2.9 - 3.9	3	13.6	14.0	81.8
3.9 - 4.4	1	4.5	9.3	86.4
4.4 - 5.0	1	4.5	7.5	90.9
5.0 - 6.3	1	4.5	3.4	95.5
6.3 - 6.8	1	4.5	9.3	100.0
	22			

Geometric mean particle size: 2.0 microns
Dispersity: 2.1

Table C.31 Epping 96.8% O/W Emulsion
Primary Distribution

Particle size range (microns)	Number frequency in range	Percentage in range	Percentage per micron	Cumulative percentage less than
0.0 - 0.5	4	4.9	10.0	4.9
0.5 - 0.7	16	19.5	80.1	24.4
0.7 - 1.0	16	19.5	80.1	43.9
1.0 - 1.5	8	9.8	20.0	53.7
1.5 - 1.7	11	13.4	55.1	67.1
1.7 - 1.9	5	6.1	25.0	73.2
1.9 - 2.2	5	6.1	25.0	79.3
2.2 - 2.6	7	8.5	23.4	87.8
2.6 - 3.4	3	3.7	4.3	91.5
3.4 - 3.7	3	3.7	15.0	95.1
3.7 - 4.6	3	3.7	3.8	98.8
4.6 - 5.8	1	1.2	1.0	100.0
	82			

Geometric mean particle size: 1.2 microns
Dispersity: 2.0

Table C.32 Epping 98.0% O/W Emulsion
Primary Distribution

Particle size range (microns)	Number frequency in range	Percentage in range	Percentage per micron	Cumulative percentage less than
0.5 - 0.9	2	3.4	9.4	3.4
0.9 - 1.0	14	24.1	198.2	27.6
1.0 - 1.2	9	15.5	63.7	43.1
1.2 - 1.5	12	20.7	85.0	63.8
1.5 - 1.7	5	8.6	35.4	72.4
1.7 - 1.9	4	6.9	28.3	79.3
1.9 - 2.7	3	5.2	7.1	84.5
2.7 - 3.2	2	3.4	7.1	87.9
3.2 - 3.7	2	3.4	7.1	91.4
3.7 - 3.9	3	5.2	21.2	96.6
3.9 - 4.1	1	1.7	7.1	98.3
4.1 - 6.3	1	1.7	0.8	100.0
	58			

Geometric mean particle size: 1.4 microns
Dispersity: 1.6

Table C.33 Epping 98.4% O/W Emulsion
Primary Distribution

Particle size range (microns)	Number frequency in range	Percentage in range	Percentage per micron	Cumulative percentage less than
0.0 - 0.2	1	0.7	2.9	0.7
0.2 - 0.6	4	2.8	7.8	3.5
0.6 - 0.7	11	7.8	64.1	11.3
0.7 - 1.0	54	38.3	157.3	49.6
1.0 - 1.2	47	33.3	136.9	83.0
1.2 - 1.5	10	7.1	29.1	90.1
1.5 - 1.7	4	2.8	11.6	92.9
1.7 - 1.9	3	2.1	8.7	95.0
1.9 - 2.2	2	1.4	5.8	96.5
2.2 - 2.4	3	2.1	8.7	98.6
4.9 - 5.1	1	0.7	2.9	99.3
5.8 - 6.1	1	0.7	2.9	100.0
	141			

Geometric mean particle size: 1.0 microns
Dispersity: 1.5

Table C.34 Primrose 3.6% W/O Emulsion
Primary Distribution

Particle size range (microns)	Number frequency in range	Percentage in range	Percentage per micron	Cumulative percentage less than
0.0 - 0.1	185	8.5	69.8	8.5
0.1 - 0.2	191	8.8	72.0	17.3
0.2 - 0.4	662	30.4	249.6	47.7
0.4 - 0.5	321	14.7	121.0	62.4
0.5 - 0.6	206	9.5	77.7	71.9
0.6 - 0.7	345	15.8	130.1	87.7
0.7 - 0.9	156	7.2	58.8	94.9
0.9 - 1.0	56	2.6	21.1	97.4
1.0 - 1.1	21	1.0	7.9	98.4
1.1 - 1.2	10	0.5	3.8	98.9
1.2 - 1.3	7	0.3	2.6	99.2
1.3 - 1.5	5	0.2	1.9	99.4
1.5 - 1.6	7	0.3	2.6	99.7
1.6 - 1.7	2	0.1	0.8	99.8
1.7 - 1.8	2	0.1	0.8	99.9
1.8 - 1.9	2	0.1	0.8	100.0
	2178			

Geometric mean particle size: 0.4 microns
Dispersity: 2.0

Table C.35 Primrose 22.8% W/O Emulsion
Primary Distribution

Particle size range (microns)	Number frequency in range	Percentage in range	Percentage per micron	Cumulative percentage less than
0.0 - 0.2	16	6.8	27.7	6.8
0.2 - 0.5	27	11.4	46.8	18.1
0.5 - 0.7	30	12.7	52.0	30.8
0.7 - 1.0	23	9.7	39.9	40.5
1.0 - 1.2	15	6.3	26.0	46.8
1.2 - 1.5	23	9.7	39.9	56.5
1.5 - 1.7	22	9.3	38.1	65.8
1.7 - 1.9	16	6.8	27.7	72.6
1.9 - 2.2	6	2.5	10.4	75.1
2.2 - 2.4	9	3.8	15.6	78.9
2.4 - 2.7	7	3.0	12.1	81.9
2.7 - 3.2	9	3.8	7.8	85.7
3.2 - 3.4	9	3.8	15.6	89.5
3.4 - 3.7	5	2.1	8.7	91.6
3.7 - 3.9	4	1.7	6.9	93.2
4.1 - 4.4	4	1.7	6.9	94.9
4.4 - 4.6	2	0.8	3.5	95.8
4.6 - 4.9	6	2.5	10.4	98.3
4.9 - 5.4	2	0.8	1.7	99.2
5.8 - 6.1	1	0.4	1.7	99.6
6.1 - 6.3	1	0.4	1.7	100.0
	237			

Geometric mean particle size: 1.1 microns
Dispersity: 2.6

Table C.36 Primrose 32.0% W/O Emulsion
Primary Distribution

Particle size range (microns)	Number frequency in range	Percentage in range	Percentage per micron	Cumulative percentage less than
0.0 - 0.1	24	5.8	47.7	5.8
0.1 - 0.2	18	4.4	35.8	10.2
0.2 - 0.4	85	20.6	169.0	30.8
0.4 - 0.7	76	18.4	50.4	49.2
0.7 - 1.0	85	20.6	84.5	69.7
1.0 - 1.2	44	10.7	43.7	80.4
1.2 - 1.5	34	8.2	33.8	88.6
1.5 - 1.7	12	2.9	11.9	91.5
1.7 - 1.9	8	1.9	8.0	93.5
1.9 - 2.2	3	0.7	3.0	94.2
2.2 - 2.4	9	2.2	8.9	96.4
2.4 - 2.7	7	1.7	7.0	98.1
2.7 - 3.4	2	0.5	0.7	98.5
3.4 - 5.6	2	0.5	0.2	99.0
6.7 - 9.1	2	0.5	0.2	99.5
12.2 - 13.4	1	0.2	0.2	99.8
13.4 - 14.7	1	0.2	0.2	100.0
	413			

Geometric mean particle size: 0.6 microns
Dispersity: 2.5

Table C.37 Primrose 44.8% W/O/W Emulsion
Primary Distribution

Particle size range (microns)	Number frequency in range	Percentage in range	Percentage per micron	Cumulative percentage less than
0.0 - 1.0	6	6.7	6.8	6.7
1.0 - 1.9	14	15.6	16.0	22.2
1.9 - 2.9	12	13.3	13.7	35.6
2.9 - 3.9	8	8.9	9.1	44.4
3.9 - 5.0	12	13.3	12.2	57.8
5.0 - 5.8	11	12.2	14.3	70.0
5.8 - 6.8	12	13.3	13.7	83.3
6.8 - 8.3	6	6.7	4.6	90.0
9.0 - 10.3	3	3.3	2.5	93.3
10.3 - 11.6	2	2.2	1.8	95.6
11.6 - 12.8	2	2.2	1.8	97.8
15.8 - 18.3	1	1.1	0.5	98.9
18.3 - 21.9	1	1.1	0.3	100.0
	90			

Geometric mean particle size: 3.6 microns
Dispersity: 2.3

Table C.38 Primrose 44.8% W/O/W Emulsion
Secondary Distribution

Particle size range (microns)	Number frequency in range	Percentage in range	Percentage per micron	Cumulative percentage less than
0.0 - 0.2	4	4.0	16.4	4.0
0.2 - 0.5	5	5.0	20.5	9.0
0.5 - 0.7	11	11.0	45.2	20.0
0.7 - 1.0	12	12.0	49.3	32.0
1.0 - 1.2	17	17.0	69.8	49.0
1.2 - 1.5	13	13.0	53.4	62.0
1.5 - 1.7	8	8.0	32.9	70.0
1.7 - 1.9	6	6.0	24.6	76.0
1.9 - 2.2	6	6.0	24.6	82.0
2.2 - 2.4	3	3.0	12.3	85.0
2.4 - 2.7	6	6.0	24.6	91.0
2.7 - 3.2	2	2.0	4.1	93.0
3.2 - 3.4	2	2.0	8.2	95.0
3.7 - 3.9	2	2.0	8.2	97.0
3.9 - 4.1	1	1.0	4.1	98.0
4.9 - 5.1	1	1.0	4.1	99.0
6.3 - 6.8	1	1.0	2.1	100.0
	100			

Geometric mean particle size: 1.2 microns
Dispersity: 2.1

Table C.39 Primrose 48.2% W/O/W Emulsion
Primary Distribution

Particle size range (microns)	Number frequency in range	Percentage in range	Percentage per micron	Cumulative percentage less than
0.0 - 0.2	17	7.1	29.2	7.1
0.2 - 0.5	33	13.8	56.7	20.9
0.5 - 0.7	25	10.5	43.0	31.4
0.7 - 1.0	32	13.4	55.0	44.8
1.0 - 1.2	20	8.4	34.4	53.1
1.2 - 1.5	10	4.2	17.2	57.3
1.5 - 1.7	14	5.9	24.1	63.2
1.7 - 1.9	10	4.2	17.2	67.4
1.9 - 2.2	11	4.6	18.9	72.0
2.2 - 2.4	8	3.3	13.7	75.3
2.4 - 2.7	13	5.4	22.3	80.8
2.7 - 2.9	10	4.2	17.2	84.9
2.9 - 3.4	10	4.2	8.6	89.1
3.4 - 3.7	3	1.3	5.2	90.4
3.7 - 3.9	5	2.1	8.6	92.5
3.9 - 4.1	4	1.7	6.9	94.1
4.1 - 4.4	4	1.7	6.9	95.8
4.4 - 4.6	3	1.3	5.2	97.1
4.6 - 4.9	2	0.8	3.4	97.9
4.9 - 5.6	2	0.8	1.1	98.7
5.6 - 5.8	1	0.4	1.7	99.2
6.3 - 6.6	1	0.4	1.7	99.6
6.6 - 6.8	1	0.4	1.7	100.0
	239			

Geometric mean particle size: 1.1 microns
Dispersity: 2.6

Table C.40 Primrose 48.2% W/O/W Emulsion
Secondary Distribution

Particle size range (microns)	Number frequency in range	Percentage in range	Percentage per micron	Cumulative percentage less than
0.0 - 0.2	17	7.8	32.2	7.8
0.2 - 0.5	29	13.4	54.9	21.2
0.5 - 0.7	24	11.1	45.4	32.3
0.7 - 1.0	24	11.1	45.4	43.3
1.0 - 1.2	17	7.8	32.2	51.2
1.2 - 1.5	10	4.6	18.9	55.8
1.5 - 1.7	9	4.1	17.0	59.9
1.7 - 1.9	10	4.6	18.9	64.5
1.9 - 2.2	14	6.5	26.5	71.0
2.2 - 2.4	9	4.1	17.0	75.1
2.4 - 2.7	15	6.9	28.4	82.0
2.7 - 2.9	4	1.8	7.6	83.9
2.9 - 3.2	7	3.2	13.2	87.1
3.2 - 3.4	6	2.8	11.4	89.9
3.4 - 3.7	6	2.8	11.4	92.6
3.7 - 3.9	4	1.8	7.6	94.5
3.9 - 4.1	1	0.5	1.9	94.9
4.1 - 4.4	4	1.8	7.6	96.8
4.4 - 4.6	5	2.3	9.5	99.1
4.6 - 4.9	1	0.5	1.9	99.5
4.9 - 5.1	1	0.5	1.9	100.0
	217			

Geometric mean particle size: 1.1 microns
Dispersity: 2.7

Table C.41 Primrose 62.4% W/O/W Emulsion
Primary Distribution

Particle size range (microns)	Number frequency in range	Percentage in range	Percentage per micron	Cumulative percentage less than
0.0 - 0.5	3	11.1	22.8	11.1
3.4 - 11.7	6	22.2	2.7	33.3
11.7 - 15.1	7	25.9	7.6	59.3
15.1 - 18.5	3	11.1	3.3	70.4
18.5 - 20.5	2	7.4	3.8	77.8
20.5 - 21.4	2	7.4	7.6	85.2
21.4 - 27.8	1	3.7	0.6	88.9
27.8 - 33.1	1	3.7	0.7	92.6
33.1 - 43.8	1	3.7	0.3	96.3
43.8 - 47.2	1	3.7	1.1	100.0
	27			

Geometric mean particle size: 9.4 microns
Dispersity: 4.1

Table C.42 Primrose 62.4% W/O/W Emulsion
Secondary Distribution

Particle size range (microns)	Number frequency in range	Percentage in range	Percentage per micron	Cumulative percentage less than
0.0 - 0.2	1	1.2	4.9	1.2
0.2 - 0.6	4	4.8	13.2	6.0
0.6 - 0.7	20	24.1	197.9	30.1
0.7 - 1.0	14	16.9	69.3	47.0
1.0 - 1.2	4	4.8	19.8	51.8
1.2 - 1.5	6	7.2	29.7	59.0
1.5 - 1.7	5	6.0	24.7	65.1
1.7 - 1.9	5	6.0	24.7	71.1
1.9 - 2.2	5	6.0	24.7	77.1
2.2 - 2.4	2	2.4	9.9	79.5
2.4 - 2.7	2	2.4	9.9	81.9
2.7 - 2.9	2	2.4	9.9	84.3
3.2 - 3.4	1	1.2	4.9	85.5
3.7 - 3.9	2	2.4	9.9	88.0
3.9 - 4.4	2	2.4	4.9	90.4
4.4 - 4.6	1	1.2	4.9	91.6
4.6 - 5.4	1	1.2	1.6	92.8
5.4 - 6.6	1	1.2	1.0	94.0
6.6 - 7.5	2	2.4	2.5	96.4
7.5 - 8.5	2	2.4	2.5	98.8
8.5 - 9.3	1	1.2	1.6	100.0
	83			

Geometric mean particle size: 1.3 microns
Dispersity: 2.3

Table C.43 Primrose 64.4% W/O/W Emulsion
Primary Distribution

Particle size range (microns)	Number frequency in range	Percentage in range	Percentage per micron	Cumulative percentage less than
0.0 - 3.0	2	4.9	1.6	4.9
3.0 - 6.1	6	14.6	4.8	19.5
6.1 - 9.7	11	26.8	7.3	46.3
9.7 - 12.2	6	14.6	6.0	61.0
12.2 - 14.6	4	9.8	4.0	70.7
14.6 - 19.5	4	9.8	2.0	80.5
19.5 - 21.9	4	9.8	4.0	90.2
21.9 - 24.4	1	2.4	1.0	92.7
24.4 - 28.0	1	2.4	0.7	95.1
28.0 - 41.4	2	4.9	0.4	100.0
	41			

Geometric mean particle size: 10.0 microns
Dispersity: 2.0

Table C.44 Primrose 64.4% W/O/W Emulsion
Secondary Distribution

Particle size range (microns)	Number frequency in range	Percentage in range	Percentage per micron	Cumulative percentage less than
0.0 - 0.2	1	0.9	3.8	0.9
0.2 - 0.5	7	6.4	26.4	7.3
0.5 - 0.7	47	43.1	177.1	50.5
0.7 - 1.0	25	22.9	94.2	73.4
1.0 - 1.2	11	10.1	41.4	83.5
1.2 - 1.5	4	3.7	15.1	87.2
1.5 - 1.7	5	4.6	18.8	91.7
1.7 - 2.2	3	2.8	5.7	94.5
2.2 - 2.4	1	0.9	3.8	95.4
2.4 - 2.7	3	2.8	11.3	98.2
3.2 - 3.4	1	0.9	3.8	99.1
3.4 - 3.7	1	0.9	3.8	100.0
	109			

Geometric mean particle size: 0.8 microns
Dispersity: 1.7

Table C.45 Primrose 78.5% O/W Emulsion
Primary Distribution

Particle size range (microns)	Number frequency in range	Percentage in range	Percentage per micron	Cumulative percentage less than
0.0 - 0.2	2	3.8	15.5	3.8
0.2 - 0.5	6	11.3	46.5	15.1
0.5 - 0.7	12	22.6	93.0	37.7
0.7 - 1.7	10	18.9	19.4	56.6
1.7 - 1.9	6	11.3	46.5	67.9
1.9 - 2.2	5	9.4	38.7	77.4
2.2 - 2.7	4	7.5	15.5	84.9
2.7 - 2.9	4	7.5	31.0	92.5
2.9 - 6.1	2	3.8	1.2	96.2
6.1 - 7.3	1	1.9	1.5	98.1
7.3 - 8.5	1	1.9	1.5	100.0
	53			

Geometric mean particle size: 1.2 microns
Dispersity: 2.5

Table C.46 Primrose 82.4% O/W Emulsion
Primary Distribution

Particle size range (microns)	Number frequency in range	Percentage in range	Percentage per micron	Cumulative percentage less than
0.0 - 0.5	2	3.9	8.1	3.9
0.5 - 1.0	16	31.4	64.4	35.3
1.0 - 1.5	6	11.8	24.2	47.1
1.5 - 1.9	9	17.6	36.2	64.7
1.9 - 2.4	3	5.9	12.1	70.6
2.4 - 3.4	4	7.8	8.1	78.4
3.4 - 3.9	3	5.9	12.1	84.3
3.9 - 4.9	3	5.9	6.0	90.2
4.9 - 5.4	3	5.9	12.1	96.1
5.4 - 5.8	1	2.0	4.0	98.0
5.8 - 6.1	1	2.0	8.1	100.0
	51			

Geometric mean particle size: 1.5 microns
Dispersity: 2.2

Table C.47 Primrose 88.8% O/W Emulsion
Primary Distribution

Particle size range (microns)	Number frequency in range	Percentage in range	Percentage per micron	Cumulative percentage less than
0.0 - 0.7	9	7.8	10.6	7.8
0.7 - 1.0	8	6.9	28.3	14.7
1.0 - 1.2	13	11.2	46.0	25.9
1.2 - 1.5	7	6.0	24.8	31.9
1.5 - 1.7	14	12.1	49.6	44.0
1.7 - 1.9	13	11.2	46.0	55.2
1.9 - 2.2	7	6.0	24.8	61.2
2.2 - 2.4	7	6.0	24.8	67.2
2.4 - 2.7	3	2.6	10.6	69.8
2.7 - 2.9	4	3.4	14.2	73.3
2.9 - 3.2	4	3.4	14.2	76.7
3.2 - 3.3	3	2.6	21.2	79.3
3.3 - 3.7	8	6.9	18.9	86.2
3.7 - 3.9	2	1.7	7.1	87.9
3.9 - 4.4	5	4.3	8.9	92.2
4.4 - 5.1	3	2.6	3.5	94.8
5.1 - 5.6	3	2.6	5.3	97.4
5.6 - 6.1	1	0.9	1.8	98.3
6.1 - 6.3	1	0.9	3.5	99.1
6.3 - 6.6	1	0.9	3.5	100.0
	116			

Geometric mean particle size: 1.8 microns
Dispersity: 2.0

Table C.48 Primrose 95.2% O/W Emulsion
Primary Distribution

Particle size range (microns)	Number frequency in range	Percentage in range	Percentage per micron	Cumulative percentage less than
0.0 - 0.2	2	2.9	12.1	2.9
0.2 - 0.5	9	13.2	54.4	16.2
0.5 - 0.7	9	13.2	54.4	29.4
0.7 - 0.9	4	5.9	48.3	35.3
0.9 - 1.2	7	10.3	28.2	45.6
1.2 - 1.5	3	4.4	18.1	50.0
1.5 - 1.7	5	7.4	30.2	57.4
1.7 - 1.9	5	7.4	30.2	64.7
1.9 - 2.2	5	7.4	30.2	72.1
2.2 - 2.7	8	11.8	24.2	83.8
2.7 - 3.2	3	4.4	9.1	88.2
3.2 - 3.7	2	2.9	6.0	91.2
3.7 - 4.6	2	2.9	3.0	94.1
4.6 - 5.6	2	2.9	3.0	97.1
5.6 - 5.8	1	1.5	6.0	98.5
6.8 - 10.2	1	1.5	0.4	100.0
	68			

Geometric mean particle size: 1.2 microns
Dispersity: 2.4

Table C.49 Primrose 98.6% O/W Emulsion
Primary Distribution

Particle size range (microns)	Number frequency in range	Percentage in range	Percentage per micron	Cumulative percentage less than
0.0 - 0.2	3	5.6	22.8	5.6
0.2 - 0.5	6	11.1	45.6	16.7
0.5 - 0.7	5	9.3	38.0	25.9
0.7 - 1.0	12	22.2	91.3	48.1
1.0 - 1.2	5	9.3	38.0	57.4
1.2 - 1.5	3	5.6	22.8	63.0
1.5 - 1.9	4	7.4	15.2	70.4
1.9 - 2.4	4	7.4	15.2	77.8
2.4 - 2.7	4	7.4	30.4	85.2
2.7 - 2.9	3	5.6	22.8	90.7
3.5 - 4.4	3	5.6	6.5	96.3
4.4 - 4.6	1	1.9	7.6	98.1
4.6 - 5.6	1	1.9	1.9	100.0
	54			

Geometric mean particle size: 1.1 microns
Dispersity: 2.4